NAVAL AIR WARFARE CENTER AIRCRAFT DIVISION
PATUXENT RIVER, MARYLAND

TECHNICAL REPORT

REPORT NO: NAWCADPAX/TR-2015/241

CALCULATION OF MOMENT MATRIX ELEMENTS FOR BILINEAR QUADRILATERALS AND HIGHER-ORDER BASIS FUNCTIONS

by

John S. Asvestas

6 January 2016

DEPARTMENT OF THE NAVY
NAVAL AIR WARFARE CENTER AIRCRAFT DIVISION
PATUXENT RIVER, MARYLAND

NAWCADPAX/TR-2015/241
6 January 2016

CALCULATION OF MOMENT MATRIX ELEMENTS FOR BILINEAR QUADRILATERALS AND HIGHER-ORDER BASIS FUNCTIONS

by

John S. Asvestas

RELEASED BY:

6 Jan 2016

DOUGLAS P. McLAUGHLIN / AIR-4.5.5 / DATE
Head, Radar and Antenna Systems Division
Naval Air Warfare Center Aircraft Division

REPORT DOCUMENTATION PAGE

Form Approved
OMB No. 0704-0188

1. REPORT DATE:	2. REPORT TYPE	3. DATES COVERED
6 January 2016	Technical Report	

4. TITLE AND SUBTITLE:

Calculation of Moment Matrix Elements for Bilinear Quadrilaterals and Higher-Order Basis Functions.

5a. CONTRACT NUMBER

5b. GRANT NUMBER

5c. PROGRAM ELEMENT NUMBER

6. AUTHOR(S)

John S. Asvestas

5d. PROJECT NUMBER

5e. TASK NUMBER

5f. WORK UNIT NUMBER

7. PERFORMING ORGANIZATION NAME(S) AND ADDRESS(ES)

Naval Air Warfare Center Aircraft Division
48110 Shaw Road
Patuxent River, Maryland 20670

8. PERFORMING ORGANIZATION REPORT NUMBER

NAWCADPAX/TR-2015/241

9. SPONSORING/MONITORING AGENCY NAME(S) AND ADDRESS(ES)

Naval Air Systems Command
47123 Buse Road Unit IPT
Patuxent River, Maryland 20670-1547

10. SPONSOR/MONITOR'S ACRONYM(S)
NISE

11. SPONSOR/MONITOR'S REPORT NUMBER(S): N/A

12. DISTRIBUTION/AVAILABILITY STATEMENT

Approved for public release; distribution is unlimited.

13. SUPPLEMENTARY NOTES

14. ABSTRACT

We present a new method for computing the impedance matrix (IM) elements in the method of moments for geometries described by bilinear quadrilaterals (BQ) and for higher-order basis functions. Our method is restricted to the Electric Field Integral Equation and focuses on the self-elements of the IM and elements for which the observation point is near the integration BQ. The method is based on the simple idea of analytical integration along one of the BQ's parameters and numerical integration along the remaining one. For the singular (or nearly so) part of the integral, we show through analysis and examples that our method can provide precision to 15 significant digits.

15. SUBJECT TERMS

Method of Moments (MoM); Electric Field Integral Equation (EFIE); Bilinear Quadrilaterals (BQ).

16. SECURITY CLASSIFICATION OF:			17. LIMITATION OF ABSTRACT	18. NUMBER OF PAGES	19a. NAME OF RESPONSIBLE PERSON
a. REPORT	b. ABSTRACT	c. THIS PAGE			John S. Asvestas
Unclassified	Unclassified	Unclassified	SAR	108	19b. TELEPHONE NUMBER (include area code) 631-673-8176

Standard Form 298 (Rev. 8-98)
Prescribed by ANSI Std. Z39-18

SUMMARY

We present a new method for computing the impedance matrix (IM) elements in the method of moments for geometries described by bilinear quadrilaterals (BQ) and for higher-order basis functions. Our method is restricted to the Electric Field Integral Equation and focuses on the self-elements of the IM and elements for which the observation point is near the integration BQ. The method is based on the simple idea of analytical integration along one of the BQ's parameters and numerical integration along the remaining one. For the singular (or nearly so) part of the integral, we show through analysis and examples that our method can provide precision to 15 significant digits.

Contents

List of Tables

List of Figures

LIST OF ACRONYMS

BIE	Boundary Integral Equation
BQ	Bilinear Quadrilateral(s)
CEM	Computational EM
DEQ	Double-Exponential Quadrature (a.k.a. TSQ)
DP	Double Precision
EFIE	Electric Field Integral Equation
EM	Electromagnetic(s)
GKQ	Gauss-Kronrod Quadrature
IM	Impedance Matrix
IP	Integration Point
M&S	Modeling and Simulation
OP	Observation Point
QL	Quadrilateral
SD	Significant Digit(s)
SP	Single Precision
TSQ	Tanh-Sinh Quadrature (a.k.a. DEQ)

SECTION 1: INTRODUCTION

Electromagnetic (EM) modeling and simulation (M&S) is increasingly used in the design stage to predict the behavior of electromagnetic systems in diverse and complex environments. Typical examples are antenna design, in-situ antenna-to-antenna interaction, radar cross section analysis and design, EM interference and vulnerability, and many others.

The computational electromagnetics (CEM) methods that are used in developing EM M&S software tools divide into two broad categories: those that operate in the time domain and those in the frequency domain. In the latter case, we can distinguish again two categories: methods that approximate the physics of the problem, and methods that do not. In turn, exact-physics methods (as the latter category is known) are split into two categories: those that operate in a volume setting and those that operate over surfaces. The latter methods are known as boundary integral equation (BIE) methods and the present study falls into this category. The numerical solution of the BIE is usually accomplished in CEM using the method of moments (MoM) [1] whereby the integral equation is converted into a system of linear equations whose unknowns are related to the currents flowing on the surface(s) of the object of interest.

In MoM, the surface of the object of interest is represented by a number of geometric panels. Currents are defined on each panel and the total current on the object's surface is expressed as a linear combination of the panel currents. Thus, in practice, the actual geometry of an object (*e.g.,* aircraft, antenna, terrain) is replaced by a finite number of surface panels: the totality of which comes close to the true geometry of the object. To-date, most MoM-based EM M&S commercial tools represent the actual geometry by means of flat, triangular panels. The solution method employed after the triangular discretization is, usually, that of Rao, Wilton, and Glisson [2]. The drawback of using flat, triangular panels is that a few million may be required in faithfully reproducing a large and complex geometry. Since the number of unknowns in the resulting system of equations is related to the number of triangle edges, this may result in a system with millions of unknowns, requiring substantial computer resources and long execution times. It is obvious then that use of higher-order panels (panels representable by higher-order polynomials) could result in a large reduction in the number of panels that represent the actual geometry. This could lead to a substantial reduction in the size of the system of equations. A very well written review of efforts in this direction up to 2008 is given by Notaroš [3]. At this time (2015), however, EM M&S software based on the methods in [3] are still in the research stage with one exception: software based on representing geometry using bilinear quadrilaterals (BQ) [4], [5]. BQs are surfaces in space that are represented in terms of two parameters. The representation is linear in each of the parameters but it also contains their product. They are the simplest curved panels in use in CEM.

An important part of the application of MoM to an object comprising a number of BQs is the calculation of the matrix elements of the resulting system of linear equations. In the case of the electric field integral equation (EFIE) ([1], [2]), the matrix element consists of two iterated integrals. The inner integral involves the product of the free-space Green's function for the Helmholtz equation multiplied by an appropriate basis function and integrated over the BQ to which the source point belongs. The outer integral involves the result of the first integration, multiplied by a test function and integrated over the BQ to which the test function belongs.

It is the inner integral of the EFIE matrix element that we study in this report. The free-space Green's function is of the form $\exp(ikR) / R$, where k is the wavenumber while R is the distance between the source point on the integration BQ and the observation point (OP). Thus, the inner integral has an integrable singularity when the OP lies on the integration BQ. In terms of numerical integration using finite precision, this singularity manifests itself not only when R is equal to zero but, also, when it is close to it.

There is a considerable amount of literature on the evaluation of this integral [3], [4], [6]. In [6], the authors consider quadrilaterals of arbitrary order and present a numerical-integration scheme based on Duffy's method [7]. The scheme is valid only if the OP lies on the integration QL. They then proceed to compare their method to four other methods: singularity extraction ([3], [4]), polar-coordinate transformation [8], and quadratic [9] and cubic [10] rectangular transformation.

All of the methods just mentioned hold for arbitrary degree QL panels. In the present study, we focus on a BQ. This allows us to take advantage of the functional form of the distance function and develop formulas that compute the singular or near-singular part to machine precision. In Section 2, we review a BQ's geometry. In Section 3, we present three QLs that we use to test our method. In Section 4, we present arguments why some of the present approaches may not yield the precision that a specific problem may require. In Section 5, we examine the integral under consideration and we split it into two integrals: one that is proper (not singular) and can be evaluated numerically using standard methods, and an improper one that contains an integrable singularity. We then show that the latter integral (which represents a Newtonian potential of polynomial density in the two variables of integration) can be reduced through repeated integrations by parts with respect to one of the variables to a double integral over the BQ of a Newtonian potential of density one and a series of single integrals that are not singular and, hence, can be computed through standard numerical methods. In Section 6, we deal with the remaining singular integral as an iterated double integral in the BQ's variables and we show that we can evaluate either of the two single integrals analytically. The remaining single integral contains a logarithmic singularity, as expected. Through numerical examples using two quite distinct quadratures, we show that, as the OP approaches the integration BQ, we keep losing significant digit(s) (SD) for the remaining integral. At this point it appears that the present approach does not work as well as expected. It is worth mentioning, however, that the precision we obtain does not go below eight SD.

In Section 7, we revisit the result of Section 6 and, upon close examination; we are able to pinpoint the reason for the loss of SD. The logarithm's argument involves the difference of two numbers that are almost identical at the origin. This leads to a numerical instability and eventual loss of SD. By manipulating the logarithmic argument, we are able to stabilize it and show that the last remaining single integral can be evaluated numerically to double precision (DP) (15 SD) for the OP not only close but on the BQ itself. In Section 8, we use the third BQ with additional OPs on it to provide further evidence of the validity of our approach. In Section 9, we deal mostly with irregular BQs (Section 2) and we perform sensitivity studies on our algorithms to determine how close we can get to an irregular BQ before we start losing precision.

The integration routines we used in our calculations are from Mathematica® 7 [11]: the Gauss-Kronrod Quadrature (GKQ) and the Double-Exponential Quadrature (DEQ), also known as the Tanh-Sinh Quadrature (TSQ). We set the maximum number of subdivisions at 12 and asked for 15 SD.

THIS PAGE INTENTIONALLY LEFT BLANK

SECTION 2: GEOMETRY OF A BILINEAR QUADRILATERAL

In this section, we provide a basic description of a BQ. With respect to a rectangular coordinate system *xyz*, we define a BQ by

$$\mathbf{r}(p,q) = \frac{1}{4}\left[\mathbf{r}_{11}(1-p)(1-q) + \mathbf{r}_{12}(1-p)(q+1) + \mathbf{r}_{21}(p+1)(1-q) + \mathbf{r}_{22}(p+1)(q+1)\right], \quad |p| \le 1, \quad |q| \le 1. \tag{2.1}$$

The four constant vectors $\mathbf{r}_{ij}$ denote the four corners of the BQ. We note that (-1, -1) maps to $\mathbf{r}_{11}$, (-1, 1) maps to $\mathbf{r}_{12}$, (1, 1) maps to $\mathbf{r}_{22}$ and (1, -1) maps to $\mathbf{r}_{21}$. We show this in Fig. 2.1.

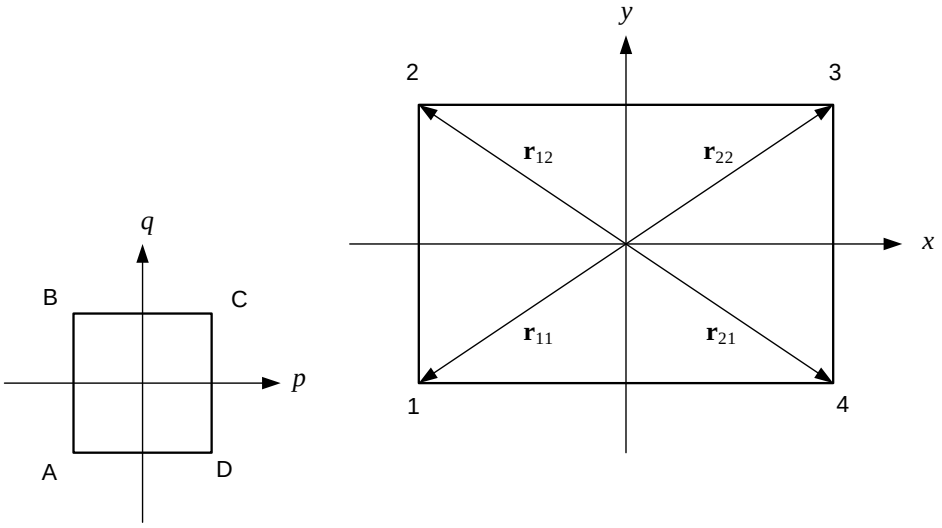

Figure 2.1. An example of how the basic square in the *pq*-plane maps to a BQ in the *xy*-plane that occupies the region $|x| \le 3$, $|y| \le 2$. The point A maps to 1, the point B to 2, point C to 3 and point D to 4.

We collect terms in *p*, *q,* and their product in (1.1) to write

$$\mathbf{r}(p,q) = \mathbf{r}_{00} + \mathbf{r}_p p + \mathbf{r}_q q + \mathbf{r}_{pq} pq, \quad |p| \le 1, \quad |q| \le 1 \tag{2.2}$$

where

$$\mathbf{r}_{00} = \frac{1}{4}\left[\mathbf{r}_{11} + \mathbf{r}_{12} + \mathbf{r}_{21} + \mathbf{r}_{22}\right] \tag{2.3}$$

$$\mathbf{r}_p = \frac{1}{4}\left[-\mathbf{r}_{11} - \mathbf{r}_{12} + \mathbf{r}_{21} + \mathbf{r}_{22}\right], \quad \mathbf{r}_q = \frac{1}{4}\left[-\mathbf{r}_{11} + \mathbf{r}_{12} - \mathbf{r}_{21} + \mathbf{r}_{22}\right] \tag{2.4}$$

$$\mathbf{r}_{pq} = \frac{1}{4}\left[\mathbf{r}_{11} - \mathbf{r}_{12} - \mathbf{r}_{21} + \mathbf{r}_{22}\right]. \tag{2.5}$$

For the example of Figure 2.1: $\mathbf{r}_{00} = \mathbf{0}$, $\mathbf{r}_p = 3\hat{x}$, $\mathbf{r}_q = 2\hat{y}$, $\mathbf{r}_{pq} = \mathbf{0}$.

The function in (2.2) maps points from the square $|p| \le 1$, $|q| \le 1$ to points in the *xyz*-space. The matrix of this transformation is

$$M = \begin{Vmatrix} \frac{\partial}{\partial p}(\hat{x}\cdot\mathbf{r}) & \frac{\partial}{\partial p}(\hat{y}\cdot\mathbf{r}) & \frac{\partial}{\partial p}(\hat{z}\cdot\mathbf{r}) \\ \frac{\partial}{\partial q}(\hat{x}\cdot\mathbf{r}) & \frac{\partial}{\partial q}(\hat{y}\cdot\mathbf{r}) & \frac{\partial}{\partial q}(\hat{z}\cdot\mathbf{r}) \end{Vmatrix} = \begin{Vmatrix} \hat{x}\cdot(\mathbf{r}_p + \mathbf{r}_{pq}q) & \hat{y}\cdot(\mathbf{r}_p + \mathbf{r}_{pq}q) & \hat{z}\cdot(\mathbf{r}_p + \mathbf{r}_{pq}q) \\ \hat{x}\cdot(\mathbf{r}_q + \mathbf{r}_{pq}p) & \hat{y}\cdot(\mathbf{r}_q + \mathbf{r}_{pq}p) & \hat{z}\cdot(\mathbf{r}_q + \mathbf{r}_{pq}p) \end{Vmatrix} \quad (2.6)$$

and it must be of rank 2 if we are not to have any singular points. This means that

$$\frac{\partial\mathbf{r}(p,q)}{\partial p} \times \frac{\partial\mathbf{r}(p,q)}{\partial q} \neq \mathbf{0} \quad (2.7)$$

at every non-singular point (p, q). This follows from the fact that the three 2 x 2 sub-matrices must have a non-zero determinant. Since the first of these vectors is tangent to a constant q-curve while the second to a constant p-curve, condition (2.7) says that the two vectors should not be collinear at a point ([12], pp. 56 – 57). What does this mean geometrically? From (2.2) we have that

$$\frac{\partial\mathbf{r}(p,q)}{\partial p} \times \frac{\partial\mathbf{r}(p,q)}{\partial q} = \left(\mathbf{r}_p + \mathbf{r}_{pq}q\right) \times \left(\mathbf{r}_q + \mathbf{r}_{pq}p\right) = \mathbf{r}_p \times \mathbf{r}_q + \mathbf{r}_{pq} \times \left(\mathbf{r}_q q - \mathbf{r}_p p\right). \quad (2.8)$$

If we assume that r_p and r_q are not collinear (and, hence, their cross product is not zero), then they define a plane in space. The vector $\left(\mathbf{r}_q q - \mathbf{r}_p p\right)$ lies on that plane. Then, a necessary condition for (2.8) to be equal to zero is that the vector $\mathbf{r}_{pq}$ does not have a component normal to that plane. Differently stated, for (2.8) to become zero, we must have the last three vectors in (2.2) lying on the same plane. In such a case, (2.2) describes a planar BQ. From this discussion, it is clear that the test for determining whether a BQ is planar is that $\mathbf{r}_{pq} \cdot \left(\mathbf{r}_p \times \mathbf{r}_q\right) = 0$. It is obvious from this condition that if $\mathbf{r}_p$ and $\mathbf{r}_q$ are collinear, we then have an irregular BQ. We substantiate these statements with mathematics in Appendix A.

Although (2.8) can be equal to zero only for a planar BQ, the converse is not true, *i.e.*, (2.8) is not zero for *all* planar BQ. We investigate this further. For a planar BQ, we can resolve the last vector in (2.2) along the directions of the preceding two vectors

$$\mathbf{r}_{pq} = \alpha\mathbf{r}_p + \beta\mathbf{r}_q \quad (2.9)$$

where α and β are scalars. In place of (2.2), we now have

$$\mathbf{r}(p,q) = \mathbf{r}_{00} + \mathbf{r}_p p\left(1 + \alpha q\right) + \mathbf{r}_q q\left(1 + \beta p\right), \quad |p| \le 1, \quad |q| \le 1. \quad (2.10)$$

Using this, we get

$$\frac{\partial \mathbf{r}(p,q)}{\partial p} \times \frac{\partial \mathbf{r}(p,q)}{\partial q} = \left[\mathbf{r}_p\left(1+\alpha q\right)+\mathbf{r}_q \beta q\right] \times \left[\mathbf{r}_p \alpha p + \mathbf{r}_q\left(1+\beta p\right)\right]$$
$$= \left(\mathbf{r}_q \times \mathbf{r}_p\right)\alpha\beta pq + \left(\mathbf{r}_p \times \mathbf{r}_q\right)(1+\alpha q)(1+\beta p) = \left(\mathbf{r}_p \times \mathbf{r}_q\right)(1+\alpha q+\beta p). \tag{2.11}$$

If the cross product is zero, then we have a straight line in space. We exclude this case. When is the scalar part zero? We let

$$P = \beta p, \quad Q = \alpha q. \tag{2.12}$$

From the conditions on p and q in (2.2), we have that

$$|P| = |\beta||p| \le |\beta|, \quad |Q| = |\alpha||q| \le |\alpha|. \tag{2.13}$$

We also set the scalar factor in (2.11) equal to zero

$$1 + Q + P = 0. \tag{2.14}$$

We want to know whether this equation is satisfied with values of P and Q in the range of (2.13). In Figure 2.2, the lower left corner of the rectangle is the point closest to the straight line. The value of P there is $-|\beta|$ and the value of Q for the straight line is $-1 + |\beta|$. For no intersection, we want $-1 + |\beta|$ to be smaller than $-|\alpha|$; for one intersection point, we want $-1 + |\beta|$ to be equal to $-|\alpha|$; and, for an uncountable number of intersection points, we want $-1 + |\beta|$ to be greater than $-|\alpha|$. We summarize these results in Table 2.1.

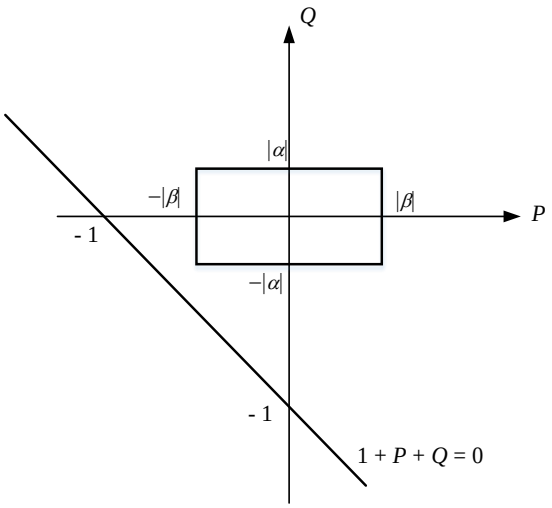

Figure 2.2. Geometry for the intersection of the straight line with the rectangle.

Table 2.1: Solutions of (2.14) subject to (2.13).

$\lvert\alpha\rvert+\lvert\beta\rvert<1$	No intersection points	No solution of (2.14)	Regular BQ
$\lvert\alpha\rvert+\lvert\beta\rvert=1$	One intersection point	One solution of (2.14)	Irregular BQ
$\lvert\alpha\rvert+\lvert\beta\rvert>1$	Many intersection points	Many solutions of (2.14)	Irregular BQ

We demonstrate these results using three BQs. The position vector for the first is

$$\mathbf{r}(p,q)=\mathbf{r}_p p(1+0.2q)+\mathbf{r}_q q(1+0.3p),\quad (\alpha=0.2,\beta=0.3) \tag{2.15}$$

and its graph is shown in Figure 2.3. This is a regular BQ. The position vector of the second BQ is

$$\mathbf{r}(p,q)=\mathbf{r}_p p(1+0.5q)+\mathbf{r}_q q(1+0.5p),\quad (\alpha=0.5,\beta=0.5) \tag{2.16}$$

and its graph is shown in Figure 2.4. This is an irregular BQ in the form of a triangle. The position vector of the third BQ is

$$\mathbf{r}(p,q)=\mathbf{r}_p p(1+2q)+\mathbf{r}_q q(1+3p),\quad (\alpha=2,\beta=3). \tag{2.17}$$

Its graph is given in Figure 2.5. This is also an irregular BQ. In all three cases, $\mathbf{r}_p=(3,0,-0.5)$ while $\mathbf{r}_q=(0,2,-0.5)$.

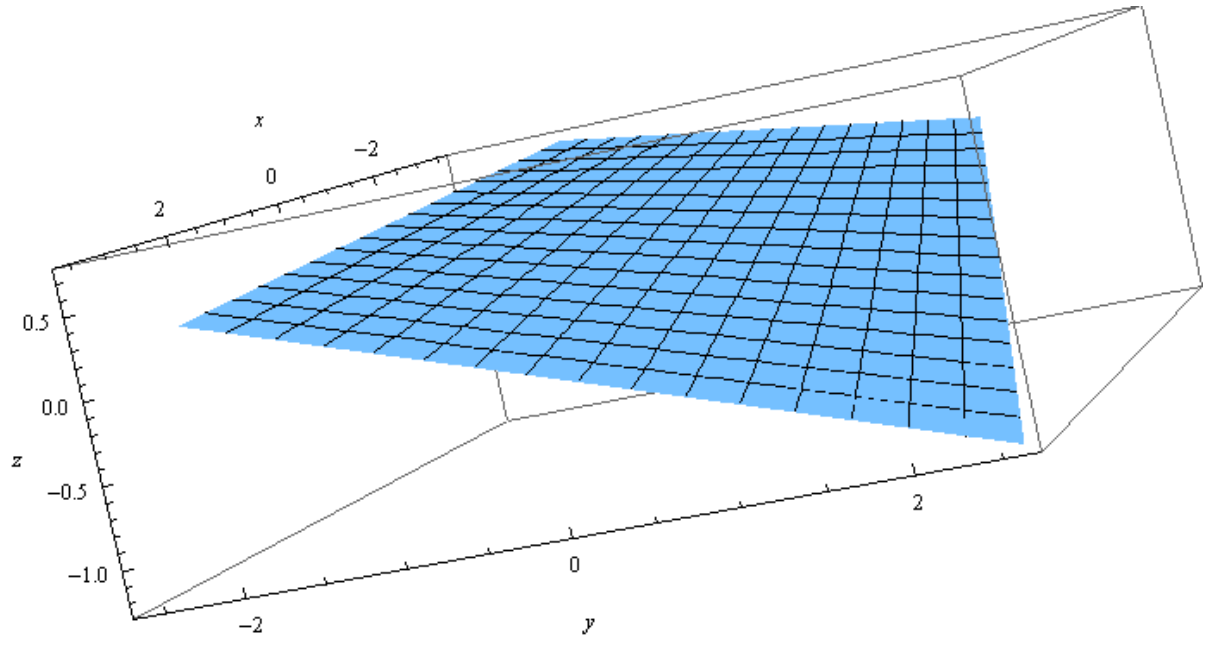

Figure 2.3: Graph of (2.15); a planar, regular BQ.

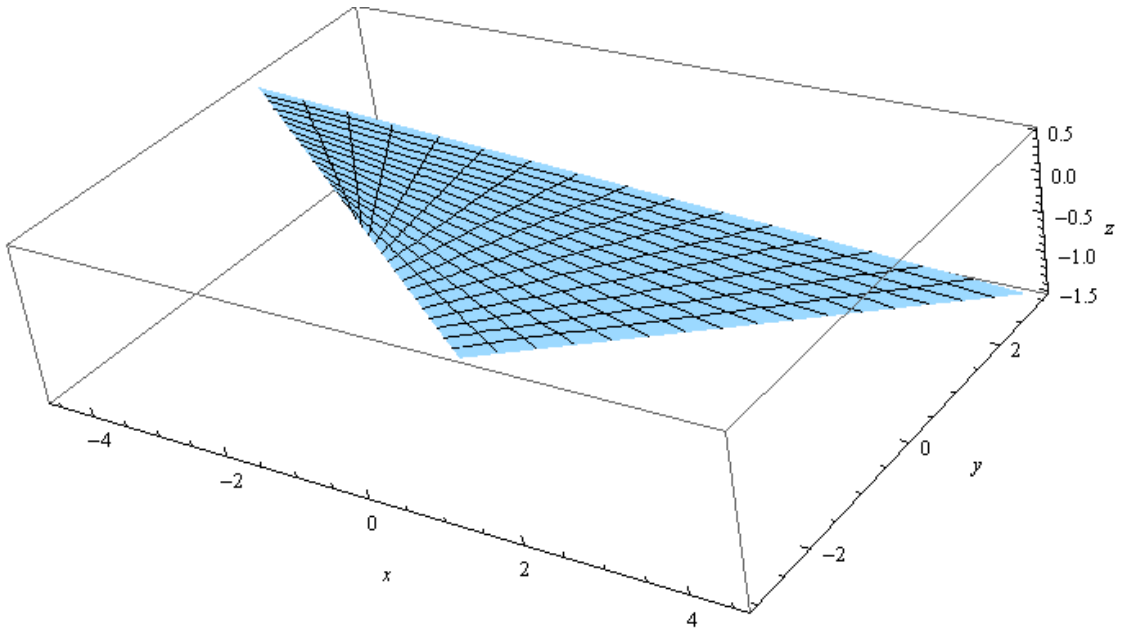

Figure 2.4: The graph of (2.16); a planar, barely irregular BQ.

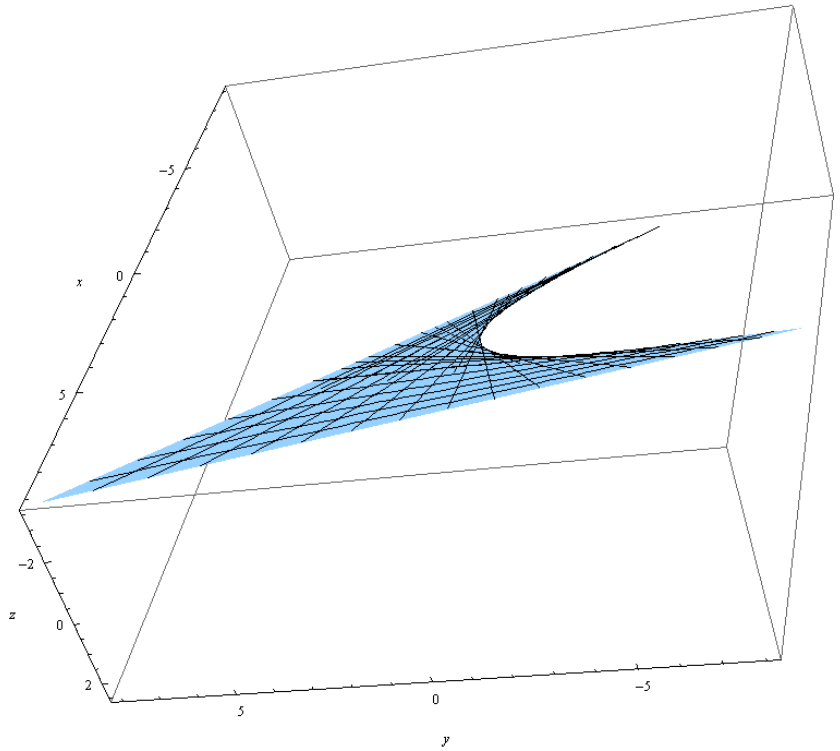

Figure 2.5: The graph of (2.17); a planar, highly irregular BQ.

The unit normal at a point on the surface is given by ([12], p. 62)

$$\hat{n} = \frac{\dfrac{\partial \mathbf{r}(p,q)}{\partial p} \times \dfrac{\partial \mathbf{r}(p,q)}{\partial q}}{\left| \dfrac{\partial \mathbf{r}(p,q)}{\partial p} \times \dfrac{\partial \mathbf{r}(p,q)}{\partial q} \right|} \tag{2.18}$$

and we note that we could also have defined it as the negative of this. The surface element at a point is defined by

$$dS = \left| \frac{\partial \mathbf{r}(p,q)}{\partial p} \times \frac{\partial \mathbf{r}(p,q)}{\partial q} \right| dpdq\,. \tag{2.19}$$

If we hold one of the parameters constant, we can measure arc length along the other according to the formula ([12], p. 58)

$$s = \int_{p_1}^{p_2} \left| \frac{\partial \mathbf{r}(p,q)}{\partial p} \right| dp = \int_{p_1}^{p_2} \left| \mathbf{r}_p + \mathbf{r}_{pq} q \right| dp = \left| \mathbf{r}_p + \mathbf{r}_{pq} q \right| \left(p_2 - p_1 \right), \quad -1 \le p_1 < p_2 \le 1, \quad q = \text{const.} \tag{2.20}$$

Similarly,

$$s = \int_{q_1}^{q_2} \left| \frac{\partial \mathbf{r}(p,q)}{\partial q} \right| dq = \left| \mathbf{r}_q + \mathbf{r}_{pq} p \right| \left(q_2 - q_1 \right), \quad -1 \le q_1 < q_2 \le 1, \quad p = \text{const.} \tag{2.21}$$

We point out that if we have a curve on the BQ described parametrically by $p(t)$ and $q(t)$, then we have a more general formula for its arc length ([12], p. 58). In any case, the above formulas make sense since we are moving along straight lines.

We consider next a point $\left(p_0 \; q_0 \right)$ in the interior of the square of definition of these variables. This maps to the point $\mathbf{r}_0$, a point in the interior of the BQ

$$\mathbf{r}_0 = \mathbf{r}\left(p_0, q_0 \right) = \mathbf{r}_{00} + \mathbf{r}_p p_0 + \mathbf{r}_q q_0 + \mathbf{r}_{pq} p_0 q_0, \quad \left| p_0 \right| < 1, \quad \left| q_0 \right| < 1. \tag{2.22}$$

We can reference (2.2) to this point by expanding in a Taylor series about it

$$\mathbf{r}(p,q) = \mathbf{r}_0 + \left(\mathbf{r}_p + \mathbf{r}_{pq} q_0 \right)\left(p - p_0 \right) + \left(\mathbf{r}_q + \mathbf{r}_{pq} p_0 \right)\left(q - q_0 \right) + \mathbf{r}_{pq} \left(p - p_0 \right)\left(q - q_0 \right). \tag{2.23}$$

This expression is exact. We can easily show this by collecting terms in powers of *p*, *q,* and *pq*. At the point r_0, we define coordinates $p_0 q_0 n$. The unit vectors are

$$\hat{p}_0 = \frac{\dfrac{\partial \mathbf{r}(p_0, q_0)}{\partial p_0}}{\left|\dfrac{\partial \mathbf{r}(p_0, q_0)}{\partial p_0}\right|}, \quad \hat{q}_0 = \frac{\dfrac{\partial \mathbf{r}(p_0, q_0)}{\partial q_0}}{\left|\dfrac{\partial \mathbf{r}(p_0, q_0)}{\partial q_0}\right|}, \quad \hat{n} = \frac{\dfrac{\partial \mathbf{r}(p_0, q_0)}{\partial p_0} \times \dfrac{\partial \mathbf{r}(p_0, q_0)}{\partial q_0}}{\left|\dfrac{\partial \mathbf{r}(p_0, q_0)}{\partial p_0} \times \dfrac{\partial \mathbf{r}(p_0, q_0)}{\partial q_0}\right|}. \tag{2.24}$$

Although $\hat{p}_0$ and $\hat{q}_0$ are perpendicular to $\hat{n}$, they are not necessarily perpendicular to each other. Letting

$$\mathbf{p}_0 = \frac{\partial \mathbf{r}(p_0, q_0)}{\partial p_0}, \quad \mathbf{q}_0 = \frac{\partial \mathbf{r}(p_0, q_0)}{\partial q_0} \tag{2.25}$$

we can write for (2.23)

$$\mathbf{r}(p, q) = \mathbf{r}_0 + \mathbf{p}_0 u + \mathbf{q}_0 v + \mathbf{r}_{pq} uv \tag{2.26}$$

where

$$u = p - p_0, \quad v = q - q_0; \quad -(1 + p_0) \le u \le 1 - p_0, \quad -(1 + q_0) \le v \le 1 - q_0. \tag{2.27}$$

In the next section, we will describe three BQs that we will use for testing purposes.

THIS PAGE INTENTIONALLY LEFT BLANK

SECTION 3: TEST BILINEAR QUADRILATERALS

We will use three BQs for testing our ideas. We describe them below. The corners of the first BQ are given by

$$\mathbf{r}_{11} = (-3,-2,1), \quad \mathbf{r}_{22} = (3,2,-1), \quad \mathbf{r}_{12} = (-3,2,0), \quad \mathbf{r}_{21} = (3,-2,0) \tag{3.1}$$

From (2.3) – (2.5)

$$\mathbf{r}_0 = (0,0,0), \quad \mathbf{r}_p = \frac{1}{2}(6,0,-1), \quad \mathbf{r}_q = \frac{1}{2}(0,4,-1), \quad \mathbf{r}_{pq} = (0,0,0). \tag{3.2}$$

From (2.2), we then have

$$\mathbf{r}(p,q) = \frac{1}{2}(6,0,-1)\,p + \frac{1}{2}(0,4,-1)\,q, \quad |p| \le 1, \quad |q| \le 1. \tag{3.3}$$

The graph of the BQ is shown in Figure 3.1. This is a flat BQ. The normal is given by (2.18).

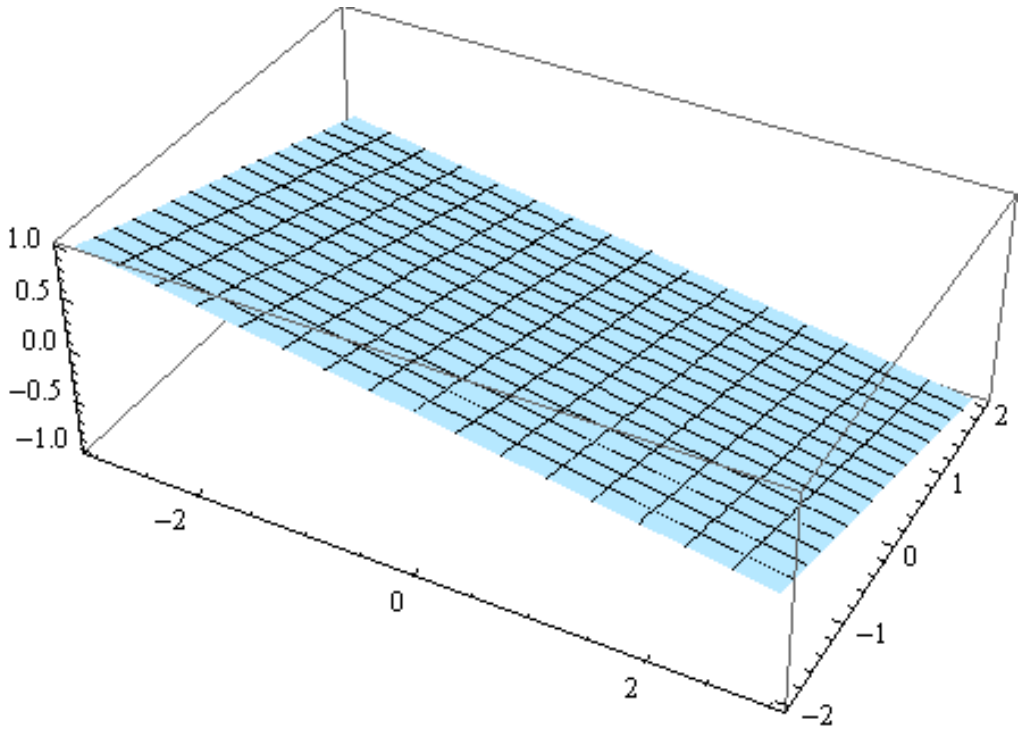

Figure 3.1: The BQ of Equation (3.3).

The second BQ has corner vectors

$$\mathbf{r}_{11} = (-3,-2,1), \quad \mathbf{r}_{22} = (3,2,1), \quad \mathbf{r}_{12} = (-3,2,-1), \quad \mathbf{r}_{21} = (3,-2,-1) \tag{3.4}$$

from which

$$\mathbf{r}_0 = (0,0,0), \quad \mathbf{r}_p = (3,0,0), \quad \mathbf{r}_q = (0,2,0), \quad \mathbf{r}_{pq} = (0,0,1) \tag{3.5}$$

so that

$$\mathbf{r}(p,q) = (3,0,0)\,p + (0,2,0)\,q + (0,0,1)\,pq, \quad |p| \le 1, \quad |q| \le 1. \tag{3.6}$$

The graph of this BQ is shown in Figure 3.2.

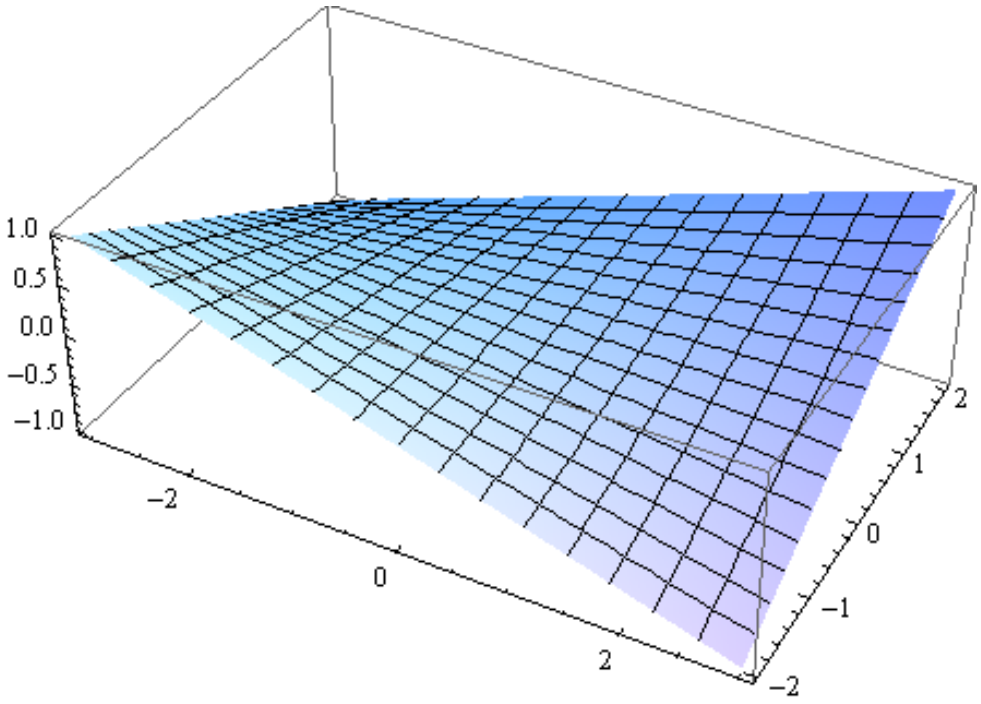

Figure 3.2: The BQ of Equation (3.6).

We go next to an extreme case

$$\mathbf{r}_{11} = (-3,-2,10), \quad \mathbf{r}_{22} = (3,2,10), \quad \mathbf{r}_{12} = (-3,2,-10), \quad \mathbf{r}_{21} = (3,-2,-10) \tag{3.7}$$

so that

$$\mathbf{r}_0 = (0,0,0), \quad \mathbf{r}_p = (3,0,0), \quad \mathbf{r}_q = (0,2,0), \quad \mathbf{r}_{pq} = (0,0,10) \tag{3.8}$$

and

$$\mathbf{r}(p,q) = (3,0,0)\,p + (0,2,0)\,q + (0,0,10)\,pq, \quad |p| \le 1, \quad |q| \le 1. \tag{3.9}$$

The graph of this BQ is shown in Figure 3.3.

We note that condition (2.7) is satisfied at all points of these QLs. For example, for the last BQ we have

$$\begin{aligned}\frac{\partial \mathbf{r}(p,q)}{\partial p}\times\frac{\partial \mathbf{r}(p,q)}{\partial q} &= \left[(3,0,0)+(0,0,10)q\right]\times\left[(0,2,0)+(0,0,10)p\right]\\ &= (3,0,0)\times(0,2,0)+(3,0,0)\times(0,0,10)p+(0,0,10)\times(0,2,0)q\\ &= 6\hat{z}-30p\hat{y}-20q\hat{x}\end{aligned} \tag{3.10}$$

and the magnitude of this vector is always greater than zero. This means that we have a tangent plane at every point of the BQ with a normal given by (2.18). For the example

$$\hat{n}=\frac{-20q\hat{x}-30p\hat{y}+6\hat{z}}{\sqrt{(20q)^2+(30p)^2+36}}\,. \tag{3.11}$$

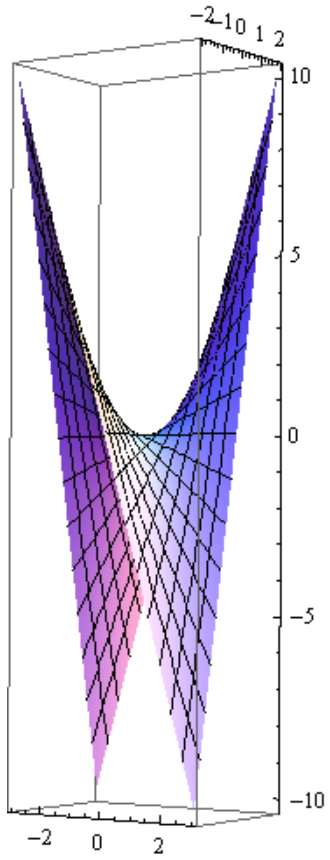

Figure 3.3: The BQ of Equation (3.9).

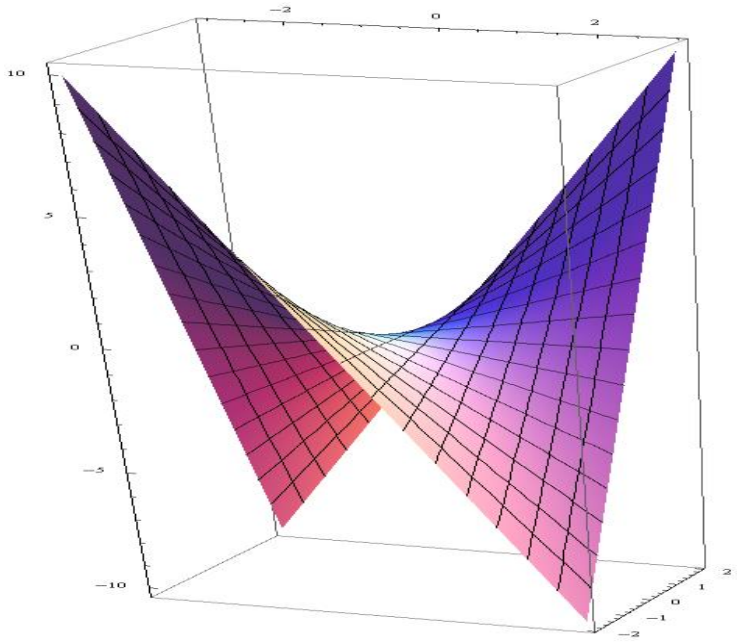

Figure 3.4: Another view of the graph of the BQ of Equation (3.9).

SECTION 4: REVIEW OF EVALUATION OF AN INTEGRAL

We justify here the need for a new way to evaluate the integral

$$P_{lm} = \int_{-1}^{1}\int_{-1}^{1} p^l q^m \frac{\mathrm{e}^{ikR}}{R} dpdq\,, \quad l,m = 0,1,2,... \tag{4.1}$$

over a BQ. The function R represents the distance between the integration point (IP) r (on the BQ) and another point, r′, that we call the OP. This integral is well behaved when the OP is some distance away from the BQ; however, when the OP is very near or on the BQ, then the integrand has a singularity since the distance function R can become equal to zero or very nearly so. Hence, the principal issue with this integral is how to calculate it when the OP is very near or on the BQ. Two principal methods exist for evaluating (4.1). One relies on singularity extraction and the use of an auxiliary tangent plane ([3], [4]) while the other on coordinate transformation ([6], [8], [9], [10]). We first discuss the former method.

Kolundzija and Djordjević ([4], p. 350, 2002) advocate the following splitting of the integral so as to isolate its singular part

$$P_{lm} = \int_{-1}^{1}\int_{-1}^{1}\left[p^l q^m \frac{\mathrm{e}^{ikR}}{R} - {p_0}^l {q_0}^m \frac{1}{R_0} \right] dpdq + {p_0}^l {q_0}^m \int_{-1}^{1}\int_{-1}^{1} \frac{1}{R_0} dpdq, \quad l,m = 0,1,2,... \tag{4.2}$$

where (p_0, q_0) corresponds to a point in the interior of the BQ and is the projection of the OP onto the BQ, while R_0 is the distance between the OP and the purely linear part of the BQ's position vector. The second integral can be evaluated analytically. For the first integral, the authors write, "The integrand of the first integral...tends to zero when the source point (IP) approaches the field point (OP). Hence, the numerical integration of this integral is much more efficient than the numerical evaluation of the complete ... integral". We will show below that this statement does not stand to scrutiny.

Notaroš ([3], p. 2265) mentions the same splitting of the integral as in (4.2) and, for the first integral in (4.2) suggests "using Gauss-Legendre quadrature formulas". What is most likely meant here is that the Gauss-Legendre formulas are to be applied along the p and q coordinates.

We proceed to examine these statements closely. The worst case scenario is when the OP is on the BQ, *i.e.*, the point (p_0, q_0). For the position vector to any point on the BQ, we have from (2.23) that

$$\mathbf{r}(p,q) = \mathbf{r}* + (\mathbf{r}_p + \mathbf{r}_{pq} q_0)(p - p_0) + (\mathbf{r}_q + \mathbf{r}_{pq} p_0)(q - q_0) + \mathbf{r}_{pq}(p - p_0)(q - q_0), \quad \mathbf{r}* = \mathbf{r}(p_0, q_0)\,. \tag{4.3}$$

We let

$$\mathbf{p}(p_0,q_0)=\frac{d\mathbf{r}(p_0,q_0)}{dp_0}=\mathbf{p}_0\,,\quad \mathbf{q}(p_0,q_0)=\frac{d\mathbf{r}(p_0,q_0)}{dq_0}=\mathbf{q}_0 \tag{4.4}$$

and we also make the change of variables (2.27)

$$u=p-p_0\,,\quad v=q-q_0\,;\quad -(1+p_0)\le u\le 1-p_0\,,\quad -(1+q_0)\le v\le 1-q_0\,. \tag{4.5}$$

We can then write for (4.3)

$$\mathbf{r}(p,q)=\mathbf{r}*+\mathbf{p}_0u+\mathbf{q}_0v+\mathbf{r}_{pq}uv\,. \tag{4.6}$$

The linear part of this

$$\mathbf{r}_0(p,q)=\mathbf{r}*+\mathbf{p}_0u+\mathbf{q}_0v \tag{4.7}$$

is a vector to a point on the plane tangent to the BQ at **r***. With this notation, we have that

$$R=|\mathbf{r}-\mathbf{r}*|\,,\quad R_0=|\mathbf{r}_0-\mathbf{r}*|\,. \tag{4.8}$$

For the first integrand in (4.2), we write

$$f(u,v)=(u+p_0)^l(v+q_0)^m\frac{e^{ikR(u,v)}}{R(u,v)}-{p_0}^l{q_0}^m\frac{1}{R_0(u,v)}\,. \tag{4.9}$$

and proceed to evaluate the limit at the origin. We let first *u* go to zero

$$f(0,v)={p_0}^l(v+q_0)^m\frac{e^{ikR(0,v)}}{R(0,v)}-{p_0}^l{q_0}^m\frac{1}{R_0(0,v)}\,. \tag{4.10}$$

From (4.7) - (4.8), we get that

$$f(0,v)={p_0}^l(v+q_0)^m\frac{e^{ik|\mathbf{q}_0v|}}{|\mathbf{q}_0v|}-{p_0}^l{q_0}^m\frac{1}{|\mathbf{q}_0v|}\,. \tag{4.11}$$

We proceed to expand the binomial

$$\begin{aligned}f(0,v)&={p_0}^l\frac{e^{ik|v||\mathbf{q}_0|}}{|v||\mathbf{q}_0|}\sum_{n=0}^{m}\binom{m}{n}v^n{q_0}^{m-n}-{p_0}^l{q_0}^m\frac{1}{|v||\mathbf{q}_0|}\\&={p_0}^l{q_0}^m\frac{e^{ik|v||\mathbf{q}_0|}-1}{|v||\mathbf{q}_0|}+{p_0}^l\frac{e^{ik|v||\mathbf{q}_0|}}{|v||\mathbf{q}_0|}\sum_{n=1}^{m}\binom{m}{n}v^n{q_0}^{m-n}\end{aligned} \tag{4.12}$$

We take now the limit as *v* goes to zero

$$\lim_{v\to 0} f\left(0,v\right) = ikp_0{}^l q_0{}^m \pm \frac{mp_0{}^l q_0{}^{m-1}}{\left|\mathbf{q}_0\right|}. \tag{4.13}$$

where the plus sign corresponds to positive values of v and the minus to negative. We see that the imaginary part of the integrand does possess a limit. This is to be expected because the imaginary part has no singularity since it is of the form $\sin(x)/x$. The real part, however, does not possess a limit since the limit value depends on the direction from which the point in question is approached.

We next let v be equal to zero in (4.9)

$$\begin{aligned} f\left(u,0\right) &= \left(u+p_0\right)^l q_0{}^m \frac{\mathrm{e}^{ikR(u,0)}}{R\left(u,0\right)} - p_0{}^l q_0{}^m \frac{1}{R_0\left(u,0\right)} \\ &= \left(u+p_0\right)^l q_0{}^m \frac{\mathrm{e}^{ik\left|\mathbf{p}\left(p_0,q_0\right)\right||u|}}{\left|\mathbf{p}\left(p_0,q_0\right)\right||u|} - p_0{}^l q_0{}^m \frac{1}{\left|\mathbf{p}_0\right||u|} \\ &= q_0{}^m \frac{\mathrm{e}^{ik|\mathbf{p}_0||u|}}{\left|\mathbf{p}_0\right||u|} \sum_{n=0}^{l} \binom{l}{n} u^n p_0{}^{l-n} - p_0{}^l q_0{}^m \frac{1}{\left|\mathbf{p}_0\right||u|} \\ &= \frac{p_0{}^l q_0{}^m}{\left|\mathbf{p}_0\right||u|}\left[\mathrm{e}^{ik|\mathbf{p}_0||u|} - 1\right] + q_0{}^m \frac{\mathrm{e}^{ik\left|\mathbf{p}\left(p_0,q_0\right)\right||u|}}{\left|\mathbf{p}_0\right||u|} \sum_{n=1}^{l} \binom{l}{n} u^n p_0{}^{l-n}. \end{aligned} \tag{4.14}$$

We now take the limit as u tends to zero

$$\lim_{u\to 0} f\left(u,0\right) = ikp_0{}^l q_0{}^m \pm \frac{lp_0{}^{l-1} q_0{}^m}{\left|\mathbf{p}_0\right|} \tag{4.15}$$

with the dual sign as in the previous case. Again, the imaginary part of the integrand has a limit while the real part does not.

We see that, for the real part of the integrand, the two operations produce different limits; moreover, within each operation the limit is direction dependent. This means that the limit of the real part of the integrand at $\left(p_0,q_0\right)$ does not exist and, hence, the function is not and cannot become continuous there. In terms of a numerical evaluation of the first integral in (4.2), this means that we need a superior cubature in order to produce good results. We also observe that, if l and m are equal to zero, then the limit does exist for the real part and is equal to zero. Thus, the claim of Kolundzija and Djordjević [4] that the integrand goes to zero at this point is correct only for this case. We present additional evidence below, based on numerical calculations.

In performing numerical demonstrations, we use the three BQs we presented in Section 3. In all three cases, we place the singular point at

$$p_0 = q_0 = 1/4 \tag{4.16}$$

so that

$$u = p - \frac{1}{4}, \quad v = q - \frac{1}{4}; \quad -1.25 \le u \le 0.75, \quad -1.25 \le v \le 0.75. \tag{4.17}$$

We will deal only with the real part of the integrand since the imaginary does not present a problem.

$$\mathrm{Re}\left\{ f_j(u,v) \right\} = \left(u + \frac{1}{4} \right)^l \left(v + \frac{1}{4} \right)^m \frac{\cos\left[kR_j(u,v) \right]}{R_j(u,v)} - \left(\frac{1}{4} \right)^{l+m} \frac{1}{R_{0,j}(u,v)}, \quad j = 1,2,3 \tag{4.18}$$

with the subscript *j* referring to one of the three BQs. Moreover, from the expansion of the cosine about zero, we see that only the leading term is singular, while the rest go to zero with R_j. We dispense with those terms and write

$$h_j(u,v) = \left(u + \frac{1}{4} \right)^l \left(v + \frac{1}{4} \right)^m \frac{1}{R_j(u,v)} - \left(\frac{1}{4} \right)^{l+m} \frac{1}{R_{0,j}(u,v)}, \quad j = 1,2,3. \tag{4.19}$$

This is the surface we will plot about the origin.

We begin with the flat BQ of Figure 3.1. The position vector is given by (3.3) and, hence,

$$R_1(u,v) = \left| \frac{1}{2}(6,0,-1)u + \frac{1}{2}(0,4,-1)v \right| = \frac{1}{2}\left| \hat{x}6u + \hat{y}4v - \hat{z}(u+v) \right| = \frac{1}{2}\sqrt{(6u)^2 + (4v)^2 + (u+v)^2} \tag{4.20}$$

Moreover,

$$R_{0,1}(u,v) = R_1(u,v). \tag{4.21}$$

From (4.19)

$$h_1(u,v) = \left[\left(u + \frac{1}{4} \right)^l \left(v + \frac{1}{4} \right)^m - \left(\frac{1}{4} \right)^{l+m} \right] \frac{1}{R_1(u,v)}. \tag{4.22}$$

This expression is equal to zero when $l = m = 0$, as it should. In Figs. 4.1 and 4.2, we display the cases $l = 1, m = 0$ and $l = 0, m = 1$, respectively. In the first case, we observe a signum-like behavior near the origin and along the *u*-axis while, in the second case, this behavior is along the *v*-axis. In Figure 4.3, we display the case $l = 1, m = 1$ where, as expected the signum-like behavior manifests itself along the bisector of the two axes as well as along the axes themselves. All three figures support the analysis presented above and the surfaces depicted there are not easy to duplicate numerically, even in this simple case of a flat BQ. Admittedly, the singularity can be removed through a rotation of the BQ so that the normal to the BQ points along the *z*-axis. Once

this is done, we can integrate with respect to one of the variables to remove the singularity. This can be done only for a flat BQ.

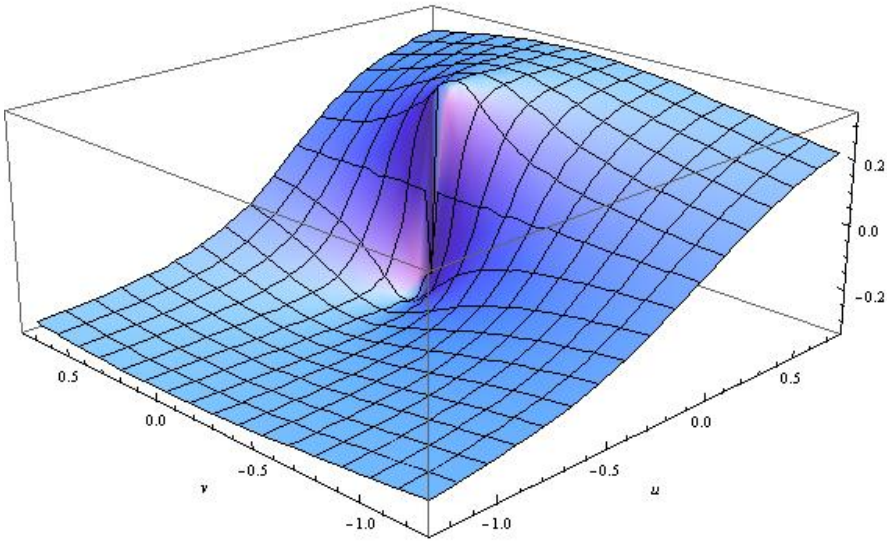

Figure 4.1: Graph of the surface (4.22) for $l=1, m=0$. The surface has a signum-like behavior near the origin and along the *u*-axis.

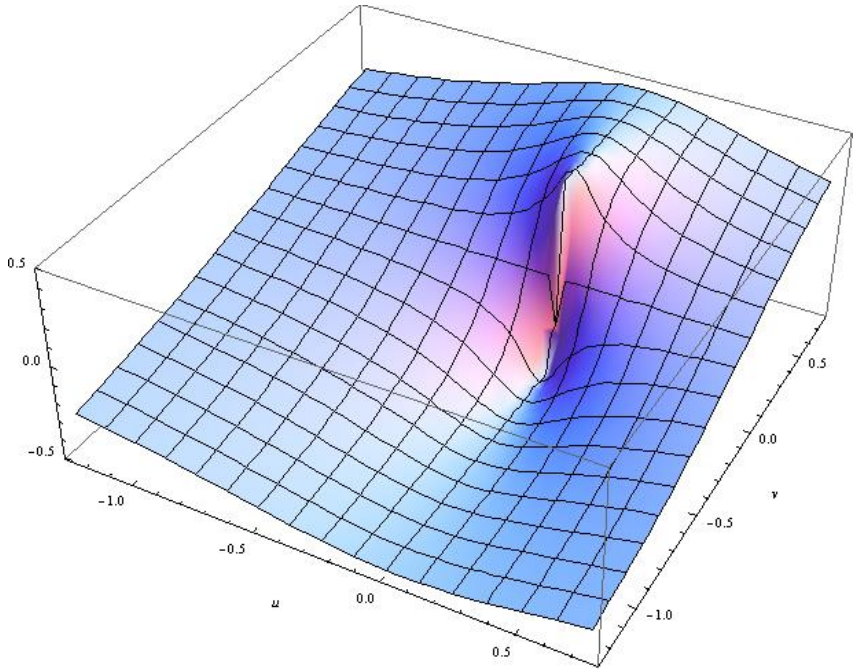

Figure 4.2: Graph of the surface (4.22) for $l=0, m=1$. The surface has a signum-like behavior near the origin and along the *v*-axis.

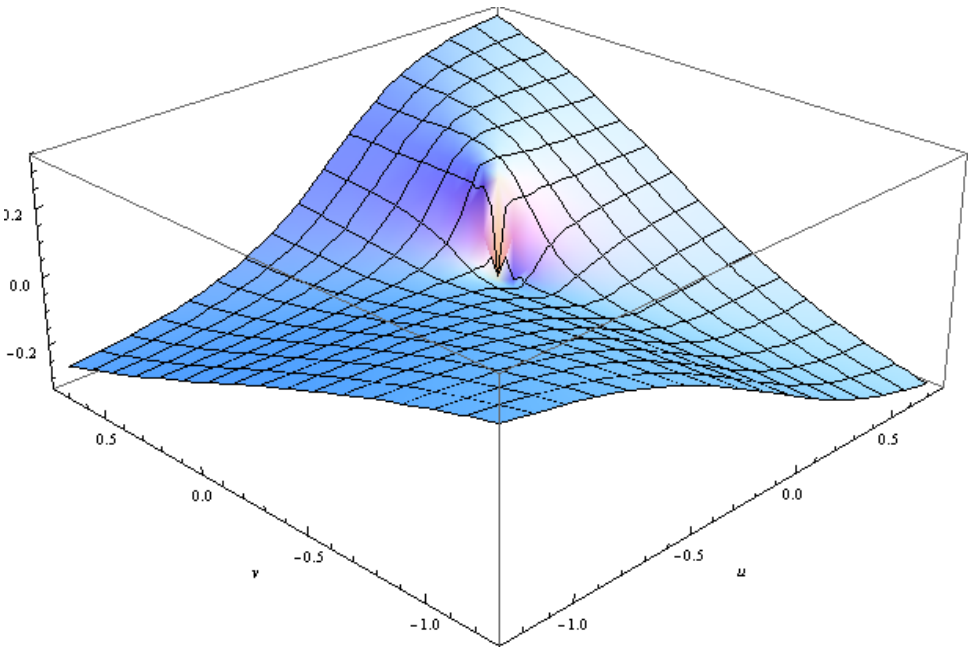

Figure 4.3: Graph of the surface (4.22) for $l=1, m=1$. The signum-like behavior near the origin manifests itself along the two axes and along a 45-deg line with respect to the two axes, as it should.

We proceed to check the values in these graphs. For the limits in (4.11) and (4.13), we write

$$\lim_{v\to 0} h_1(0,v) = \pm \frac{m}{|\mathbf{q}_0|}\left(\frac{1}{4}\right)^{l+m-1}, \quad \lim_{u\to 0} h_1(u,0) = \pm \frac{l}{|\mathbf{p}_0|}\left(\frac{1}{4}\right)^{l+m-1}. \tag{4.23}$$

Using (4.4) and (3.3), we write for these limits

$$\lim_{v\to 0} h_1(0,v) = \pm \frac{2m}{\sqrt{17}}\left(\frac{1}{4}\right)^{l+m-1} = \pm 0.4851 m\left(\frac{1}{4}\right)^{l+m-1} \tag{4.24}$$

and

$$\lim_{u\to 0} h_1(u,0) = \pm \frac{2l}{\sqrt{37}}\left(\frac{1}{4}\right)^{l+m-1} = \pm 0.3288 l\left(\frac{1}{4}\right)^{l+m-1}. \tag{4.25}$$

For the case $l=1, m=0$, we see from (4.22) that (4.24) is satisfied. Moreover, from (4.22) and (4.20)

$$h_1(u,0) = \left[\left(u+\frac{1}{4}\right)-\left(\frac{1}{4}\right)\right]\frac{1}{R_1(u,0)} = \frac{2}{\sqrt{37}}\frac{u}{|u|} \tag{4.26}$$

which is in agreement with (4.25).We display the graph of this function in Figure 4.4.

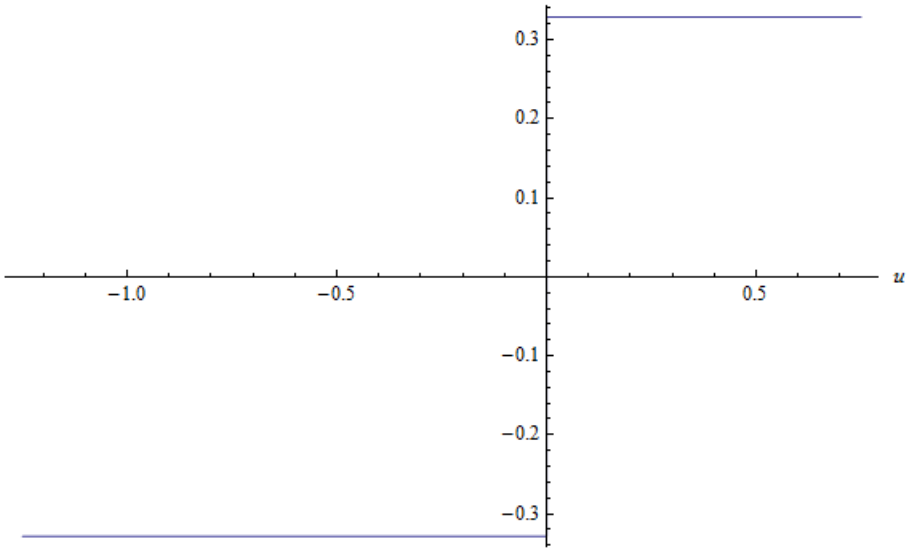

Figure 4.4: Graph of the function $h_1(u,0)$, as defined in (4.22), for $l=1, m=0$.

Similar comments can be made about the cases $l=0, m=1$. In the case $l=1, m=1$, we get results as for the other two cases but we have one more, interesting result along the bisector. Letting $v=u$ in (4.22), we get

$$h_1(u,u)=\frac{1}{\sqrt{14}}\left(|u|+\frac{1}{2}\frac{u}{|u|}\right), \quad u\neq 0. \tag{4.27}$$

We show the graph of this in Figure 4.5. This discontinuity is at least as nasty as the previous ones. We encounter the same behavior along u for $l=2, m=0$ and along v for $l=0, m=2$.

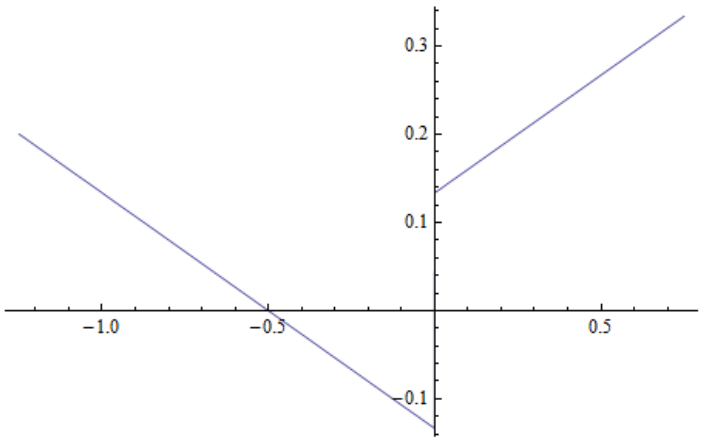

Figure 4.5: Graph of $h_1(u,u)$ for $l=1, m=1$.

So as not to crowd this section, we analyze the other two BQs of Section 3 in Appendix B. From the results there and the present analysis, we conclude that, when the OP is near or on the integration BQ, the singularity extraction technique is not sufficient if the first integral in (4.2) is to be computed in *pq*- or *uv*-coordinates. The one and only exception is when both *l* and *m* are equal to zero.

We next discuss the second method, that of a coordinate transformation. For simplicity, we concentrate on the transformation to polar coordinates ([3], [8]). If the OP lies on the integration BQ, this approach works very well. When, however, the OP is removed from the BQ, it becomes ineffective. In order to demonstrate our point, we use the second BQ of Section 3 and the point of (4.16). Using this point, we erect the normal along which we designate a distance *h* from the BQ. This is where the OP is located. We also introduce polar coordinates

$$u = \rho\cos\varphi\,, \quad v = \rho\sin\varphi\,; \quad \rho \geq 0\,, \quad 0 \leq \varphi < 2\pi \tag{4.28}$$

with *u* and *v* defined in (4.5). In Figs. 4.6.1 – 4.6.4, we plot the ratio ρ / R where *R* is the distance between the OP and the source (integration) point on the BQ. From these graphs, we see that the integrand is not very smooth near the origin. By switching to polar coordinates, we remove the (near-) singularity at the origin but we are still left with a function that is not easy to integrate to high accuracy.

To better grasp the behavior near the origin, we have also taken cuts along $u = 0$ and $v = 0$. We exhibit these graphs in Figs. 4.7.1 – 4.7.5. From the first four graphs, we see that, for *h* different from zero, we have continuity at the origin and the value there is zero. When $h = 0$, however, the limit at the origin does not exist, as we see from Figure 4.7.5. We see also that, the larger the *h* is (in absolute value), the more we have to worry about the accuracy of the result. As *h* gets small, the gap between the two sides of the curve diminishes dramatically, making the numerical evaluation easier. All in all, we conclude from this brief discussion that, even when we use polar coordinates, we have to be careful how we develop numerical integration algorithms. We note that an analytical evaluation cannot be performed on either the radial or the angular integral.

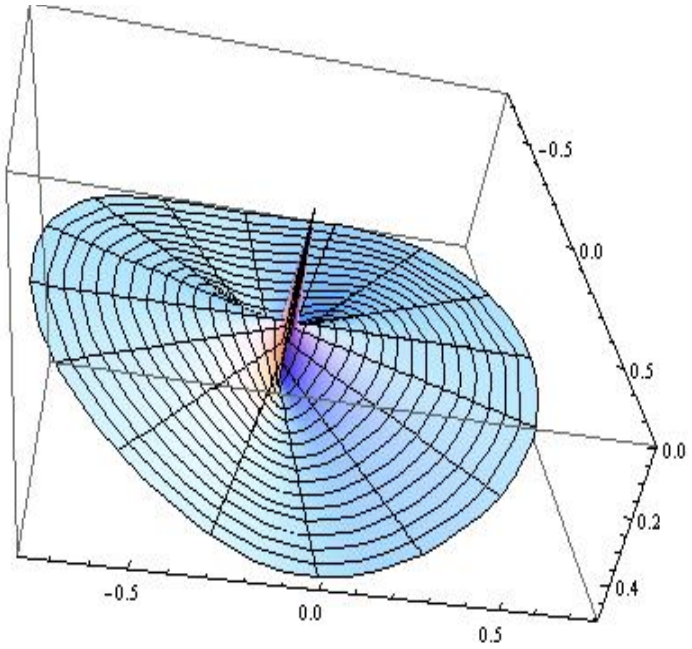

Figure 4.6.1. Graph of the integrand ρ / R for $h = 0.001$ about the origin for the second BQ of Section 3. The origin is the point (4.16). To better illustrate its properties, we show the graph in an upside-down position.

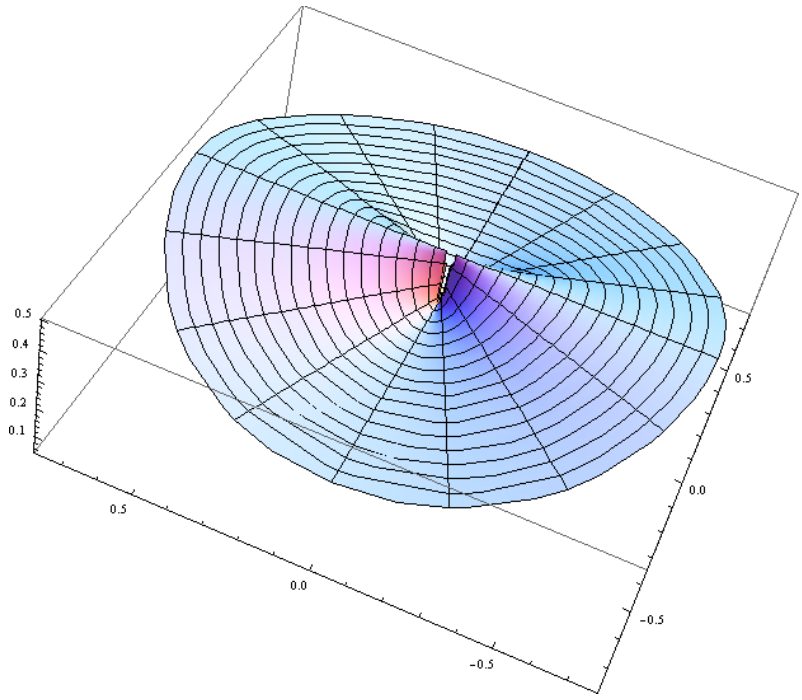

Figure 4.6.2. Graph of the integrand ρ / R for $h = 10^{-6}$ about the origin for the second BQ of Section 3. The origin is the point (4.16). If we turn this graph upside down, we get a figure that resembles Fig. 4.6.1. Conversely, if we turn Fig. 4.6.1 upside down, we get a figure that resembles the present one.

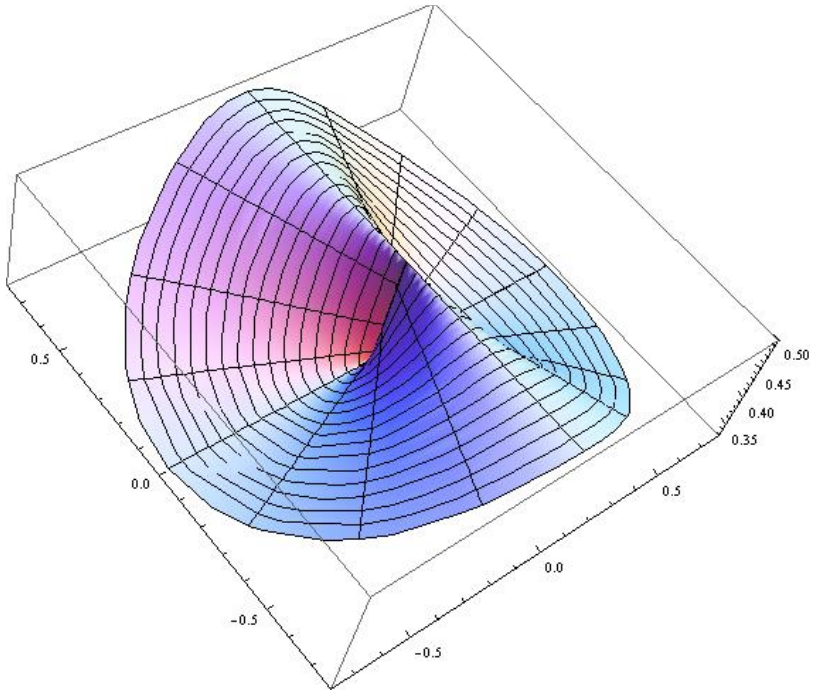

Figure 4.6.3. Graph of the integrand ρ / R for $h = 10^{-12}$ about the origin for the second BQ of Section 3. The origin is the point (4.16).

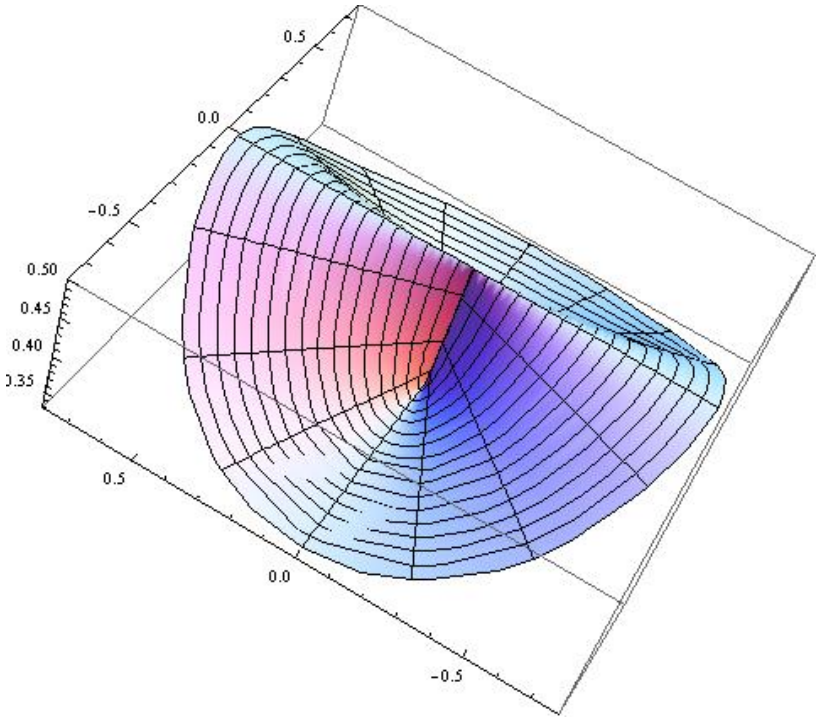

Figure 4.6.4. Graph of the integrand ρ / R for $h = 0.0$ about the origin for the second BQ of Section 3. The origin is the point (4.16).

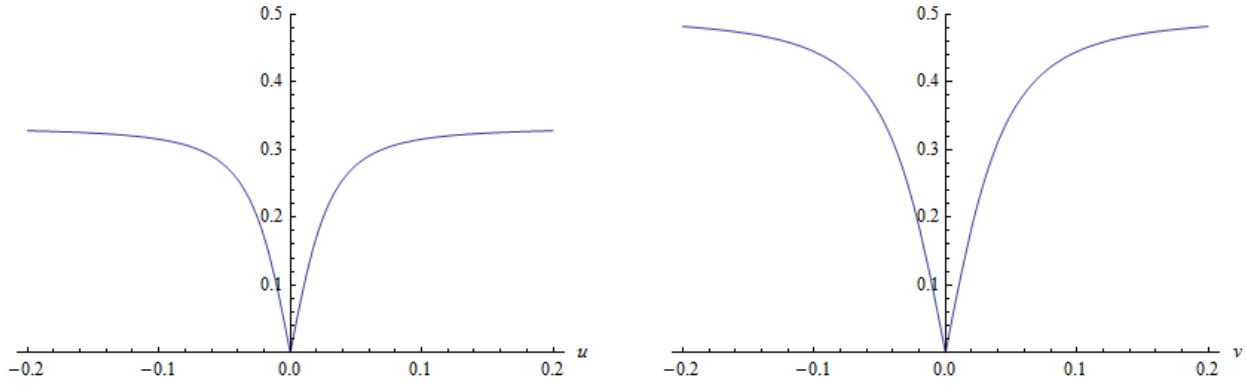

Figure 4.7.1. Graph of the integrand ρ / R for $h = 0.1$ along $v = 0$ (left) and $u = 0$ (right) for the second BQ of Section 3. The origin is the point (4.16).

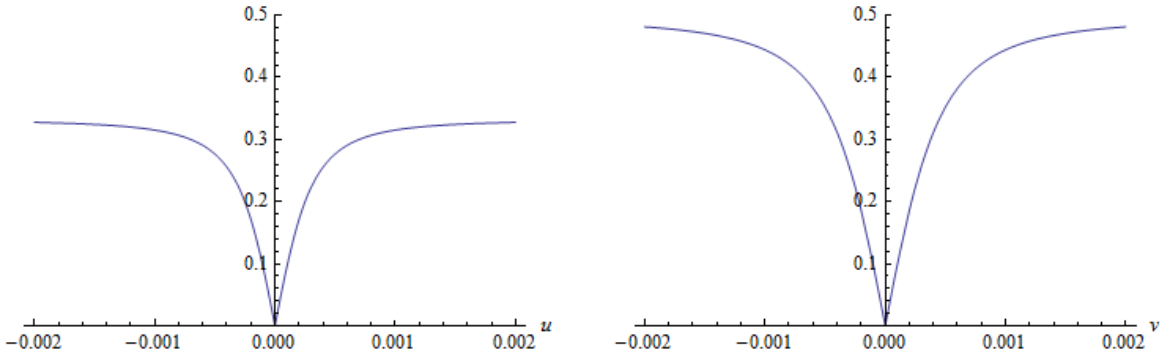

Figure 4.7.2. Graph of the integrand ρ / R for $h = 0.1$ along $v = 0$ (left) and $u = 0$ (right) for the second BQ of Section 3. The origin is the point (4.16).

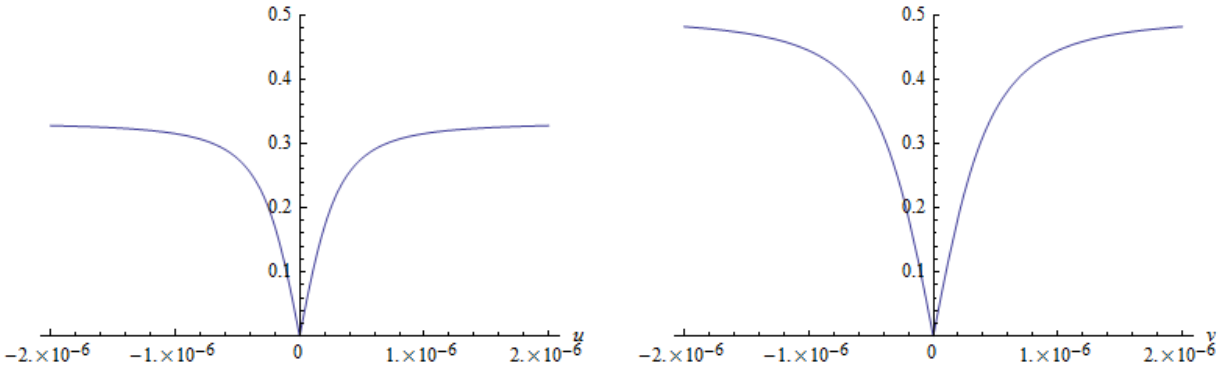

Figure 4.7.3. Graph of the integrand ρ / R for $h = 10^{-6}$ along $v = 0$ (left) and $u = 0$ (right) for the second BQ of Section 3. The origin is the point (4.16).

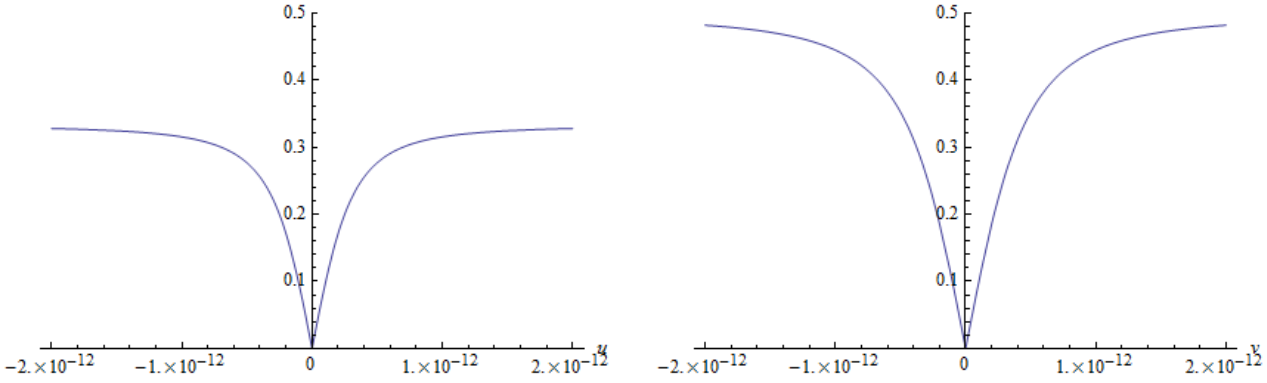

Figure 4.7.4. Graph of the integrand ρ / R for $h = 10^{-12}$ along $v = 0$ (left) and $u = 0$ (right) for the second BQ of Section 3. The origin is the point (4.16).

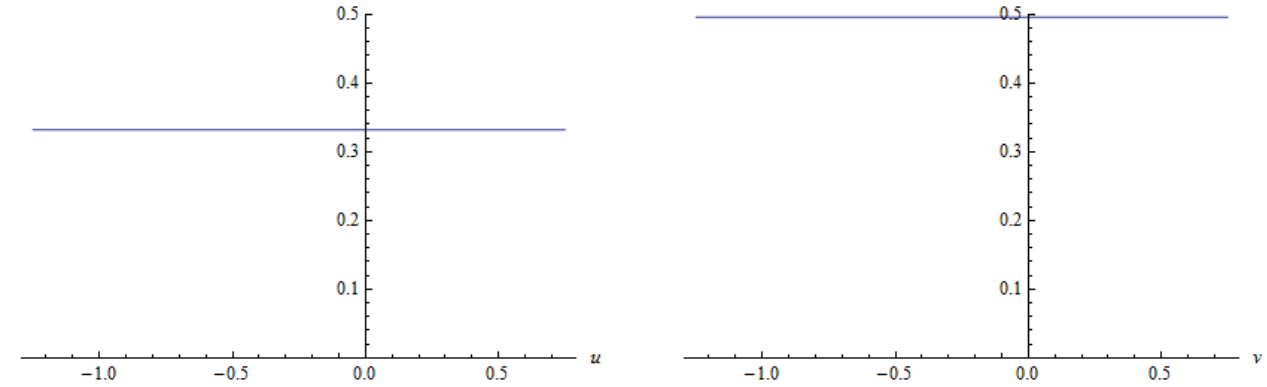

Figure 4.7.5. Graph of the integrand ρ / R for $h = 0.0$ along $v = 0$ (left) and $u = 0$ (right) for the second BQ of Section 3. The origin is the point (4.16).

The next question we may ask is: what if we use polar coordinates and the tangent-plane approximation? We employ (4.8) and compute the integrand $\rho\left((1/R)-(1/R_0)\right)$. We display the graph of this function in Figs. 4.8.1 – 4.8.5. We see that the graphs have no singularities and that they are relatively smooth; in fact, it appears that the smaller the h, the smoother the graph. Since the integral of $1 / R_0$ can be evaluated analytically, this approach may lead to good accuracies in computing (4.1). In the following sections, we propose an approach in rectangular coordinates that makes the use of the auxiliary tangent plane unnecessary.

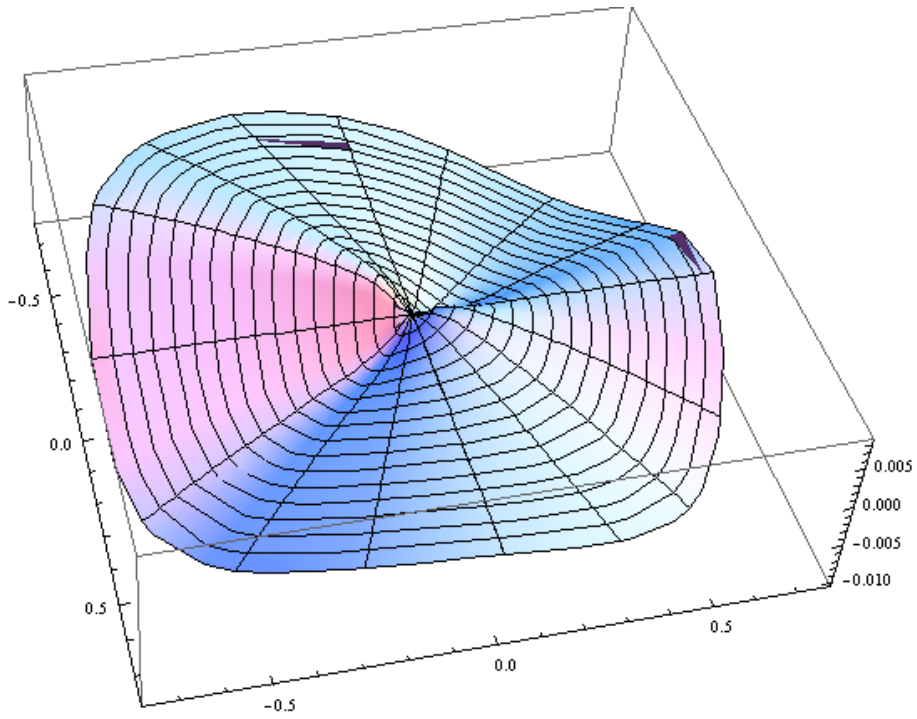

Figure 4.8.1. The integrand $\rho\left((1/R)-(1/R_0)\right)$ for the second BQ of Section 3 and for h = 0.1. The origin is the point (4.16).

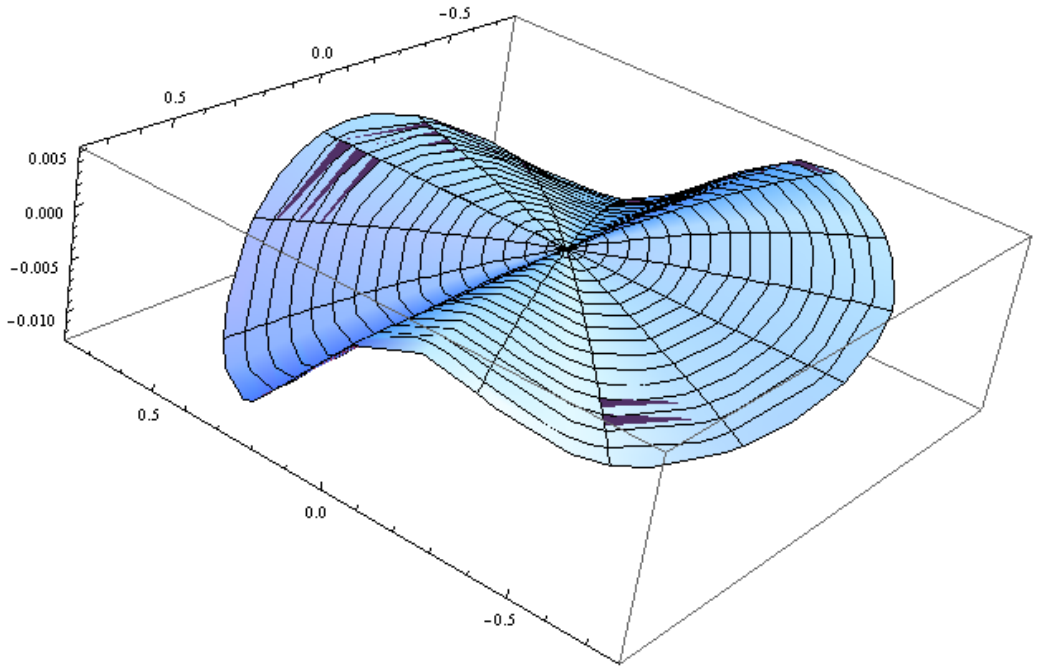

Figure 4.8.2. The integrand $\rho\left((1/R)-(1/R_0)\right)$ for the second BQ of Section 3 and for h = 0.001. The origin is the point (4.16).

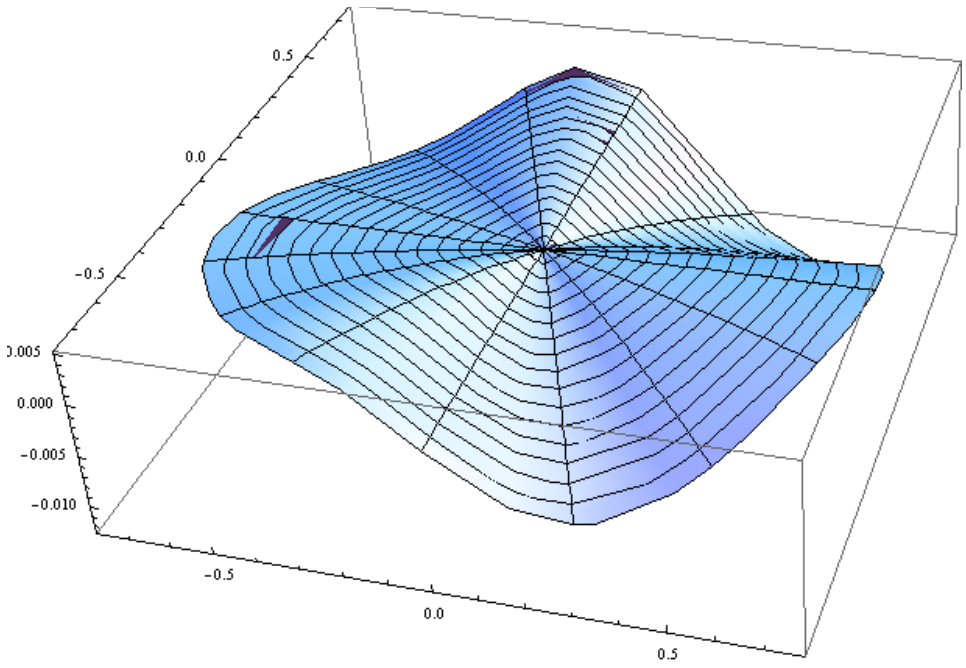

Figure 4.8.3. The integrand $\rho\left((1/R)-(1/R_0)\right)$ for the second BQ of Section 3 and for $h = 10^{-6}$. The origin is the point (4.16).

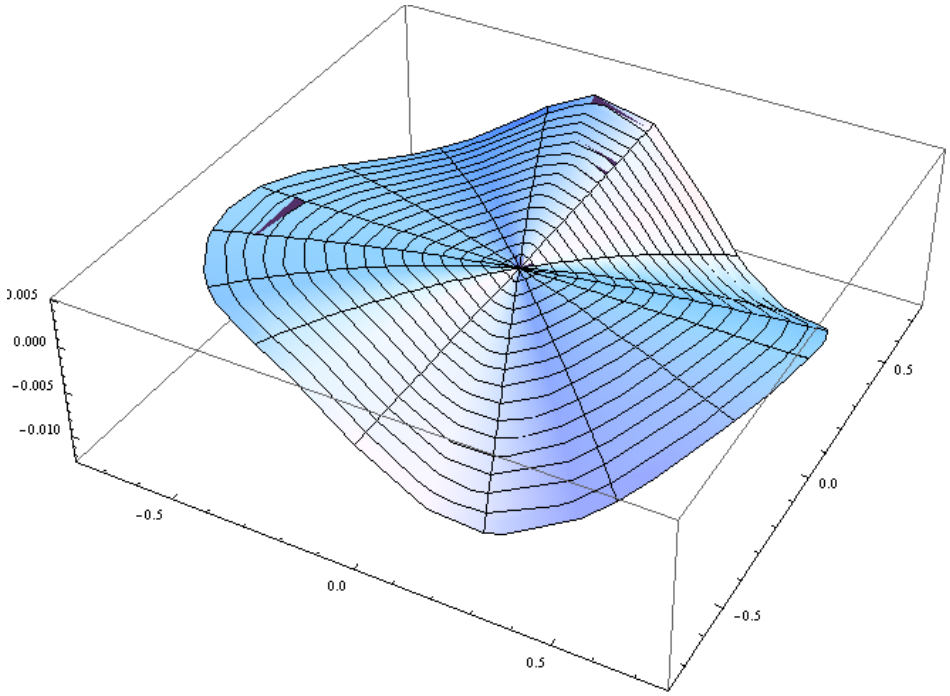

Figure 4.8.4. The integrand $\rho\left((1/R)-(1/R_0)\right)$ for the second BQ of Section 3 and for $h = 10^{-12}$. The origin is the point (4.16).

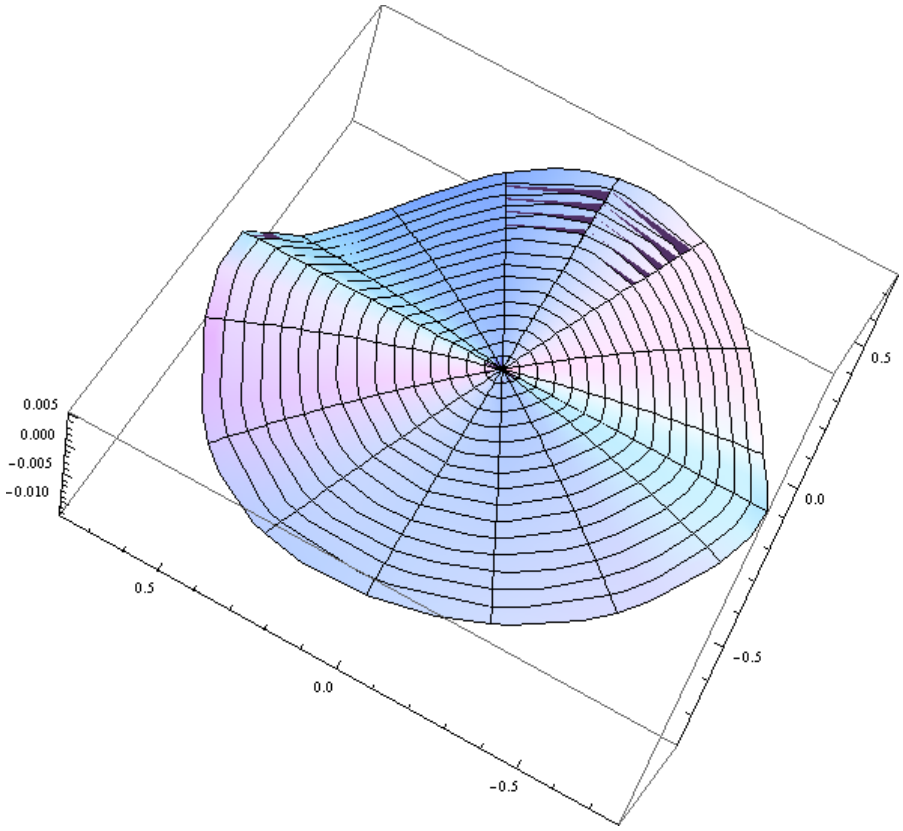

Figure 4.8.5. The integrand $\rho\left((1/R)-(1/R_0)\right)$ for the second BQ of Section 3 and for h = 0.0. The origin is the point (4.16).

THIS PAGE INTENTIONALLY LEFT BLANK

SECTION 5: EXAMINATION OF ORIGINAL INTEGRAL

In this section we take a closer look at the integral in (4.1). We show that we can split the integral into two parts: one with an analytical integrand and one with an integrable singularity. For the latter, we show that we can employ integration by parts to perform analytically the integration with respect to one of its variables, leaving an integral with respect to the other variable whose integrand contains at worst a logarithmic singularity. In subsequent sections, we will show that the remaining integral is computable to machine precision. We begin by re-writing (4.1) in the form

$$P_{lm} = \int_{-1}^{1}\int_{-1}^{1} p^l q^m \frac{\cos(kR)}{R}\,dpdq + ik\int_{-1}^{1}\int_{-1}^{1} p^l q^m \frac{\sin(kR)}{kR}\,dpdq\,, \quad l,m = 0,1,2,... \tag{5.1}$$

Since the function $\sin(x)/x$ can be computed to all available precision for any value of x, no matter how small, the integral of the imaginary part can be computed using established quadratures. Most of the contribution will come from the neighborhood of $R = 0$. We dispense then with the imaginary part of (5.1) and concentrate on the real part

$$\mathrm{Re}\{P_{lm}\} = \int_{-1}^{1}\int_{-1}^{1} p^l q^m \frac{\cos(kR)}{R}\,dpdq\,, \quad l,m = 0,1,2,... \tag{5.2}$$

The integrand has an integrable singularity when R is equal to zero or, for finite-precision arithmetic, in a neighborhood of it. Just as in Section 4, we assume that the OP is an interior point (p_0, q_0) of the BQ and employ the notation of (4.3) through (4.8). As we shall show below, the point can be anywhere on the BQ, including the BQ's boundary.

We proceed to work on (5.2) and write

$$\begin{aligned}
\mathrm{Re}\{P_{lm}\} &= \int_{-1}^{1}\int_{-1}^{1} p^l q^m \frac{\cos(kR)-1}{R}\,dpdq + \int_{-1}^{1}\int_{-1}^{1} \frac{p^l q^m}{R}\,dpdq \\
&= -2\int_{-1}^{1}\int_{-1}^{1} p^l q^m \frac{\sin^2(kR/2)}{R}\,dpdq + \int_{-1}^{1}\int_{-1}^{1} \frac{p^l q^m}{R}\,dpdq \\
&= -\frac{k}{2}\int_{-1}^{1}\int_{-1}^{1} p^l q^m (kR)\left[\frac{\sin(kR/2)}{kR/2}\right]^2 dpdq + \int_{-1}^{1}\int_{-1}^{1} \frac{p^l q^m}{R}\,dpdq
\end{aligned} \tag{5.3}$$

and substitute the result in (5.1)

$$P_{lm} = -\frac{k}{2}\int_{-1}^{1}\int_{-1}^{1} p^l q^m (kR)\left[\frac{\sin(kR/2)}{kR/2}\right]^2 dpdq + \int_{-1}^{1}\int_{-1}^{1} \frac{p^l q^m}{R}\,dpdq + ik\int_{-1}^{1}\int_{-1}^{1} p^l q^m \frac{\sin(kR)}{kR}\,dpdq$$

$$= ik\int_{-1}^{1}\int_{-1}^{1} p^l q^m \frac{\sin(kR/2)\cos(kR/2)}{kR/2}\,dpdq - \frac{k}{2}\int_{-1}^{1}\int_{-1}^{1} p^l q^m (kR)\left[\frac{\sin(kR/2)}{kR/2}\right]^2 dpdq + \int_{-1}^{1}\int_{-1}^{1} \frac{p^l q^m}{R}\,dpdq$$

$$= ik\int_{-1}^{1}\int_{-1}^{1} p^l q^m \left[\frac{\sin(kR/2)}{kR/2}\right]\left[\cos(kR/2)+i\sin(kR/2)\right]dpdq + \int_{-1}^{1}\int_{-1}^{1}\frac{p^l q^m}{R}dpdq \tag{5.4}$$

or

$$P_{lm} = ik\int_{-1}^{1}\int_{-1}^{1} p^l q^m \left[\frac{\sin(kR/2)}{kR/2}\right]e^{ikR/2}dpdq + \int_{-1}^{1}\int_{-1}^{1}\frac{p^l q^m}{R}dpdq\,, \quad l,m = 0,1,2,\ldots. \tag{5.5}$$

The first of these integrals has no singularity and can be evaluated numerically using standard methods. We note that the since function emphasizes the values of the integrand about $R = 0$ and de-emphasizes those away from it; moreover, the frequency has been cut in half, resulting in a less oscillatory integrand.

To work on the last integral, we need the expression for the distance function. We will assume that the OP projects to a point (p_0, q_0) of the BQ. From (2.23), the position vector to a point (p_0, q_0) of BQ is

$$\mathbf{r}(p,q) = \mathbf{r}_0 + \left(\mathbf{r}_p + \mathbf{r}_{pq}q_0\right)(p-p_0) + \left(\mathbf{r}_q + \mathbf{r}_{pq}p_0\right)(q-q_0) + \mathbf{r}_{pq}(p-p_0)(q-q_0). \tag{5.6}$$

Using (2.25), we can write this in the form

$$\mathbf{r}(p,q) = \mathbf{r}_0 + \mathbf{p}_0(p-p_0) + \mathbf{q}_0(q-q_0) + \mathbf{r}_{pq}(p-p_0)(q-q_0). \tag{5.7}$$

This is the IP on the BQ. The vectors p_0 and q_0 define a plane tangent to the BQ at the origin. We define the OP by

$$\mathbf{r}' = \mathbf{r}_0 + \frac{\mathbf{p}_0\times\mathbf{q}_0}{|\mathbf{p}_0\times\mathbf{q}_0|}h = \mathbf{r}_0 + \hat{n}h. \tag{5.8}$$

With (2.27), we can then write for the distance function,

$$\begin{aligned} R(u,v)^2 = |\mathbf{r}-\mathbf{r}'|^2 &= r^2 - 2\mathbf{r}\cdot\mathbf{r}' + r'^2 = \left|\mathbf{p}_0u + \mathbf{q}_0v + \mathbf{r}_{pq}uv\right|^2 - 2\left(\mathbf{p}_0u + \mathbf{q}_0v + \mathbf{r}_{pq}uv\right)\cdot\hat{n}h + h^2 \\ &= \left|\mathbf{p}_0u + \mathbf{q}_0v\right|^2 + \left|\mathbf{r}_{pq}\right|^2(uv)^2 + 2\left(\mathbf{p}_0u + \mathbf{q}_0v\right)\cdot\mathbf{r}_{pq}uv - 2\left(\mathbf{p}_0u + \mathbf{q}_0v + \mathbf{r}_{pq}uv\right)\cdot\hat{n}h + h^2. \end{aligned} \tag{5.9}$$

We return to the last integral in (5.5) and write for it

$$I(p_0,q_0,l,m) = \int_{-1}^{1}\int_{-1}^{1}\frac{p^l q^m}{R}dpdq\,, \quad l,m = 0,1,2,\ldots \tag{5.10}$$

With the transformation (2.27), we get integrals of the form

$$I(p_0,q_0,l,m) = \int_{-(1+q_0)}^{1-q_0}\int_{-(1+p_0)}^{1-p_0}\frac{u^l v^m}{R}dudv\,, \quad l,m = 0,1,2,\ldots \tag{5.11}$$

We show below how this double integral can be reduced to a single integral.

Case 1: $l = m = 0$.

$$I\left(p_0, q_0, 0, 0\right) = I = \int_{-(1+q_0)}^{1-q_0} \int_{-(1+p_0)}^{1-p_0} \frac{dudv}{R}. \tag{5.12}$$

The distance function, given by (5.9), can be considered as a second degree polynomial in u or in v. As such, one of the two integrals can be evaluated analytically ([13], p. 81, Formula 2.261). The resulting expression involves the logarithm of a complicated function of the remaining variable. This function goes to infinity when the remaining variable is zero and as h tends to zero. We shall study this integral in detail in subsequent sections. As an example, we consider the distance as a function of u. From (5.9), we write

$$R(u,v) = \sqrt{C^2(v)u^2 + B(v,h)u + A(v,h)}, \quad C(v) > 0 \tag{5.13}$$

where

$$A(v,h) = \left|\mathbf{q}_0\right|^2 v^2 + h^2, \quad B(v,h) = 2\left[\mathbf{q}_0 \cdot \left(\mathbf{p}_0 + \mathbf{r}_{pq} v\right) - \hat{n} \cdot \mathbf{r}_{pq} h\right] v, \quad C(v) = \left|\mathbf{p}_0 + \mathbf{r}_{pq} v\right|. \tag{5.14}$$

If we integrate (5.12) with respect to u, we get

$$I = \int_{-(1+q_0)}^{1-q_0} \ln\left|\frac{2C(v)R(1-p_0,v) + 2C^2(v)(1-p_0) + B(v,h)}{2C(v)R\left(-(1+p_0),v\right) - 2C^2(v)(1+p_0) + B(v,h)}\right| \frac{dv}{C(v)}. \tag{5.15}$$

We can easily verify that the denominator of the logarithmic argument becomes zero at $v = 0$ and $h = 0$. The numerator becomes zero when $p_0 = 1$ and v and h are both zero.

Case 2: $l = 0$, $m = 1$.

$$I\left(p_0, q_0, 0, 1\right) = \int_{-(1+q_0)}^{1-q_0} v dv \int_{-(1+p_0)}^{1-p_0} \frac{du}{R} \tag{5.16}$$

In this case, we proceed as in Case 1 to get the same expression as in (5.15) but with the integrand multiplied by v. The limit for the integrand as v tends to zero and $h = 0$ now exists and is zero. Thus, in the numerical evaluation of the outer integral in (5.16), all we need do is to define the value of the integrand at zero to be zero. If $l = 0$ and $m = 1$, then we consider the integral with respect to v as the inner integral and proceed as above.

Case 3: $l \geq 1, m \geq l$.

The integral is

$$I(p_0,q_0,l,m) = \int_{-(1+q_0)}^{1-q_0} dv v^m \int_{-(1+p_0)}^{1-p_0} \frac{u^l}{\sqrt{C^2(v)u^2 + B(v,h)u + A(v,h)}} du$$
$$= \frac{1}{2}\int_{-(1+q_0)}^{1-q_0} dv \frac{v^m}{C^2(v)} \int_{-(1+p_0)}^{1-p_0} \frac{u^{l-1}\left[2C^2(v)u + B(v,h)\right]}{\sqrt{C^2(v)u^2 + B(v,h)u + A(v,h)}} du$$
$$-\frac{1}{2}\int_{-(1+q_0)}^{1-q_0} dv \frac{v^m B(v,h)}{C^2(v)} \int_{-(1+p_0)}^{1-p_0} \frac{u^{l-1}}{\sqrt{C^2(v)u^2 + B(v,h)u + A(v,h)}} du . \quad (5.17)$$

For the first inner integral on the right-hand side, we can write

$$I_1(p_0,q_0,l) = \frac{1}{2}\int_{-(1+p_0)}^{1-p_0} \frac{u^{l-1}\left[2C^2(v)u + B(v,h)\right]}{\sqrt{C^2(v)u^2 + B(v,h)u + A(v,h)}} du = u^{l-1}R(u,v)\Big|_{u=-(1+p_0)}^{u=1-p_0}$$
$$-(l-1)\int_{-(1+p_0)}^{1-p_0} u^{l-2}\sqrt{C^2(v)u^2 + B(v,h)u + A(v,h)}\,du . \quad (5.18)$$

The last integral in this expression can be evaluated using the recursion formulas in Gradshteyn and Ryzhik ([13], Section 2.26, p. 81). From ([13], Formula 2.260.1, p. 81), we have that

$$\int_{-(1+p_0)}^{1-p_0} u^{l-2}R(u,v)\,du = \frac{u^{l-3}R^3}{lC^2(v)}\Big|_{u=-(1+p_0)}^{u=1-p_0} - \frac{(2l-3)B(v,h)}{2lC^2(v)}\int_{-(1+p_0)}^{1-p_0} u^{l-3}R(u,v)\,du$$
$$-\frac{(l-3)A(v,h)}{lC^2(v)}\int_{-(1+p_0)}^{1-p_0} u^{l-4}R(u,v)\,du . \quad (5.19)$$

If we use this formula repeatedly, we end up with a number of rational functions of *v*, with no poles in the interval of integration, and an integral of the distance function multiplied by a rational function of *v*. From ([13], Formula 2.262.1, p. 82), we have that

$$\int_{-(1+p_0)}^{1-p_0} R(u,v)\,du = \frac{\left[2C^2(v)u + B(v,h)\right]}{4C^2(v)}R(u,v)\Big|_{u=-(1+p_0)}^{u=1-p_0} + \frac{4A(v,h)C^2(v) - B^2(v,h)}{8C^2(v)}\int_{-(1+p_0)}^{1-p_0} \frac{du}{R(u,v)} \quad (5.20)$$

We will show how to compute the last integral in the next section.

For the inner integral of the second integral on the right-hand side of (5.16), we see that we have an integrand of exactly the same form as the integral we started with, except that the power of u has been reduced by one. We can then apply the same rule to this integral.

If $m > 1$ and $l \geq m$, then we consider the integral with respect to v as the inner integral and proceed as above. In conclusion, we see that the integral we must study is the integral $I(p_0, q_0, 0,0)$ in (5.12). We proceed to do that in the next section.

THIS PAGE INTENTIONALLY LEFT BLANK

SECTION 6: EVALUATION OF THE INTEGRAL OF 1/*R* IN RECTANGULAR COORDINATES

As we demonstrated in the last section, the integral in (5.11) can be reduced to a number of well-behaved single integrals and an integral of the form

$$I = \int_{-1-q_0}^{1-q_0} dv \int_{-1-p_0}^{1-p_0} \frac{du}{R(u,v)}. \tag{6.1}$$

We have omitted from the integrand a function of v that is at least continuous since its presence or absence does not affect our argument. We examine here how well we can compute this integral. From (5.7) and (5.8), we have that

$$R(u,v) = |\mathbf{r} - \mathbf{r}'|, \quad \mathbf{r} = \mathbf{r}_0 + \mathbf{p}_0 u + \mathbf{q}_0 v + \mathbf{r}_{pq} uv, \quad \mathbf{r}' = \mathbf{r}_0 + \frac{\mathbf{p}_0 \times \mathbf{q}_0}{|\mathbf{p}_0 \times \mathbf{q}_0|} h = \mathbf{r}_0 + \hat{n}h. \tag{6.2}$$

The definitions of the various symbols are as in (2.23) and the equations following it. The IP is **r** while the OP is **r**´. The OP is near the BQ and projects to a point of the BQ that corresponds to the point (p_0, q_0). This point is the new origin of rectangular coordinates (u, v).

We consider now the inner integral

$$I_u = \int_{-1-p_0}^{1-p_0} \frac{du}{R(u,v)} \tag{6.3}$$

For the distance function, we write

$$\begin{aligned} R^2(u,v) &= |\mathbf{r}|^2 - 2\mathbf{r}\cdot\mathbf{r}' + |\mathbf{r}'|^2 = |\mathbf{p}_0 u + \mathbf{q}_0 v|^2 + 2(\mathbf{p}_0 u + \mathbf{q}_0 v)\cdot\mathbf{r}_{pq} uv + |\mathbf{r}_{pq}|^2 (uv)^2 - 2\mathbf{r}_{pq}\cdot\hat{n}huv + h^2 \\ &= |\mathbf{p}_0|^2 u^2 + 2\mathbf{p}_0\cdot\mathbf{q}_0 uv + |\mathbf{q}_0|^2 v^2 + 2(\mathbf{p}_0 u + \mathbf{q}_0 v - \hat{n}h)\cdot\mathbf{r}_{pq} uv + |\mathbf{r}_{pq}|^2 (uv)^2 + h^2 \\ &= \left(|\mathbf{p}_0|^2 + 2\mathbf{p}_0\cdot\mathbf{r}_{pq} v + |\mathbf{r}_{pq}|^2 v^2\right) u^2 + 2\left[\mathbf{p}_0\cdot\mathbf{q}_0 + (\mathbf{q}_0 v - \hat{n}h)\cdot\mathbf{r}_{pq}\right] vu + |\mathbf{q}_0|^2 v^2 + h^2 \\ &= |\mathbf{p}_0 + \mathbf{r}_{pq} v|^2 u^2 + 2\left[\mathbf{q}_0\cdot(\mathbf{p}_0 + \mathbf{r}_{pq} v) - \hat{n}\cdot\mathbf{r}_{pq} h\right] vu + |\mathbf{q}_0|^2 v^2 + h^2 \end{aligned} \tag{6.4}$$

or

$$R(u,v) = \sqrt{|\mathbf{p}_0 + \mathbf{r}_{pq} v|^2 u^2 + 2\left[\mathbf{q}_0\cdot(\mathbf{p}_0 + \mathbf{r}_{pq} v) - \hat{n}\cdot\mathbf{r}_{pq} h\right] vu + |\mathbf{q}_0|^2 v^2 + h^2}. \tag{6.5}$$

We let

$$A(v,h) = |\mathbf{q}_0|^2 v^2 + h^2, \quad B(v,h) = 2\left[\mathbf{q}_0\cdot(\mathbf{p}_0 + \mathbf{r}_{pq} v) - \hat{n}\cdot\mathbf{r}_{pq} h\right] v, \quad C(v) = |\mathbf{p}_0 + \mathbf{r}_{pq} v|. \tag{6.6}$$

We assume that C is different from zero and apply the Euler transformation ([13], p. 80)

$$R = \sqrt{C^2u^2 + Bu + A} = t - Cu\,. \tag{6.7}$$

We square both sides and solve for u

$$u = \frac{t^2 - A}{B + 2Ct}\,. \tag{6.8}$$

From this

$$du = \frac{2t\left(B + 2Ct\right) - 2C\left(t^2 - A\right)}{\left(B + 2Ct\right)^2}dt = 2\frac{Ct^2 + Bt + CA}{\left(B + 2Ct\right)^2}dt \tag{6.9}$$

and

$$\frac{du}{R} = \frac{1}{t - Cu}2\frac{Ct^2 + Bt + CA}{\left(B + 2Ct\right)^2}dt = \frac{2}{t - C\dfrac{t^2 - A}{B + 2Ct}}\frac{Ct^2 + Bt + CA}{\left(B + 2Ct\right)^2}dt = \frac{2dt}{B + 2Ct}\,. \tag{6.10}$$

Applying the transformation to (6.3), we get that

$$\begin{aligned} I_u &= \int_{\sqrt{C^2(1+p_0)^2 - B(1+p_0) + A} - C(1+p_0)}^{\sqrt{C^2(1-p_0)^2 + B(1-p_0) + A} + C(1-p_0)} \frac{2dt}{B + 2Ct} = \frac{1}{C}\ln\left|2Ct + B\right|\Bigg|_{\sqrt{C^2(1+p_0)^2 - B(1+p_0) + A} - C(1+p_0)}^{\sqrt{C^2(1-p_0)^2 + B(1-p_0) + A} + C(1-p_0)} \\ &= \frac{1}{C}\ln\left|\frac{2C\left[\sqrt{C^2\left(1 - p_0\right)^2 + B\left(1 - p_0\right) + A} + C\left(1 - p_0\right)\right] + B}{2C\left[\sqrt{C^2\left(1 + p_0\right)^2 - B\left(1 + p_0\right) + A} - C\left(1 + p_0\right)\right] + B}\right|. \end{aligned} \tag{6.11}$$

In place of the double integral in (6.1), we now have a single integral with a more complicated integrand

$$I = \int_{-1-q_0}^{1-q_0} \ln\left|\frac{2C\left(v\right)\left[R\left(1 - p_0, v\right) + C\left(v\right)\left(1 - p_0\right)\right] + B\left(v,h\right)}{2C\left(v\right)\left[R\left(-\left(1 + p_0\right), v\right) - C\left(v\right)\left(1 + p_0\right)\right] + B\left(v,h\right)}\right|\frac{dv}{C\left(v\right)} \tag{6.12}$$

where A, B, and C are given by (6.6).

We note that the denominator of the fraction in the algorithm's argument is equal to zero when h and v are both zero. The numerator, however, is a positive number for these values, as we will show at the end of this section. We thus have a logarithmic singularity at the origin when h

is equal to zero and the integrand goes to infinity at this point. We turn to the second BQ of Section 3 and use it to test how well Mathematica's numerical subroutines can handle the integral in (6.12). The value of p_0 and q_0 is as in (4.16). From (B.2), and omitting the constant vector, we find that the IP is

$$\mathbf{r}(u,v)=\left(3,0,\frac{1}{4}\right)u+\left(0,2,\frac{1}{4}\right)v+(0,0,1)uv \tag{6.13}$$

from which we find that the unit normal at the origin is

$$\hat{n}=\frac{\left(3,0,\frac{1}{4}\right)\times\left(0,2,\frac{1}{4}\right)}{\left|\left(3,0,\frac{1}{4}\right)\times\left(0,2,\frac{1}{4}\right)\right|}=\frac{-2\hat{x}-3\hat{y}+24\hat{z}}{\sqrt{589}}. \tag{6.14}$$

From (6.6) and (6.13),

$$A=\frac{65}{16}v^2+h^2,\quad B=\left(v+\frac{1}{4}-\frac{96}{\sqrt{589}}h\right)\frac{v}{2},\quad C=\sqrt{9+\left(v+\frac{1}{4}\right)^2}. \tag{6.15}$$

We substitute these results in the integrand of (6.12). In Figure 6.1, we display the graph of the integrand as a function of v over the range of integration, [-1.25, 0.75], for three values of h. We see that, as h tends to zero, we do get the logarithmic singularity mentioned above. In terms of numerical integration, this tells us that we have a singularity-type behavior at the origin not only when $h = 0$ but also when h is a small, non-zero number.

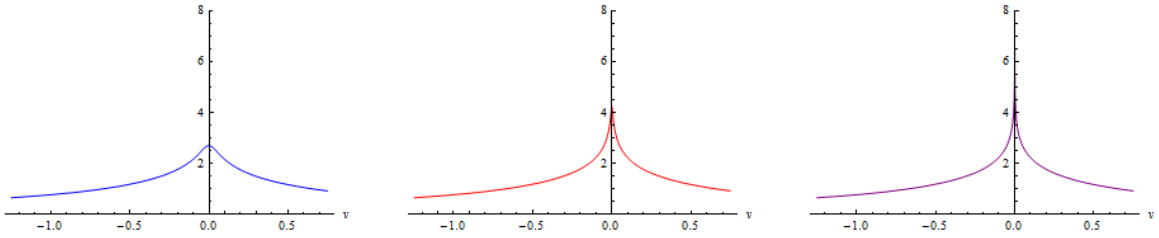

Figure 6.1. The integrand of (6.12) for the second BQ (*i.e.*, with (6.15) substituted in it) as a function of v over the range of integration. From left to right: $h = 0.1, 0.01, 0.00$. Though it is not clear from this picture, the function is singular at the origin when $h = 0$.

We have used two numerical integration routines in Mathematica [11] to compute (6.12) as a function of h. The first method is the GKQ ([14], p. 106) while the second method is the DEQ [15], ([14], p. 214) which is also known as the TSQ. We exhibit typical results in Table 6.1.1 and 6.1.2. For each of these methods, Mathematica allows the specification of singular and nearly singular points. In the present case, we have one such point. It is the origin when h is equal to zero or close to it. The designation "with" means that we have specified this point in Mathematica,

while the designation "w/out" means that we have not. We set the maximum number of recursive subdivisions of the integration interval to 12 (MaxRecursion → 12). We also record the execution time in CPU sec and the maximum number of SD we were able to get from each method. It is clear that specifying the (near) singularity reduces execution time by about an order of magnitude. It also provides more SD. We also see that GKQ is faster than the double exponential method but the latter provides more SD. Whether the extra SD are worth the time expense depends on the application. Finally, in Figure 6.2, we display the graph of the integral in (6.12) as a function of *h*. Although the integral appears to be an even function of *h*, it is not. This is because the BQ is not flat, the only time this property would hold. Simply put, the distance from $\hat{n}h$ to a point on the BQ is not the same as the distance from $-\hat{n}h$ to the same point. From these two tables, we also note that if single precision (SP) is desired, then these algorithms do provide that.

A note of caution: the CPU times are given for the purpose of comparison only, as for example specifying the singular point vs. not specifying it. The computer on which we ran these calculations is a laptop with a first-generation Intel i7 CPU.

Table 6.1.1. The value of the integral in (6.12) for five values of *h* calculated using GKQ with and without specifying the singular point. The execution time is in CPU seconds. We also display the maximum number of SD obtainable from each method. Second BQ. Singular or nearly singular point at ($p_0 = q_0 = 0.25$).

	GKQ w/out			GKQ with		
h	Value	Time	SD	Value	Time	SD
1.00E-01	2.6488500450514	0.437	14	2.6488500450514	0.031	14
1.00E-04	2.74952	0.109	6	2.74951658706	0.047	12
1.00E-08	2.7496	0.109	5	2.7496197	0.016	8
1.00E-12	2.7496	0.141	5	2.7496196	0.015	8
0.00E+00	2.7496	0.109	5	2.7496196	0.031	8

Table 6.1.2. The value of the integral in (6.12) for five values of *h* calculated using DEQ with and without specifying the singular point. The execution time is in CPU seconds. We also display the maximum number of SD obtainable from each method. Second BQ. Singular or nearly singular point at ($p_0 = q_0 = 0.25$).

	DEQ w/out			DEQ with		
h	Value	Time	SD	Value	Time	SD
1.00E-01	2.6488500450514	0.53	14	2.6488500450514	0.032	14
1.00E-04	2.7495	5.35	5	2.7495165870543	0.358	14
1.00E-08	2.7496	5.289	5	2.749619652	1.201	10
1.00E-12	2.7496	5.351	5	2.74961965	0.031	9
0.00E+00	2.7496	5.024	5	2.74961965	0.031	9

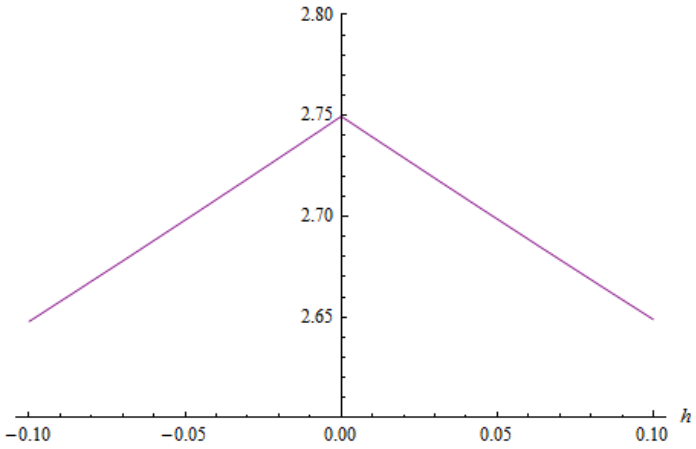

Figure 6.2: Integral in (6.12) as a function of *h*.

We turn now to the third BQ of Section 3. From (B.18), we have that

$$\mathbf{r}(u,v) = (3,0,2.5)u + (0,2,2.5)v + (0,0,10)uv \tag{6.16}$$

so that

$$\hat{n} = \frac{\left(3,0,\frac{10}{4}\right)\times\left(0,2,\frac{10}{4}\right)}{\left|\left(3,0,\frac{10}{4}\right)\times\left(0,2,\frac{10}{4}\right)\right|} = \frac{-20\hat{x} - 30\hat{y} + 24\hat{z}}{\sqrt{1876}} \tag{6.17}$$

and

$$A = \frac{41}{4}v^2 + h^2\,, \quad B = 5\left[10v + \frac{10}{4} - \frac{96}{\sqrt{1876}}h\right]v\,, \quad C = \sqrt{9 + (10v + 2.5)^2}\,. \tag{6.18}$$

We substitute these results in the integrand of (6.12). In Figure 6.3, we display the graph of the integrand as a function of *v* over the range of integration, [-1.25, 0.75], for three values of *h*. The behavior is the same as for the second BQ. We also compute the integral in (6.12) and form Tables 6.2, tables analogous to Tables 6.1. The conclusions we draw from the new tables are the same as those for Tables 6.1. If we need more than SP, a straight-forward numerical evaluation of the integral in (6.12) is not sufficient. In the next section, we proceed to re-write this integral so as to make it computable to machine (double) precision.

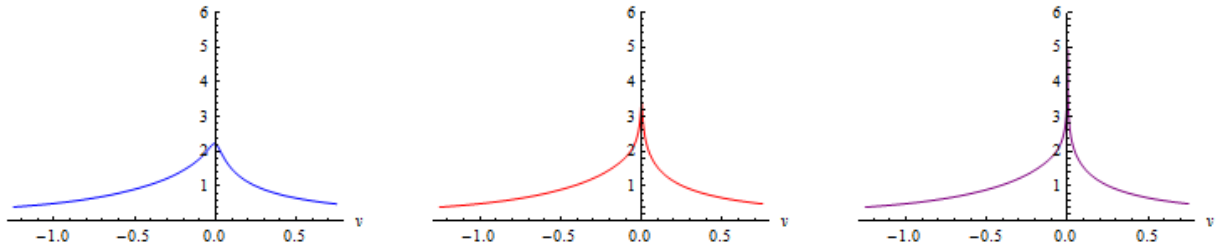

Figure 6.3. The integrand of (6.12) for the third BQ (*i.e.*, with (6.18) substituted in it) as a function of v over the range of integration. From left to right: $h = 0.1, 0.01, 0.00$. Though it is not clear from this picture, the function is singular at the origin when $h = 0$.

Table 6.2.1. The value of the integral in (6.12) for five values of h calculated using GKQ with and without specifying the singular point. The execution time is in CPU seconds. We also display the maximum number of SD obtainable from each method. Third BQ. Singular or nearly singular point at ($p_0 = q_0 = 0.25$).

	GKQ w/out			GKQ with		
h	Value	Time	SD	Value	Time	SD
1.00E-01	1.8704724171441	0.453	14	1.8704724171441	0.016	14
1.00E-04	1.92438	0.109	6	1.92437645094	0.031	12
1.00E-08	1.9244	0.125	5	1.9244343	0.031	8
1.00E-12	1.9244	0.156	5	1.9244343	0.015	8
0.00E+00	1.9244	0.094	5	1.9244343	0.032	8

Table 6.2.2. The value of the integral in (6.12) for five values of h calculated using DEQ with and without specifying the singular point. The execution time is in CPU seconds. We also display the maximum number of SD obtainable from each method. Third BQ. Singular or nearly singular point at ($p_0 = q_0 = 0.25$).

	DEQ w/out			DEQ with		
h	Value	Time	SD	Value	Time	SD
1.00E-01	1.8704724171441	0.655	14	1.8704724171441	0.015	14
1.00E-04	1.9244	5.445	5	1.92437645094	0.187	13
1.00E-08	1.9244	5.429	5	1.924434344	0.640	10
1.00E-12	1.9244	5.507	5	1.92443434	0.062	9
0.00E+00	1.9244	5.116	5	1.92443434	0.047	9

Before proceeding further, we point out that we can also reverse the order of integration in (6.1) and integrate first with respect to *v*. In this case, we get

$$I = \int_{-1-p_0}^{1-p_0} \ln \left| \frac{2F(u)\left[\sqrt{F(u)^2(1-q_0)^2 + E(u,h)(1-q_0) + D(u,h)} + F(u)(1-q_0)\right] + E(u,h)}{2F(u)\left[\sqrt{F(u)^2(1+q_0)^2 - E(u,h)(1+q_0) + D(u,h)} - F(u)(1+q_0)\right] + E(u,h)} \right| \frac{du}{F(u)} \tag{6.19}$$

where

$$D(u,h) = |\mathbf{p}_0|^2 u^2 + h^2\,, \quad E(u,h) = 2\left[\mathbf{p}_0 \cdot (\mathbf{q}_0 + \mathbf{r}_{pq}u) - h\hat{n}\cdot\mathbf{r}_{pq}\right]u\,, \quad F(u) = |\mathbf{q}_0 + \mathbf{r}_{pq}u|\,. \tag{6.20}$$

Using (6.19) is advantageous when the power *m* in the last integral in (5.3) is smaller than the power *l*.

Before leaving this section, we remark that the numerator in (6.12) becomes zero only when the singular point is an edge point of the BQ. The proof is as follows. Setting the numerator equal to zero, we have that

$$\sqrt{C^2(1-p_0)^2 + B(1-p_0) + A} = -\frac{B}{2C} - C(1-p_0)\,. \tag{6.21}$$

If $p_0 = 1$, an edge point, then we have that

$$\sqrt{A} = -\frac{B}{2C}\,. \tag{6.22}$$

From (6.6), this can be satisfied if, and only if, $v = h = 0$.

If $p_0 < 1$, then, squaring both sides of (6.21), we get

$$A = \left(\frac{B}{2C}\right)^2\,. \tag{6.23}$$

From (6.21) we have that

$$\frac{B}{2C} + C(1-p_0) \le 0\,. \tag{6.24}$$

Substituting (6.23) in this, we get

$$\sqrt{A} + C(1-p_0) \le 0 \tag{6.25}$$

which, by (6.6), becomes

$$\sqrt{\left|\mathbf{q}_0\right|^2 v^2 + h^2} + \left|\mathbf{p}_0 + \mathbf{r}_{pq} v\right| (1 - p_0) \le 0 . \tag{6.26}$$

This expression can never be negative. For it to be zero, both terms must be equal to zero. The first term is equal to zero when both *v* and *h* are equal to zero; the second, however, is not. The second term becomes zero when

$$v = \frac{-\left(\mathbf{p}_0 \cdot \mathbf{r}_{pq}\right) \pm \sqrt{\left(\mathbf{p}_0 \cdot \mathbf{r}_{pq}\right)^2 - \left|\mathbf{p}_0\right|^2 \left|\mathbf{r}_{pq}\right|^2}}{\left|\mathbf{r}_{pq}\right|^2} . \tag{6.27}$$

The value of *v* here is real only when the two vectors are collinear; in this case,

$$v = -\frac{\left(\mathbf{p}_0 \cdot \mathbf{r}_{pq}\right)}{\left|\mathbf{r}_{pq}\right|^2} \tag{6.28}$$

which makes the second term in (6.26) equal to zero but not the first.

SECTION 7: EVALUATION OF THE INTEGRAL IN (6.12)

In this section we develop a procedure for evaluating the integral in (6.12) to machine (double) precision.

As we showed at the end of Section 6, the numerator of the logarithmic argument in (6.12) is never equal to zero for interior singular points and, hence, it presents no computational difficulties. For this reason, we re-write (6.12) in the form

$$I = \int_{-1-q_0}^{1-q_0} \ln\left|2C(v)\left[R(1-p_0,v)+C(v)(1-p_0)\right]+B(v,h)\right|\frac{dv}{C(v)}$$
$$-\int_{-1-q_0}^{1-q_0} \ln\left|2C(v)\left[R(-(1+p_0),v)-C(v)(1+p_0)\right]+B(v,h)\right|\frac{dv}{C(v)} = I_1 - I_2 \qquad (7.1)$$

where $R(u, v)$ is defined in (6.2). We can evaluate the first integral numerically using either of the two methods of Section 6. The term in the square brackets in the second integral may become unstable when both v and h are close to zero for, in such a case, it represents the difference of two almost identical numbers. In Tables 7.1.1 and 7.1.2, we have computed these terms and their difference at $v = 0$. We note that, as h gets smaller, the value of R approaches that of $(1+p_0)C(v)$ (which is independent of h) so that their difference is correct to very few digits. This happens not only at $v = 0$ but in an entire neighborhood of the origin. The BQs we used are the second and third ones of Section 3 and the BQ point is (0.25, 0.25).

Table 7.1.1. The terms in square brackets in the second integrand of (7.1) for $v = 0$ and for the second BQ. As h tends to zero, the difference between the two terms loses accuracy and tends to zero, which is the wrong answer if h is different from zero.

h	$R(-(1+p_0),v)$	$(1+p_0)C(v)$	Difference
1.0E-01	3.76432679904389E+00	3.76299830587259E+00	1.32849317129535E-03
1.0E-04	3.76299830720132E+00	3.76299830587259E+00	1.32872779445847E-09
1.0E-08	3.76299830587259E+00	3.76299830587259E+00	0.00000000000000E+00
1.0E-12	3.76299830587259E+00	3.76299830587259E+00	0.00000000000000E+00
1.0E-16	3.76299830587259E+00	3.76299830587259E+00	0.00000000000000E+00

Table 7.1.2. The terms in square brackets in the second integrand of (7.1) for $v = 0$ and for the third BQ. As h tends to zero, the difference between the two terms loses accuracy and tends to zero, which is the wrong answer if h is different from zero.

h	$R(-(1+p_0),v)$	$(1+p_0)C(v)$	Difference
1.0E-01	4.88243023503665E+00	4.88140604744166E+00	1.02418759498679E-03
1.0E-04	4.88140604846595E+00	4.88140604744166E+00	1.02429531523285E-09
1.0E-08	4.88140604744166E+00	4.88140604744166E+00	0.00000000000000E+00
1.0E-12	4.88140604744166E+00	4.88140604744166E+00	0.00000000000000E+00
1.0E-16	4.88140604744166E+00	4.88140604744166E+00	0.00000000000000E+00

We correct for this as follows. We let

$$g(v,h) = 2C(v)\left[R(-(1+p_0),v) - (1+p_0)C(v)\right] + B(v,h) \tag{7.2}$$

From (6.5)

$$R(u,v) = \sqrt{C^2(v)u^2 + B(v,h)u + A(v,h)} \tag{7.3}$$

and, from (6.6),

$$A = |\mathbf{q}_0|^2 v^2 + h^2\,, \quad B = 2\left[\mathbf{q}_0 \cdot (\mathbf{p}_0 + \mathbf{r}_{pq}v) - \hat{n}\cdot\mathbf{r}_{pq}h\right]v\,, \quad C = |\mathbf{p}_0 + \mathbf{r}_{pq}v| \tag{7.4}$$

For g we write

$$g(v,h) = 2C(v)\left[\frac{R^2(-(1+p_0),v) - (1+p_0)^2C^2(v)}{R(-(1+p_0),v) + (1+p_0)C(v)}\right] + B(v,h)$$

$$= 2C(v)\left[\frac{-(1+p_0)B(v,h) + A(v,h)}{R(-(1+p_0),v) + (1+p_0)C(v)}\right] + B(v,h)$$

$$= \frac{2C(v)\left[-(1+p_0)B(v,h) + A(v,h)\right] + B(v,h)\left[R(-(1+p_0),v) + (1+p_0)C(v)\right]}{R(-(1+p_0),v) + (1+p_0)C(v)}$$

$$= \frac{B(v,h)\left[R(-(1+p_0),v) - (1+p_0)C(v)\right] + 2A(v,h)C(v)}{R(-(1+p_0),v) + (1+p_0)C(v)}\,. \tag{7.5}$$

The denominator of this fraction is never zero for an interior point. In the numerator, the troublesome term is multiplied by *B*. As we can see from (7.4), *B* is of *O*(*v*), as *v* tends to zero, and sends the product of the two terms to zero; in fact,

$$B(v,h)\left[R\left(-(1+p_0),v\right)-(1+p_0)C(v)\right]+2A(v,h)C(v)\xrightarrow[v\to 0]{}2\left|\mathbf{p}_0\right|h^2 \tag{7.6}$$

with the contribution coming from the second term. From (7.5) and (7.1), we have that

$$I_2=\int_{-1-q_0}^{1-q_0}\ln\left|\frac{B(v,h)\left[R\left(-(1+p_0),v\right)-(1+p_0)C(v)\right]+2A(v,h)C(v)}{R\left(-(1+p_0),v\right)+(1+p_0)C(v)}\right|\frac{dv}{C(v)}. \tag{7.7}$$

Going back to (7.1) again, we write

$$\begin{aligned}I=&\int_{-1-q_0}^{1-q_0}\ln\left|2C(v)\left[R(1-p_0,v)+C(v)(1-p_0)\right]+B(v,h)\right|\frac{dv}{C(v)}\\&-\int_{-1-q_0}^{1-q_0}\ln\left|\frac{B(v,h)\left[R\left(-(1+p_0),v\right)-(1+p_0)C(v)\right]+2A(v,h)C(v)}{R\left(-(1+p_0),v\right)+(1+p_0)C(v)}\right|\frac{dv}{C(v)}.\end{aligned} \tag{7.8}$$

We display results for this expression in Tables 7.2.1 (second BQ) and 7.2.2 (third BQ). For both integration methods, we have specified the origin as a singular point. We have also specified the maximum number of recursions to be 12. Only on one occasion (h = 0.1) do the two methods differ and only in the last digit and by one unit. The times quoted are the CPU sec for the two integrations in (7.8). We have not been able to find information in Mathematica as to what zero time means. In any case, the times are shown here simply for comparing the two integration methods. If we compare these tables with the right-hand side (the "with" column) of Tables 6.1 and 6.2, we notice two things. First, that the results of Tables 6.1 agree with the present ones to the number of SD specified there. Second, for approximately the same time-expense, we get 15 SD with the present approach.

The most interesting part about the tables below is the last line. It clearly indicates that both integration routines can handle even the case h = 0 and to 15 SD! As we show in the next section, this case can be handled separately and that the results we will get there are in agreement with the ones here.

Table 7.2.1. The value of the expression in (7.8) for five values of *h* calculated using GKQ and DEQ methods and specifying the singular point. The execution time is in CPU seconds. We also display the maximum number of SD obtainable from each method. Second BQ. Singular or nearly singular point at ($p_0 = q_0 = 0.25$).

	GKQ			DEQ		
h	Value	Time	SD	Value	Time	SD
1.00E-01	2.64885004505136	0.032	15	2.64885004505135	0.046	15
1.00E-04	2.74951658705434	0.046	15	2.74951658705434	0.031	15
1.00E-08	2.74961966479829	0.032	15	2.74961966479829	0.063	15
1.00E-12	2.74961967510630	0.032	15	2.74961967510630	0.046	15
1.00E-16	2.74961967510733	0.016	15	2.74961967510733	0	15
0.00E+00	2.74961967510733	0.031	15	2.74961967510733	0	15

Table 7.2.2. The value of the expression in (7.8) for five values of *h* calculated using GKQ and DEQ methods and specifying the singular point. The execution time is in CPU seconds. We also display the maximum number of SD obtainable from each method. Third BQ. Singular or nearly singular point at ($p_0 = q_0 = 0.25$).

	GKQ			DEQ		
h	Value	Time	SD	Value	Time	SD
1.00E-01	1.87047241714406	0	15	1.87047241714406	0.032	15
1.00E-04	1.92437645094211	0.031	15	1.92437645094211	0.032	15
1.00E-08	1.92443435241883	0.047	15	1.92443435241883	0.048	15
1.00E-12	1.92443435820941	0.063	15	1.92443435820941	0.032	15
1.00E-16	1.92443435820999	0.047	15	1.92443435820999	0.016	15
0.00E+00	1.92443435820999	0.030	15	1.92443435820999	0	15

The two integrals in (7.8) can be combined into a single one

$$I = \int_{-1-q_0}^{1-q_0} \ln \left| \frac{\left\{2C(v)\left[R(1-p_0,v)+C(v)(1-p_0)\right]+B(v,h)\right\}\left\{R\left(-(1+p_0),v\right)+(1+p_0)C(v)\right\}}{B(v,h)\left[R\left(-(1+p_0),v\right)-(1+p_0)C(v)\right]+2A(v,h)C(v)} \right| \frac{dv}{C(v)} \tag{7.9}$$

We present results for this integral in Tables 7.3.1 and 7.3.2. The entries in bold red indicate times lower than those required by (7.8). From these we conclude that GKQ works faster with (7.9) while for DEQ there is not much time difference between (7.8) and (7.9).

From Figs. 6.1 and 6.3, we see that the integrand of (7.9) is not a simple one to evaluate numerically; nevertheless, through a simple manipulation, we were able to compute it to machine precision (15 SD).

Table 7.3.1. The value of the integral in (7.9) for five values of h calculated using GKQ and DEQ methods and specifying the singular point. The execution time is in CPU seconds. We also display the maximum number of SD obtainable from each method. Second BQ. Singular or nearly singular point at ($p_0 = q_0 = 0.25$).

	GKQ			DEQ		
h	Value	Time	SD	Value	Time	SD
1.00E-01	2.64885004505136	0.015	15	2.64885004505135	0.031	15
1.00E-04	2.74951658705434	0.031	15	2.74951658705434	0.015	15
1.00E-08	2.74961966479829	0.078	15	2.74961966479829	0.062	15
1.00E-12	2.74961967510630	0.062	15	2.74961967510630	0.032	15
1.00E-16	2.74961967510733	0.016	15	2.74961967510733	0.015	15
0.00E+00	2.74961967510733	0.031	15	2.74961967510733	0.016	15

Table 7.3.2. The value of the integral in (7.9) for five values of h calculated using GKQ and DEQ methods and specifying the singular point. The execution time is in CPU seconds. We also display the maximum number of SD obtainable from each method. Third BQ. Singular or nearly singular point at ($p_0 = q_0 = 0.25$).

	GKQ			DEQ		
h	Value	Time	SD	Value	Time	SD
1.00E-01	1.87047241714406	0.015	15	1.87047241714406	0.016	15
1.00E-04	1.92437645094211	0.015	15	1.92437645094211	0.032	15
1.00E-08	1.92443435241883	0.031	15	1.92443435241883	0.031	15
1.00E-12	1.92443435820941	0.016	15	1.92443435820941	0.031	15
1.00E-16	1.92443435820999	0.016	15	1.92443435820999	0.015	15
0.00E+00	1.92443435820999	0.016	15	1.92443435820999	0	15

In the tables above, we notice that the result for $h = 0$ is the same as for $h = 10^{-16}$. We focus on this observation in Tables 7.4. There, we vary h from 10^{-13} to 10^{-20} and we note that, for both BQs and both methods, we get the same result as for $h = 0$ for values of h equal or greater than 10^{-15}. Considering (7.6), and as a precaution, whenever h is specified as zero, we may add some more stability to the computation by giving it a small value, such as 10^{-20}.

Table 7.4.1. The value of the integral in (7.9) for small values of *h* calculated using GKQ and DEQ methods and specifying the singular point. The execution time is in CPU seconds. We also display the maximum number of SD obtainable from each method. Second BQ. Singular or nearly singular point at (0.25, 0.25).

	GKQ			DEQ		
h	Value	Time	SD	Value	Time	SD
1.00E-13	2.74961967510723	0.015	15	2.74961967510723	0.016	15
1.00E-14	2.74961967510732	0.062	15	2.74961967510732	0.016	15
1.00E-15	2.74961967510733	0.031	15	2.74961967510733	0.015	15
1.00E-16	2.74961967510733	0.015	15	2.74961967510733	0.016	15
1.00E-17	2.74961967510733	0.016	15	2.74961967510733	0.015	15
1.00E-18	2.74961967510733	0.015	15	2.74961967510733	0.000	15
1.00E-19	2.74961967510733	0.031	15	2.74961967510733	0.000	15
1.00E-20	2.74961967510733	0.031	15	2.74961967510733	0.000	15
0.00E+00	2.74961967510733	0.031	15	2.74961967510733	0.000	15

Table 7.4.2. The value of the integral in (7.9) for small values of *h* calculated using GKQ and DEQ methods and specifying the singular point. The execution time is in CPU seconds. We also display the maximum number of SD obtainable from each method. Third BQ. Singular or nearly singular point at (0.25, 0.25).

	GKQ			DEQ		
h	Value	Time	SD	Value	Time	SD
1.00E-13	1.92443435820993	0.015	15	1.92443435820993	0.016	15
1.00E-14	1.92443435820998	0.015	15	1.92443435820998	0.016	15
1.00E-15	1.92443435820999	0.015	15	1.92443435820999	0.000	15
1.00E-16	1.92443435820999	0.000	15	1.92443435820999	0.015	15
1.00E-17	1.92443435820999	0.015	15	1.92443435820999	0.000	15
1.00E-18	1.92443435820999	0.016	15	1.92443435820999	0.015	15
1.00E-19	1.92443435820999	0.000	15	1.92443435820999	0.016	15
1.00E-20	1.92443435820999	0.015	15	1.92443435820999	0.000	15
0.00E+00	1.92443435820999	0.016	15	1.92443435820999	0.015	15

In the next section, we present more examples and another way of evaluating (7.9) when $h = 0$.

SECTION 8: ADDITIONAL TEST CASES

In the previous sections, we developed a method for computing the inner integral of the IM element of EFIE. We tested the method using the BQs of Section 3 but we employed only one point in the parametric representation of each BQ, namely, the point $p_0 = q_0 = 0.25$. In this section, we expand the testing using the third BQ of Section 3. As we pointed out in that section, this extreme type of a BQ should be avoided in practice. It makes, however, for a good test case since, if our method can provide good results for this BQ, it will, in all likelihood, provide good results for more commonly used BQs, such as the second one in Section 3.

The first case we consider is the case $p_0 = q_0 = 0$. At this point the BQ has a saddle type of behavior. From (3.9), the equation for the third BQ is

$$\mathbf{r}(p,q) = (3,0,0)\,p + (0,2,0)\,q + (0,0,10)\,pq\,, \quad |p| \le 1\,, \quad |q| \le 1 \tag{8.1}$$

from which we get that

$$\frac{\partial \mathbf{r}(p,q)}{\partial p} = (3,0,0) + (0,0,10)\,q\,, \quad \frac{\partial \mathbf{r}(p,q)}{\partial q} = (0,2,0) + (0,0,10)\,p \tag{8.2}$$

and

$$\hat{n} = \frac{(3,0,10q)\times(0,2,10p)}{\left|(3,0,10q)\times(0,2,10p)\right|} = \frac{(3,0,10q)\times(0,2,10p)}{\left|(3,0,10q)\times(0,2,10p)\right|} = \frac{-20q\hat{x} - 30p\hat{y} + 6\hat{z}}{\sqrt{400q^2 + 900p^2 + 36}}\,. \tag{8.3}$$

We use this information in the integral under consideration, namely (7.9). We display the graph of the integrand for $h = 0.1$ in Figure 8.1. In Table 8.1, we display the results of the integration of (7.9) using both GKQ and DEQ, and for the same values of h that we have used in the previous sections. The conditions for the two quadratures are the same as before, with the number of recursions limited to 12. We have also specified the origin as a singular point. We obtain agreement to 15 SD, except in the last two cases where there is a disagreement of one unit in the last digit.

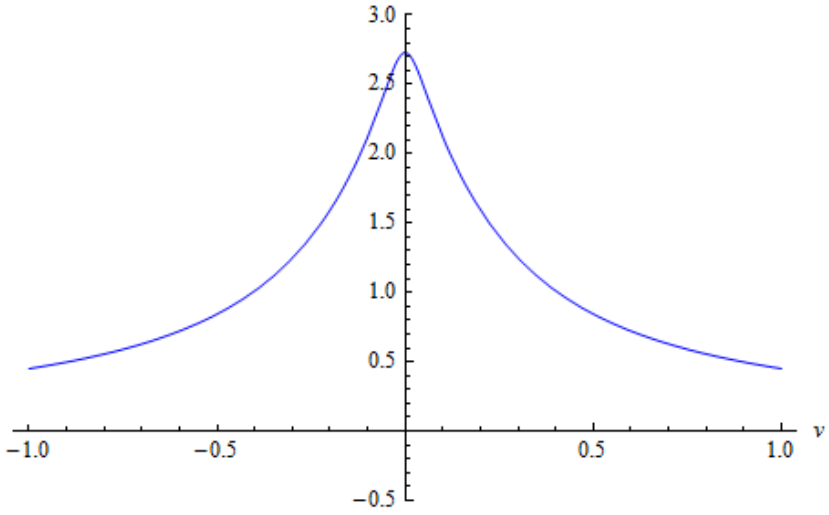

Figure 8.1. The graph of the integrand in (7.9) for the third BQ of Section 3, with $p_0 = q_0 = 0$ and $h = 0.1$. As h gets smaller, the peak moves upward. When $h = 0$, we have a logarithmic singularity at the origin.

Table 8.1. The numerical integration of (7.9) for the third BQ of Section 3 and with $p_0 = q_0 = 0$. Both methods agree except for the numbers in red, which disagree in the last digit by one unit.

	GKQ			DEQ		
h	Value	Time	SD	Value	Time	SD
1.00E-01	2.16084390813449	0.047	15	2.16084390813449	0.047	15
1.00E-04	2.25593244874981	0.015	15	2.25593244874981	0.047	15
1.00E-08	2.25603714690303	0.031	15	2.25603714690303	0.031	15
1.00E-12	2.25603715737396	0.031	15	2.25603715737396	0.031	15
1.00E-16	2.25603715737501	0.032	14	2.25603715737500	0.015	14
0.00E+00	2.25603715737501	0.016	14	2.25603715737500	0.016	14

We next give the singular point the value $p_0 = -1$, $q_0 = 1$. The position vector from (8.1) is (-3, 2, -10) and corresponds to one of the two lower corners of the BQ. In Figure 8.2, we show the graph of the integrand of (7.9) for $h = 0.1$. The same comments as above hold with the exception that the logarithmic singularity is now an endpoint of the integration interval. We have calculated the integral in (7.9) and we display the results in Table 8.2. We see that this time the two quadratures differ for large rather than small values of h. Since the difference is only in the last digit and only by a unit, we do not think it is a matter to dwell on.

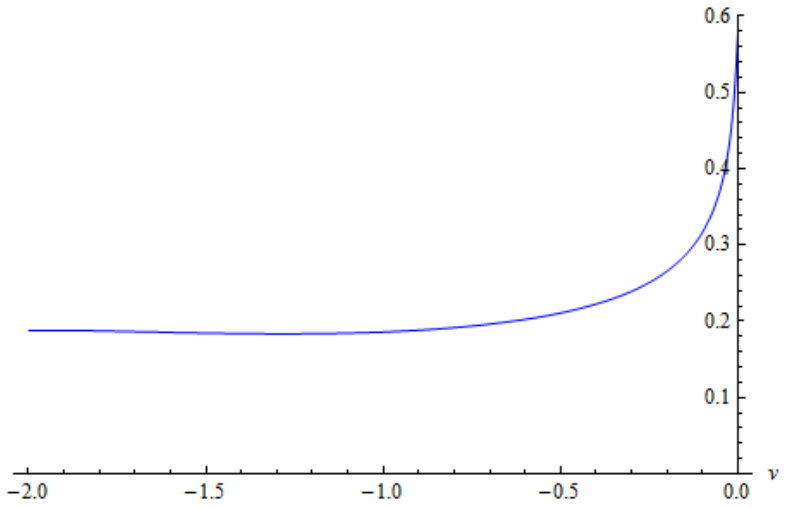

Figure 8.2. The graph of the integrand in (7.9) for the third BQ of Section 3, with p_0 = -1, q_0 = 1 and h = 0.1. As h gets smaller, the peak moves upward. When h = 0, we have a logarithmic singularity at the origin.

Table 8.2. The numerical integration of (7.9) for the third BQ of Section 3 and with p_0 = -1, q_0 = 1. Both methods agree except for the numbers in red, which disagree in the last digit by one unit.

	GKQ			DEQ		
h	Value	Time	SD	Value	Time	SD
1.00E-01	0.421015601245452	0.031	15	0.421015601245452	0.032	15
1.00E-04	0.422730809605921	0.031	14	0.422730809605920	0.031	14
1.00E-08	0.422732511450675	0.031	14	0.422732511450674	0.016	14
1.00E-12	0.422732511620856	0.032	15	0.422732511620856	0.031	15
1.00E-16	0.422732511620873	0.015	15	0.422732511620873	0.016	15
0.00E+00	0.422732511620873	0.016	15	0.422732511620873	0.031	15

We chose the next singular point to be at $p_0 = q_0 = 1$. The position vector from (8.1) is (3, 2, 10) and corresponds to one of the two upper corners of the BQ. In Figure 8.2, we show the graph of the integrand of (7.9) for h = 0.1. We have calculated the integral in (7.9) and we display the results in Table 8.2. We see that this time the two quadratures differ in all cases but one, but only in the last digit and not more than by a unit. From the last three cases, we may conclude that, in terms of the Mathematica quadratures, our method provides at least 14 SD.

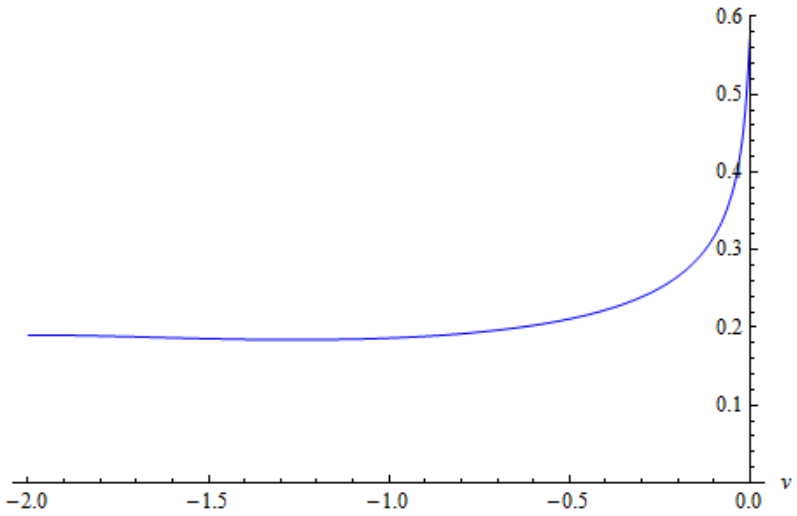

Figure 8.3. The graph of the integrand in (7.9) for the third BQ of Section 3, with $p_0 = q_0 = 1$ and $h = 0.1$. As h gets smaller, the peak moves upward. When $h = 0$, we have a logarithmic singularity at the origin.

Table 8.3. The numerical integration of (7.9) for the third BQ of Section 3 and with $p_0 = q_0 = 1$. The numbers in red indicate a disagreement in the last digit of one unit.

	GKQ			DEQ		
h	Value	Time	SD	Value	Time	SD
1.00E-01	0.422500945889474	0.016	15	0.422500945889474	0.015	15
1.00E-04	0.422732296117918	0.016	14	0.422732296117917	0.015	14
1.00E-08	0.422732511599326	0.015	14	0.422732511599325	0.016	14
1.00E-12	0.422732511620871	0.062	14	0.422732511620870	0.015	14
1.00E-16	0.422732511620873	0.016	14	0.422732511620872	0.015	14
0.00E+00	0.422732511620873	0.031	14	0.422732511620872	0	14

We also repeat the calculations as in Tables 7.4 for the three points of this section. The conclusions are the same as in Section 7: giving h a small value when it is supposed to be zero may stabilize the algorithm without altering the end result.

Table 8.4.1. The value of the integral in (7.9) for the third BQ and for small values of *h* calculated using GKQ and DEQ methods and specifying the singular point. The execution time is in CPU seconds. We also display the maximum number of SD obtainable from each method. Singular or nearly singular point at $p_0 = 0.0$, $q_0 = 0.0$.

	GKQ			DEQ		
h	Value	Time	SD	Value	Time	SD
1.00E-13	2.25603715737490	0.047	15	2.25603715737490	0.016	15
1.00E-14	2.25603715737500	0.031	14	2.25603715737499	0.016	14
1.00E-15	2.25603715737501	0.000	14	2.25603715737500	0.016	14
1.00E-16	2.25603715737501	0.032	14	2.25603715737500	0.031	14
1.00E-17	2.25603715737501	0.031	14	2.25603715737501	0.016	14
1.00E-18	2.25603715737501	0.016	14	2.25603715737500	0.015	14
1.00E-19	2.25603715737501	0.031	14	2.25603715737501	0.015	14
1.00E-20	2.25603715737501	0.031	14	2.25603715737500	0.016	14
0.00E+00	2.25603715737501	0.031	14	2.25603715737501	0.016	14

Table 8.4.2. The value of the integral in (7.9) for the third BQ and for small values of *h* calculated using GKQ and DEQ methods and specifying the singular point. The execution time is in CPU seconds. We also display the maximum number of SD obtainable from each method. Singular or nearly singular point at $p_0 = -1.0$, $q_0 = 1.0$.

	GKQ			DEQ		
h	Value	Time	SD	Value	Time	SD
1.00E-13	0.422732511620871	0.015	15	0.422732511620871	0.032	15
1.00E-14	0.422732511620873	0.016	15	0.422732511620873	0.031	15
1.00E-15	0.422732511620873	0.032	15	0.422732511620873	0.015	15
1.00E-16	0.422732511620873	0.016	15	0.422732511620873	0.031	15
1.00E-17	0.422732511620873	0	15	0.422732511620873	0.032	15
1.00E-18	0.422732511620873	0.031	15	0.422732511620873	0.015	15
1.00E-19	0.422732511620873	0.031	15	0.422732511620873	0.016	15
1.00E-20	0.422732511620873	0.015	15	0.422732511620873	0.000	15
0.00E+00	0.422732511620873	0.016	15	0.422732511620873	0.031	15

Table 8.4.3. The value of the integral in (7.9) for the third BQ and for small values of *h* calculated using GKQ and DEQ methods and specifying the singular point. The execution time is in CPU seconds. We also display the maximum number of SD obtainable from each method. Singular or nearly singular point at $p_0 = 1.0$, $q_0 = 1.0$.

	GKQ			DEQ		
h	Value	Time	SD	Value	Time	SD
1.00E-13	0.422732511620873	0.016	14	0.422732511620872	0.015	14
1.00E-14	0.422732511620873	0.046	14	0.422732511620872	0.016	14
1.00E-15	0.422732511620873	0.016	14	0.422732511620872	0.016	14
1.00E-16	0.422732511620873	0.031	14	0.422732511620872	0.016	14
1.00E-17	0.422732511620873	0.000	14	0.422732511620872	0.031	14
1.00E-18	0.422732511620873	0.031	14	0.422732511620872	0.000	14
1.00E-19	0.422732511620873	0.000	14	0.422732511620872	0.016	14
1.00E-20	0.422732511620873	0.016	14	0.422732511620872	0.015	14
0.00E+00	0.422732511620873	0.031	14	0.422732511620872	0.000	14

We next present another way of computing (7.9) when *h* is equal to zero. We repeat here (7.9) for convenience

$$I = \int_{-1-q_0}^{1-q_0} \ln \left| \frac{\left\{2C(v)\left[R(1-p_0,v)+C(v)(1-p_0)\right]+B(v,h)\right\}\left\{R\left(-(1+p_0),v\right)+(1+p_0)C(v)\right\}}{B(v,h)\left[R\left(-(1+p_0),v\right)-(1+p_0)C(v)\right]+2A(v,h)C(v)} \right| \frac{dv}{C(v)} \tag{8.4}$$

where, from (7.3),

$$R(u,v) = \sqrt{C^2(v)u^2 + B(v,h)u + A(v,h)} \tag{8.5}$$

while, from (7.4),

$$A(v,0) = \left|\mathbf{q}_0\right|^2 v^2\,, \quad B(v,0) = 2\mathbf{q}_0 \cdot \left(\mathbf{p}_0 + \mathbf{r}_{pq} v\right) v\,, \quad C(v) = \left|\mathbf{p}_0 + \mathbf{r}_{pq} v\right|. \tag{8.6}$$

We consider the case of an interior singular point. When $h = 0$, the numerator of the logarithm's argument does not become zero, nor does it become so at any other value of the integration variable. For the denominator, we write

$$g(v) = B(v,0)\left[R\left(-(1+p_0),v\right)-(1+p_0)C(v)\right]+2A(v,0)C(v)$$

$$= B(v,0)\left[\frac{R^2\left(-(1+p_0),v\right)-(1+p_0)^2 C^2(v)}{R\left(-(1+p_0),v\right)+(1+p_0)C(v)}\right]+2A(v,0)C(v)$$

$$= \frac{B(v,0)\left[R^2\left(-(1+p_0),v\right)-(1+p_0)^2 C^2(v)\right]+2A(v,0)C(v)\left[R\left(-(1+p_0),v\right)+(1+p_0)C(v)\right]}{R\left(-(1+p_0),v\right)+(1+p_0)C(v)} \tag{8.7}$$

We evaluate

$$\begin{aligned} R^2\left(-(1+p_0),v\right)-(1+p_0)^2 C^2(v) &= (1+p_0)^2 C^2(v)+B(v,0)u+A(v,0)-(1+p_0)^2 C^2(v) \\ &= -B(v,0)(1+p_0)+A(v,0) = -2(1+p_0)\mathbf{q}_0\cdot\left(\mathbf{p}_0+\mathbf{r}_{pq}v\right)v+|\mathbf{q}_0|^2 v^2 \end{aligned} \tag{8.8}$$

and substitute in (8.7)

$$g(v) = \frac{B(v,0)\left[-2(1+p_0)\mathbf{q}_0\cdot\left(\mathbf{p}_0+\mathbf{r}_{pq}v\right)v+|\mathbf{q}_0|^2 v^2\right]+2A(v,0)C(v)\left[R\left(-(1+p_0),v\right)+(1+p_0)C(v)\right]}{R\left(-(1+p_0),v\right)+(1+p_0)C(v)}$$

$$= 2v^2\,\frac{\mathbf{q}_0\cdot\left(\mathbf{p}_0+\mathbf{r}_{pq}v\right)\left[-2(1+p_0)\mathbf{q}_0\cdot\left(\mathbf{p}_0+\mathbf{r}_{pq}v\right)+|\mathbf{q}_0|^2 v\right]+|\mathbf{q}_0|^2 C(v)\left[R\left(-(1+p_0),v\right)+(1+p_0)C(v)\right]}{R\left(-(1+p_0),v\right)+(1+p_0)C(v)} \tag{8.9}$$

We set $h = 0$ in the argument of the logarithm in (8.4) and write

$$\ln\left|\frac{N(v)}{2v^2 D(v)}\right| = \ln\left|\frac{N(v)}{2D(v)}\right| - 2\ln|v| \tag{8.10}$$

where

$$N(v) = \left\{2C(v)\left[R(1-p_0,v)+C(v)(1-p_0)\right]+B(v,0)\right\}\left\{R\left(-(1+p_0),v\right)+(1+p_0)C(v)\right\}^2 \tag{8.11}$$

and

$$\begin{aligned} D(v) = {} & \mathbf{q}_0\cdot\left(\mathbf{p}_0+\mathbf{r}_{pq}v\right)\left[-2(1+p_0)\left(\mathbf{p}_0+\mathbf{r}_{pq}v\right)\cdot\mathbf{q}_0+|\mathbf{q}_0|^2 v\right] \\ & +|\mathbf{q}_0|^2 C(v)\left[R\left(-(1+p_0),v\right)+(1+p_0)C(v)\right]. \end{aligned} \tag{8.12}$$

We return to (8.4) and write

$$I(0)=\int_{-1-q_0}^{1-q_0}\frac{1}{C(v)}\ln\left|\frac{N(v)}{2v^2D(v)}\right|dv=\int_{-1-q_0}^{1-q_0}\frac{1}{C(v)}\ln\left|\frac{N(v)}{2D(v)}\right|dv-2\int_{-1-q_0}^{1-q_0}\frac{\ln|v|}{C(v)}dv=I_1(0)-2I_2(0). \tag{8.13}$$

We note that the argument of the logarithm in the first integral on the right takes on a finite value when v is equal to zero. For the second integral, we have

$$I_2(0)=\int_{-1-q_0}^{1-q_0}\frac{\ln|v|}{C(v)}dv=\int_{-1-q_0}^{0}\frac{\ln|v|}{C(v)}dv+\int_{0}^{1-q_0}\frac{\ln(v)}{C(v)}dv=\int_{0}^{1+q_0}\frac{\ln(v)}{C(-v)}dv+\int_{0}^{1-q_0}\frac{\ln(v)}{C(v)}dv. \tag{8.14}$$

We integrate the new integrals once by parts

$$\begin{aligned}I_2(0)=&\frac{(1+q_0)\left[\ln(1+q_0)-1\right]}{C(-1-q_0)}+\frac{(1-q_0)\left[\ln(1-q_0)-1\right]}{C(1-q_0)}\\&+\int_0^{1+q_0}\frac{v\left[\ln(v)-1\right]\left[|\mathbf{r}_{pq}|^2v-\mathbf{p}_0\cdot\mathbf{r}_{pq}\right]}{C^3(-v)}dv+\int_0^{1-q_0}\frac{v\left[\ln(v)-1\right]\left[|\mathbf{r}_{pq}|^2v+\mathbf{p}_0\cdot\mathbf{r}_{pq}\right]}{C^3(v)}dv.\end{aligned} \tag{8.15}$$

The last two integrals have no singularities and are stable for numerical evaluation. If we substitute this result in (8.14), we get

$$\begin{aligned}I(0)=&\int_{-1-q_0}^{1-q_0}\frac{1}{C(v)}\ln\left|\frac{N(v)}{2D(v)}\right|dv-2\left\{\frac{(1+q_0)\left[\ln(1+q_0)-1\right]}{C(-1-q_0)}+\frac{(1-q_0)\left[\ln(1-q_0)-1\right]}{C(1-q_0)}\right\}\\&-2\left\{\int_0^{1+q_0}\frac{v\left[\ln(v)-1\right]\left[|\mathbf{r}_{pq}|^2v-\mathbf{p}_0\cdot\mathbf{r}_{pq}\right]}{C^3(-v)}dv+\int_0^{1-q_0}\frac{v\left[\ln(v)-1\right]\left[|\mathbf{r}_{pq}|^2v+\mathbf{p}_0\cdot\mathbf{r}_{pq}\right]}{C^3(v)}dv\right\}.\end{aligned} \tag{8.16}$$

All the integrals in this expression are numerically stable.

We examine next the case in which p_0 takes on its extreme values. When $p_0=-1$, we still have the denominator of the logarithmic function becoming zero but not the numerator. In this case,

$$R^2(0,v)\big|_{h=0}=|\mathbf{q}_0|^2v^2,\quad R^2(2,v)\big|_{h=0}=4C^2(v)+2B(v,0)+A(v,0);\quad (p_0=-1) \tag{8.17}$$

and

$$\frac{N(v)}{2v^2D(v)}=\frac{2C(v)\left[\sqrt{4C^2(v)+2B(v,0)+A(v,0)}+2C(v)\right]+B(v,0)}{2v\left[\mathbf{q}_0\cdot\left(\mathbf{p}_0+\mathbf{r}_{pq}v\right)+|\mathbf{q}_0|C(v)\right]}. \tag{8.19}$$

If we take *v* away from the denominator, then the rest of the fraction attains a finite value at *v* = 0. We can then proceed as above.

When $p_0 = 1$, we have from the end of Section 6 that the numerator in the logarithm's argument becomes zero. In this case, we have that

$$\frac{N(v)}{2v^2 D(v)} = \frac{\left\{C(v)|\mathbf{q}_0| + \mathbf{q}_0 \cdot \left(\mathbf{p}_0 + \mathbf{r}_{pq} v\right)\right\}\left\{\sqrt{\rho(v,0)} + 2C(v)\right\}^2}{v\left\{\mathbf{q}_0 \cdot \left(\mathbf{p}_0 + \mathbf{r}_{pq} v\right)\left[-4\left(\mathbf{p}_0 + \mathbf{r}_{pq} v\right)\cdot \mathbf{q}_0 + |\mathbf{q}_0|^2 v\right] + |\mathbf{q}_0|^2 C(v)\left[\sqrt{\rho(v,0)} + 2C(v)\right]\right\}} \tag{8.20}$$

with same comments as above. The singularity is of the same kind as the one in (8.19). We recall that we used the last two values of p_0 in the examples above and all cases ran smoothly.

We return to (8.16) and we compute it for the third BQ and the same points. The results are displayed in Table 8.5. The results of the first row are in agreement with those of Table 7.3.2 (last row). The results of the second row are in agreement with those of Table 8.3.1 (last row) but took a lot longer. The results of the third row are in agreement with those of Table 8.3.2 (last row). From the CPU time, we see that GKQ struggled to get to the result while the DEQ time is the same as in Table 8.3.2. From the last row, we see that both quadratures achieved 15 SD but the CPU time they required is much higher than that listed in Table 8.3.3. The conclusion here is that we will do as well using (7.9) instead of (8.17).

Table 8.5. The value of (8.17) for the third BQ and for four values of (p_0, q_0) calculated using GKQ and DEQ methods and specifying the singular point. The execution time is in CPU seconds. We also display the maximum number of SD obtainable from each method.

	GKQ			DEQ		
(p_0, q_0)	Value	Time	SD	Value	Time	SD
(0.25, 0.25)	1.92443435820999	0.015	15	1.92443435820999	0.016	15
(0.0, 0.0)	2.25603715737501	0.046	15	2.25603715737500	0.046	15
(-1.0,1.0)	0.422732511620873	0.110	15	0.422732511620873	0.030	15
(1.0, 1.0)	0.422732511620873	0.093	15	0.422732511620873	0.048	15

We conclude this section with a brief explanation as to why some of the times in Table 8.4 are much higher than the corresponding times in the previous tables. In Figure 8.4, we display the integrand of the middle integral in (8.16) for p_0 = -1 and q_0 = 1. The fact that we are subtracting two almost equal areas may have contributed to the slow convergence of GKQ. The execution time in this case is 0.094 CPU sec vs. 0.015 for the DEQ. The same is true for the case p_0 = 1 and q_0 = 1. We display the corresponding integrand in Figure 8.5.

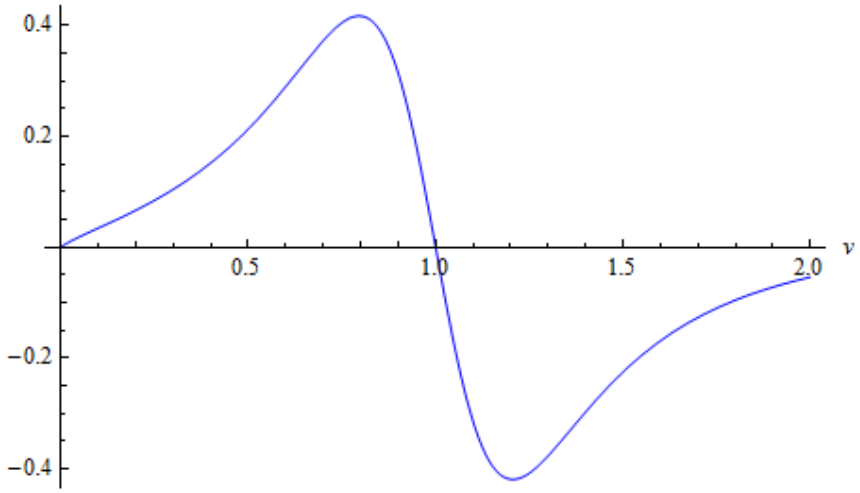

Figure 8.4: Integrand of the middle integral in (8.16) for p_0 = -1 and q_0 = 1.

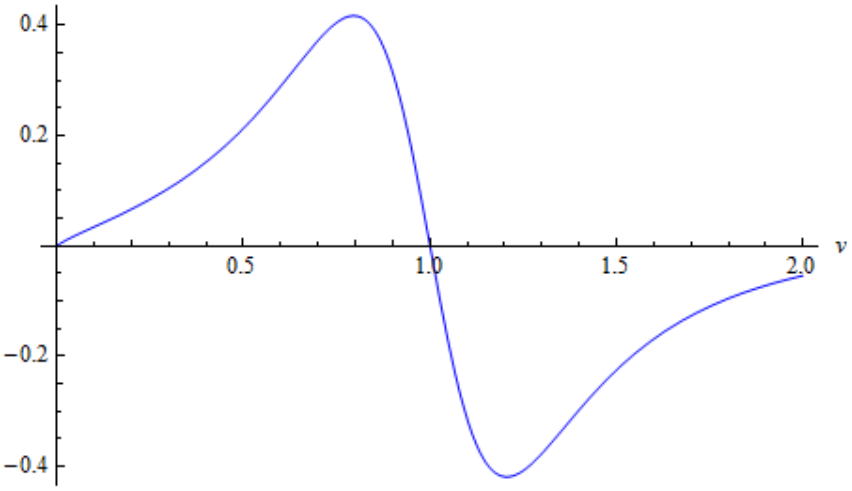

Figure 8.5: Integrand of the middle integral in (8.16) for p_0 = 1 and q_0 = 1.

SECTION 9: PROOF OF CLAIM AND SENSITIVITY ANALYSIS

In Section 6, we claimed that *C* in (6.6) is greater than zero. We show below that, if (6.6) is equal to zero, we have an irregular BQ. We also give additional examples of irregular BQs and perform a sensitivity study to determine how precision is affected as we pass from a regular to an irregular BQ. The arguments that we use here can also be used to show that *F* in (6.20) is also greater than zero. From (6.6), we have that

$$C = \left|\mathbf{p}_0 + \mathbf{r}_{pq} v\right| . \tag{9.1}$$

We assume first that $\mathbf{r}_{pq} = \mathbf{0}$. From (2.2), we see that the resulting BQ describes a planar parallelogram. For (9.1) to be zero, we must have that $\mathbf{p}_0 = \mathbf{0}$. From (2.23) the position vector to the BQ is

$$\mathbf{r}(p,q) = \mathbf{r}_0 + \left(\mathbf{r}_p + \mathbf{r}_{pq} q_0\right)(p - p_0) + \left(\mathbf{r}_q + \mathbf{r}_{pq} p_0\right)(q - q_0) + \mathbf{r}_{pq}\,(p - p_0)(q - q_0) \tag{9.2}$$

with $\mathbf{r}_0$ defined in (2.22). From (2.25)

$$\mathbf{p}_0 = \frac{\partial \mathbf{r}(p_0, q_0)}{\partial p_0}, \quad \mathbf{q}_0 = \frac{\partial \mathbf{r}(p_0, q_0)}{\partial q_0} \tag{9.3}$$

so that, from the last two,

$$\mathbf{p}_0 = \mathbf{r}_p + \mathbf{r}_{pq} q_0 . \tag{9.4}$$

We let now $\mathbf{p}_0$ and $\mathbf{r}_{pq}$ be zero in (9.2) and we get

$$\mathbf{r}(p,q) = \mathbf{r}_0 + \mathbf{r}_q \left(q - q_0\right) \tag{9.5}$$

which is the equation of a straight line in space. We thus have an irregular BQ. We could have surmised that immediately since $\mathbf{p}_0 = \mathbf{0}$ implies that (2.7) is zero.

We assume next that $\mathbf{r}_{pq} \neq \mathbf{0}$. For (9.1) to be equal to zero, we must have the two vectors there to be collinear. From this and (9.4), we conclude that $\mathbf{r}_{pq}$ and $\mathbf{r}_p$ are collinear. This implies that the BQ is planar. We write

$$\mathbf{r}_{pq} = \alpha \mathbf{r}_p . \tag{9.6}$$

If we compare this expression with (2.9), we conclude that $\beta = 0$ and Table 2.1 tells us for what values of α we will have a regular or irregular, planar BQ. We verify these values by substituting (9.6) in (9.1)

$$C = \left|\mathbf{p}_0 + \mathbf{r}_{pq} v\right| = \left|\mathbf{r}_p + \mathbf{r}_{pq} q_0 + \mathbf{r}_{pq} v\right| = \left|\mathbf{r}_p + \mathbf{r}_{pq} q\right| = \left|\mathbf{r}_p + \mathbf{r}_p \alpha q\right| = \left|\mathbf{r}_p\right| \left|1 + \alpha q\right| . \tag{9.7}$$

For this to be equal to zero, we must have that

$$q = -\frac{1}{\alpha} . \tag{9.8}$$

If $|\alpha| < 1$, the absolute value of q that makes (9.7) be zero is greater than one. Since $-1 \le q \le 1$, then (9.7) is different from zero. If $|\alpha| \ge 1$, then $|q| \le 1$ and we can have (9.7) equal to zero. What does this imply in terms of the nature of the BQ? If we substitute (9.6) in (9.2), we get

$$\begin{aligned} \mathbf{r}(p,q) &= \mathbf{r}_0 + \left(\mathbf{r}_p + \alpha \mathbf{r}_p q_0\right)(p - p_0) + \left(\mathbf{r}_q + \alpha \mathbf{r}_p p_0\right)(q - q_0) + \alpha \mathbf{r}_p (p - p_0)(q - q_0) \\ &= \mathbf{r}_0 + \mathbf{r}_p \left[(1 + \alpha q_0)(p - p_0) + \alpha p_0 (q - q_0) + \alpha (p - p_0)(q - q_0)\right] + \mathbf{r}_q (q - q_0) . \end{aligned} \tag{9.9}$$

From this, we see that we have a surface on the plane defined by the vectors $\mathbf{r}_p$ and $\mathbf{r}_q$, as we have already mentioned. We proceed to compute

$$\frac{\partial \mathbf{r}(p,q)}{\partial p} = \mathbf{r}_p \left[\left(1 + \alpha q_0\right) + \alpha \left(q - q_0\right)\right], \quad \frac{\partial \mathbf{r}(p,q)}{\partial q} = \mathbf{r}_p \alpha \left(p - p_0\right) + \mathbf{r}_q . \tag{9.10}$$

From this

$$\frac{\partial \mathbf{r}(p,q)}{\partial p} \times \frac{\partial \mathbf{r}(p,q)}{\partial q} = \left[\left(1 + \alpha q_0\right) + \alpha \left(q - q_0\right)\right]\left(\mathbf{r}_p \times \mathbf{r}_q\right) = \left(1 + \alpha q\right)\left(\mathbf{r}_p \times \mathbf{r}_q\right) \tag{9.11}$$

which is equal to zero when q is given by (9.8). These results are in agreement with Table 2.1. Thus, the only time (9.1) can be zero is when we have an irregular BQ.

We have given examples of regular and irregular BQs in Section 2. We present additional ones here by appropriately modifying the third BQ of Section 3. The relevant vectors are

$$\mathbf{r}_p = (3,0,0), \quad \mathbf{r}_q = (0,2,0), \quad \mathbf{r}_{pq} = (3\alpha,0,0) . \tag{9.12}$$

We have thus modified the last vector to be collinear with $\mathbf{r}_p$. We also set $p_0 = q_0 = 0.25$. Since the vectors in (9.12) lie in the *xy*-plane, so does the surface of the BQ. In Figure 9.1.1, we display the BQ's surface when $\alpha = 0.5$. Since (9.8) results in a value of q outside its range of values, we have a regular BQ in the *xy*-plane. Moreover, for C in (9.1) we have that

$$C = \left|\mathbf{p}_0 + \mathbf{r}_{pq} v\right| = \left|\mathbf{r}_p \left(1 + \alpha q\right)\right| = 3\left(1 + \frac{q}{2}\right) \ge \frac{3}{2} . \tag{9.13}$$

In Figure 9.1.2, we have set α = 1.0. The resulting value of -1 in (9.8) is at the lower end of the range of q and results in the QL being reduced to a triangle:

$$C = \left|\mathbf{r}_p\,(1+\alpha q)\right| = 3(1+q) \geq 0\,. \tag{9.14}$$

In Figure 9.1.3, we have set α = 2.0. The resulting value of q in (9.8) is now well within the range of values of q and we get a very irregular BQ, namely, two triangles with a common vertex.

$$-3 \leq C = 3(1+2q) \leq 9\,. \tag{9.15}$$

We can obtain similar results for F in (6.20).

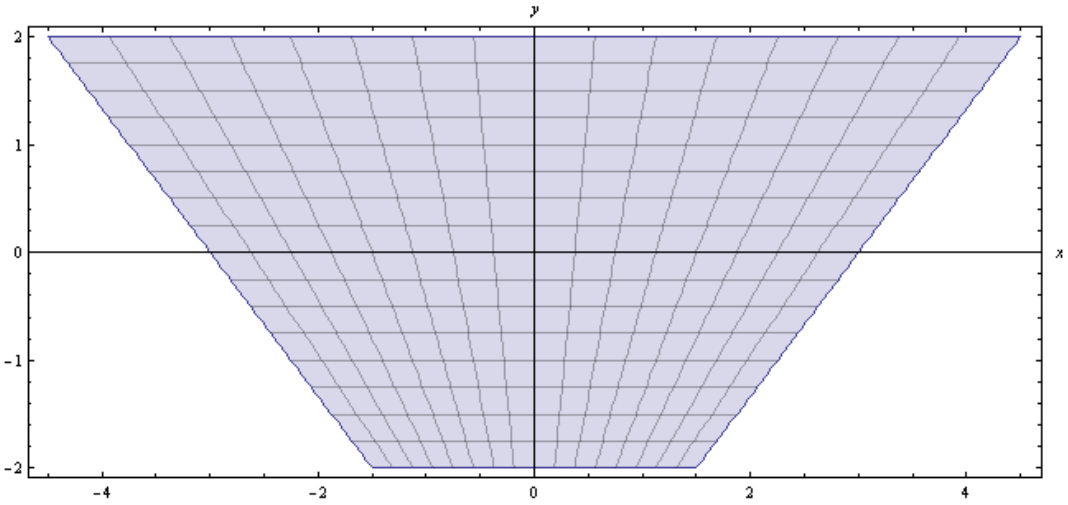

Figure 9.1.1: Graph of the BQ of (9.12) with α = 0.5.

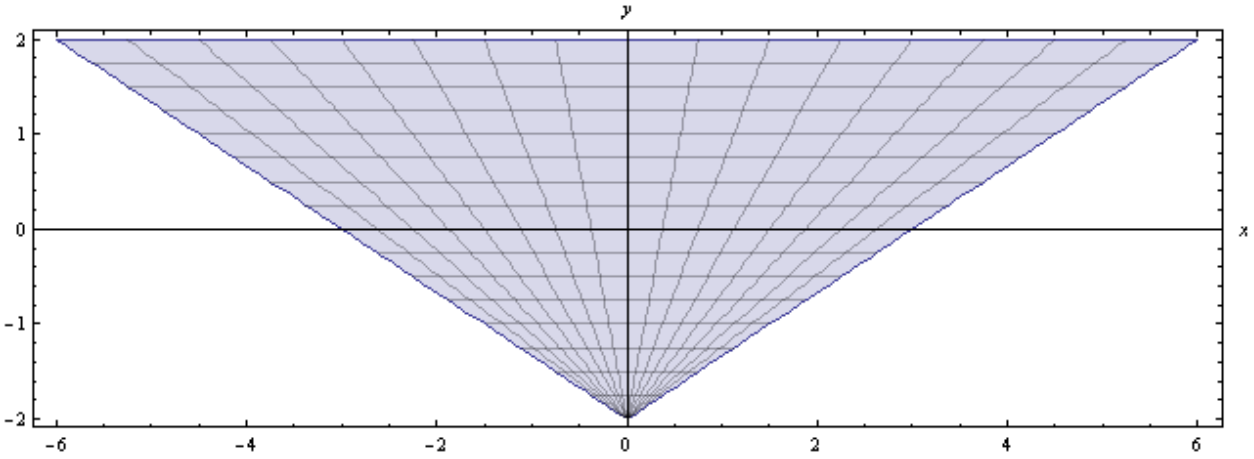

Figure 9.1.2: Graph of the BQ of (9.12) with α = 1.0.

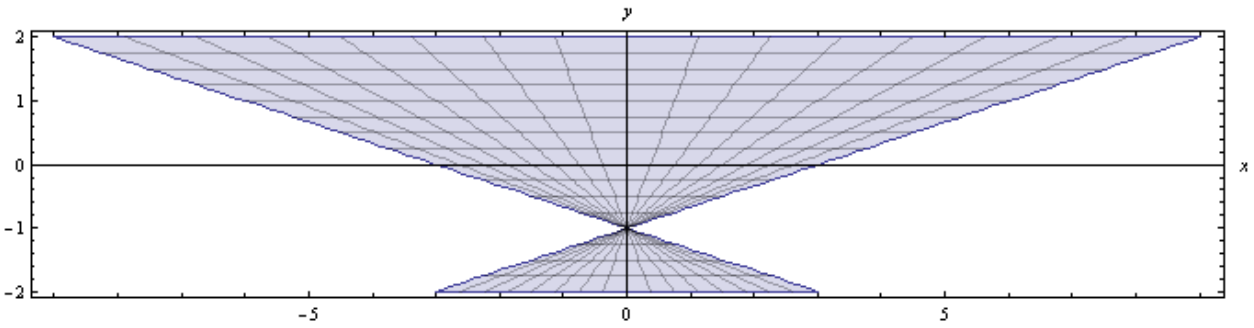

Figure 9.1.3: Graph of the BQ of (9.12) with α = 2.0.

In this last case, the position vector for the BQ is

$$\mathbf{r}(p,q) = \hat{x}p(1+2q) + \hat{y}2q\,. \tag{9.16}$$

From this we see that the line q = - 1/2 ($|p| \le 1$) maps to the single point (0, -1) in the *xy*-plane.

From the above discussion, it becomes clear that we have to exercise caution when we deal with a flat BQ. From (2.2), the position vector to a point on the BQ is

$$\mathbf{r}(p,q) = \mathbf{r}_{00} + \mathbf{r}_p p + \mathbf{r}_q q + \mathbf{r}_{pq} pq\,, \quad |p| \le 1\,, \quad |q| \le 1 \tag{9.17}$$

with the four vectors defined in (2.3) – (2.5). For this BQ to be flat, we must have the last three vectors lying on the same plane. One way to express this condition is that

$$\mathbf{r}_{pq} \cdot (\mathbf{r}_p \times \mathbf{r}_q) = 0\,. \tag{9.18}$$

If this holds, the next step is to determine the scalars in (2.9). This can be done by considering the rectangular components of this equation and solving a system of two equations in two unknowns. Once the unknowns have been determined, we can use Table 2.1 to decide whether we are dealing with a regular or irregular BQ.

We next ask the question of how sensitive the numerical integration becomes as we move from a regular BQ to an irregular one. To this end, we introduce the BQ

$$\mathbf{r}_p = (3,0,0)\,, \quad \mathbf{r}_q = (0,2,0)\,, \quad \mathbf{r}_{pq} = (0,2\beta,0)\,. \tag{9.19}$$

For this BQ, $\mathbf{r}_q$ and $\mathbf{r}_{pq}$ are collinear. In place of (9.6), we now have

$$\mathbf{r}_{pq} = \beta \mathbf{r}_q \tag{9.20}$$

while, in place of (9.8), we have

$$p' = -\frac{1}{\beta}. \tag{9.21}$$

In Figures 9.2.1 to 9.2.3, we display the graph of this BQ when β = 0.9, 0.99 and 0.999. We see that, as β tends to one, the BQ tends to look more like a triangle than a QL.

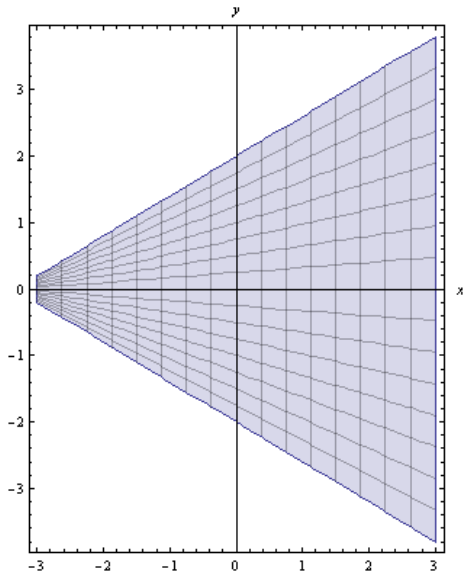

Figure 9.2.1: Graph of the BQ of (9.19) with β = 0.9 (p' = -1.1111).

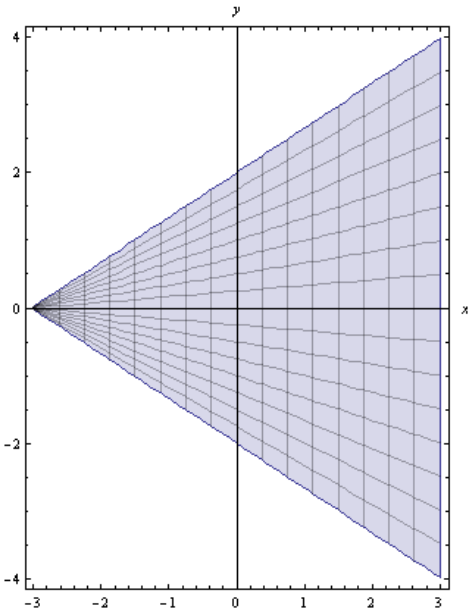

Figure 9.2.2: Graph of the BQ of (9.19) with β = 0.99 (p' = -1.0101).

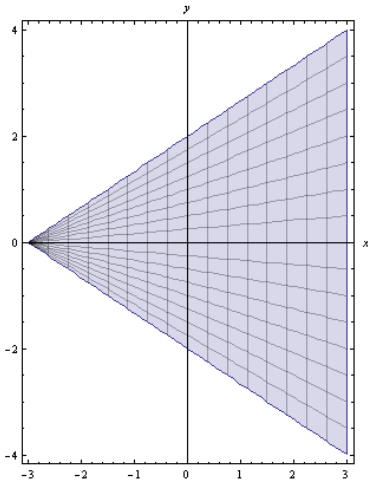

Figure 9.2.3: Graph of the BQ of (9.19) with $\beta = 0.999$ ($p' = -1.0010$).

We now examine what happens to the integral in (7.9) as β tends to one. We have computed this integral for the singular point at the center of the pq-coordinates and also at a corner point. We have considered the three values of β as well as four values of h. We display the integration results in Tables 9.1.1 to 9.2.3. We see that the two quadratures agree to at least 14 SD and, where there is a disagreement in the last digit, it is only by one unit. We also note that the cases of $h = 10^{-20}$ and $h = 0$ are in perfect agreement, which further reinforces the use of a small, non-zero h in place of zero.

Table 9.1.1: Value of the integral in (7.9) for the BQ of (9.19) and for $p_0 = q_0 = 0$ and $\beta = 0.9$.

	GKQ			DEQ		
h	Value	Time	SD	Value	Time	SD
1.00E-01	2.74665336952689	0.016	14	2.74665336952688	0.031	14
1.00E-08	2.84965918230493	0.031	15	2.84965918230493	0.032	15
1.00E-20	2.84965919277691	0.031	14	2.84965919277690	0.015	14
0.00E+00	2.84965919277691	0.031	14	2.84965919277690	0.000	14

Table 9.1.2: Value of the integral in (7.9) for the BQ of (9.19) and for $p_0 = q_0 = 0$ and $\beta = 0.99$.

	GKQ			DEQ		
h	Value	Time	SD	Value	Time	SD
1.00E-01	2.74730724784908	0.000	15	2.74730724784908	0.016	15
1.00E-08	2.85037159343782	0.032	14	2.85037159343781	0.031	14
1.00E-20	2.85037160390979	0.016	15	2.85037160390979	0.015	15
0.00E+00	2.85037160390979	0.015	15	2.85037160390979	0.015	15

Table 9.1.3: The value of the integral in (7.9) for the BQ of (9.19) and for $p_0 = q_0 = 0$ and $\beta = 0.999$.

	GKQ			DEQ		
h	Value	Time	SD	Value	Time	SD
1.00E-01	2.74736479069567	0.000	14	2.74736479069566	0.016	14
1.00E-08	2.85043525566924	0.031	15	2.85043525566924	0.031	15
1.00E-20	2.85043526614122	0.032	15	2.85043526614122	0.015	15
0.00E+00	2.85043526614122	0.016	15	2.85043526614122	0.016	15

Table 9.2.1: The value of the integral in (7.9) for the BQ of (9.19) and for $p_0 = -1$, $q_0 = 1$, and $\beta = 0.9$.

	GKQ			DEQ		
h	Value	Time	SD	Value	Time	SD
1.00E-01	2.56501461685842	0.015	15	2.56501461685842	0.032	15
1.00E-08	2.84064664644604	0.031	15	2.84064664644604	0.016	15
1.00E-20	2.84064668163297	0.016	15	2.84064668163297	0.015	15
0.00E+00	2.84064668163297	0.000	15	2.84064668163297	0.000	15

Table 9.2.2: The value of the integral in (7.9) for the BQ of (9.19) and for $p_0 = -1$, $q_0 = 1$, and $\beta = 0.99$.

	GKQ			DEQ		
h	Value	Time	SD	Value	Time	SD
1.00E-01	2.99932746262052	0.016	14	2.99932746262051	0.015	14
1.00E-08	4.26080553788516	0.015	15	4.26080553788516	0.016	15
1.00E-20	4.26080589691273	0.000	15	4.26080589691273	0.016	15
0.00E+00	4.26080589691273	0.016	15	4.26080589691273	0.015	15

Table 9.2.3: The value of the integral in (7.9) for the BQ of (9.19) and for $p_0 = -1$, $q_0 = 1$, and $\beta = 0.999$.

	GKQ			DEQ		
h	Value	Time	SD	Value	Time	SD
1.00E-01	3.02996129711238	0.000	15	3.02996129711238	0.000	15
1.00E-08	5.69681413172724	0.000	14	5.69681413172723	0.016	14
1.00E-20	5.69681772889930	0.016	14	5.69681772889929	0.015	14
0.00E+00	5.69681772889930	0.015	14	5.69681772889929	0.016	14

We may also ask the question of whether (7.9) is computable when $|\beta| \geq 1$. Here, we may run into problems if either p_0 or q_0 turns out to be zero. For example, when $\beta = 1$ and $p_0 = -1$, $q_0 = 1$, then $\mathbf{q}_0 = (0, 2(1+\beta p_0), 0) = (0, 0, 0)$. If we define the unit normal in terms of these two vectors, then in this example, we will run into the case of dividing by zero. In such a case, and since the unit normally does not change on a flat BQ we can do either of two things: select two non-collinear vectors on the BQ to define the unit normal or, even better, ignore it altogether since it only appears in B in (7.4) and, there, it is dotted to the vector $\mathbf{r}_{pq}$ which lies on the BQ's plane; thus, this product is zero and can be omitted.

In Tables 9.3 and 9.4, we present results for the BQ of (9.20) and for three different values of β. In Tables 9.3, we take the singular point to be the origin. We see that the results from the two quadratures agree to at least 14SD. We also note that the results of Tables 9.3.1 and 9.3.3 are identical. This is because the BQ (a triangle in this case) is the reflection of the BQ in the second case about the y-axis, as shown in Figs. 9.3.1 and 9.3.2. If we compare the values in Table 9.1.3 to those in Table 9.3.1, we see a smooth transition between the values for $\beta = 0.999$ and those for $\beta = 1$. We show the BQ for Table 9.3.2 in Figure 9.3.3. It comprises two triangles with a common vertex.

Table 9.3.1: The value of the integral in (7.9) for the BQ of (9.19) and for $p_0 = q_0 = 0$ and $\beta = 1$.

	GKQ			DEQ		
h	Value	Time	SD	Value	Time	SD
1.00E-01	2.74737108607702	0.031	15	2.74737108607702	0.031	15
1.00E-08	2.85044223392429	0.046	14	2.85044223392428	0.047	14
1.00E-20	2.85044224439626	0.000	15	2.85044224439626	0.016	15
0.00E+00	2.85044224439626	0.031	15	2.85044224439626	0.000	15

Table 9.3.2: The value of the integral in (7.9) for the BQ of (9.19) and for $p_0 = q_0 = 0$ and $\beta = 2$.

	GKQ			DEQ		
h	Value	Time	SD	Value	Time	SD
1.00E-01	2.73594640126082	0.016	15	2.73594640126082	0.016	15
1.00E-08	2.83994915267823	0.016	15	2.83994915267823	0.031	15
1.00E-20	2.83994916315021	0.000	15	2.83994916315021	0.015	15
0.00E+00	2.83994916315021	0.016	15	2.83994916315021	0.031	15

Table 9.3.3: The value of the integral in (7.9) for the BQ of (9.19) and for $p_0 = q_0 = 0$ and $\beta = -1$.

	GKQ			DEQ		
h	Value	Time	SD	Value	Time	SD
1.00E-01	2.74737108607702	0.016	15	2.74737108607702	0.015	15
1.00E-08	2.85044223392429	0.031	14	2.85044223392428	0.031	14
1.00E-20	2.85044224439626	0.031	15	2.85044224439626	0.000	15
0.00E+00	2.85044224439626	0.000	15	2.85044224439626	0.016	15

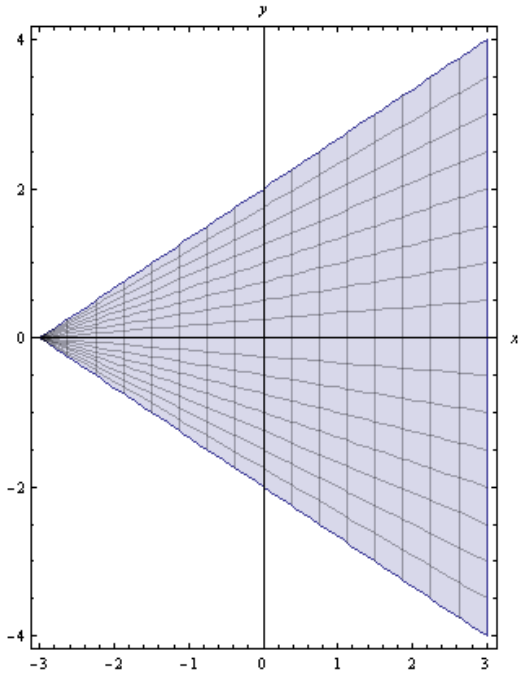

Figure 9.3.1: Graph of the BQ of (9.19) with $\beta = 1$ ($p' = -1.0$).

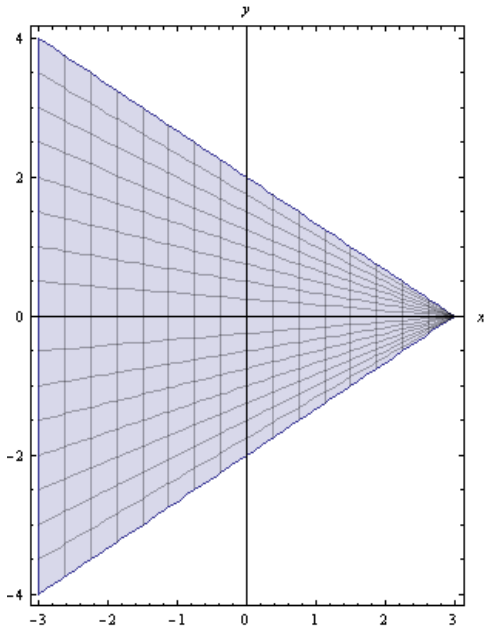

Figure 9.3.2: Graph of the BQ of (9.19) with β = -1 (p' = 1.0).

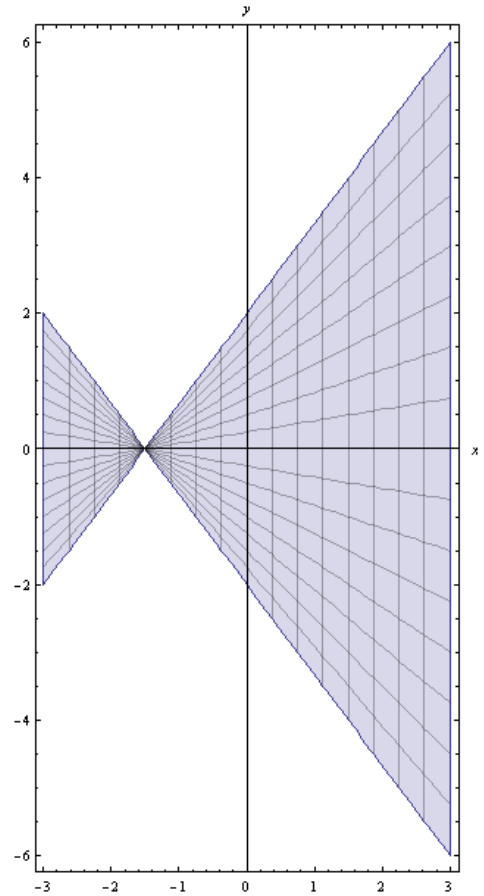

Figure 9.3.3: Graph of the BQ of (9.19) with β = 2 (p' = -0.5).

In Tables 9.4, we take the singular point to be the point (p_0 = -1, q_0 = 1). In Table 9.4.1, we present the results for β = 1. In this case, the singular point is the point (-3, 0, 0) in Figure 9.3.1. Also, we have that q_0 = (0, 0, 0), as we mentioned above. In this case, we have from (7.4) that

$$A = h^2\,, \quad B = 0\,, \quad C = \sqrt{9 + 4\left(1+v\right)^2}\,. \tag{9.23}$$

When we substitute these values into the logarithm's argument in (7.9), we get

$$I = \int_{-1-q_0}^{1-q_0} \frac{1}{C(v)} \ln \left| \frac{\sqrt{\left[2C(v)\right]^2 + h^2} + 2C(v)}{|h|} \right| dv \tag{9.24}$$

an expression that is not computable when h = 0. If we compare this table to Table 9.2.3, we see that the transition for h = 0.1 is smooth. As h gets smaller, however, we see a radical change in the integration outcome. We note that in Table 9.2.3, the value of q_0 is (0, 0.002, 0), a small value but sufficient to stabilize the integral.

Table 9.4.1. The value of the integral in (7.9) for the BQ of (9.19) and for p_0 = -1, q_0 = 1 and β = 1.

	GKQ			DEQ		
h	Value	Time	SD	Value	Time	SD
1.00E-01	3.03215129971745	0.015	14	3.03215129971744	0.016	14
1.00E-08	13.1082615780428	0.000	15	13.1082615780428	0.015	15
1.00E-20	30.3816595133087	0.031	15	30.3816595133087	0.016	15
0.00E+00	Failed to compute	N/A	N/A	Failed to compute	N/A	N/A

Table 9.4.2. The value of the integral in (7.9) for the BQ of (9.19) and for p_0 = -1, q_0 = 1 and β = 2.

	GKQ			DEQ		
h	Value	Time	SD	Value	Time	SD
1.00E-01	1.27899151358520	0.000	14	1.27899151358519	0.000	14
1.00E-08	1.29041253658337	0.016	14	1.29041253658336	0.031	14
1.00E-20	1.29041253765587	0.000	15	1.29041253765587	0.015	15
0.00E+00	1.29041253765587	0.015	15	1.29041253765587	0.031	15

Table 9.4.3. The value of the integral in (7.9) for the BQ of (9.19) and for p_0 = -1, q_0 = 1 and β = -1.

	GKQ			DEQ		
h	Value	Time	SD	Value	Time	SD
1.00E-01	0.936274735416838	0.015	14	0.936274735416837	0.016	14
1.00E-08	0.944587582282624	0.015	14	0.944587582282623	0.016	14
1.00E-20	0.944587583101619	0.016	14	0.944587583101618	0.000	14
0.00E+00	0.944587583101619	0.000	14	0.944587583101618	0.016	14

In concluding this section, we stress that we should avoid irregular BQs in practice. For flat but regular BQs, we can use (7.9) without incurring a loss of SD.

SECTION 10: SUMMARY AND CONCLUSIONS

We have presented a new approach for computing the simple layer potential of polynomial density over a BQ. The analysis focuses on the case when the OP is near or on the BQ. Our approach differs from existing ones in that it does not use a transformation of coordinates nor does it employ an auxiliary plane; instead it uses rectangular coordinates and integrates analytically along one of them and numerically along the other. We have demonstrated that, with carefully designed quadratures, this approach can yield DP for any regular BQ and any position of the OP.

In Section 2, we define the BQ mathematically and provide its geometric properties. We also make the distinction between a regular and an irregular BQ; moreover, we show that an irregular BQ is necessarily flat and we provide examples. In Section 3, we describe three BQs that we use for testing our approach. They range from a flat one to a very elongated three-dimensional one.

In Section 4, we discuss in detail the reasons for the need of a new approach to the calculation of the simple layer potential. We demonstrate through analysis and examples that, under the existing approach of the tangent-plane approximation, the limit of the integrand does not exist at the singularity point, and that the integrand may undergo rapid changes in the neighborhood of this point. We also demonstrate that the use of polar coordinates works well when the OP is on the BQ but not when it is near the BQ.

In Section 5, we introduce our approach. We split the integrand into two parts: one that has no singularities of any kind, and one that does not oscillate but contains the singularity. The integral of the formal can be evaluated numerically to good precision. For the latter we show that, through repeated integration by parts, we can reduce its integral to a number of single integrals with at least continuous integrands and one that is basically a simple layer (or Newtonian potential) of density one.

In Section 6, we consider the simple layer of density one and integrate it with respect to one of the two parameters that define the BQ. Through analysis and examples, we show that the remaining integral (with respect to the remaining parameter and which can be evaluated only numerically) loses precision as the OP approaches the BQ. In Section7, we study the cause of this behavior and find that it is due to two terms in the integrand that subtract one another. When the integration variable is equal to zero, and as the OP approaches the BQ, the two terms become almost equal and their difference appears as zero while it is not, unless the OP is on the BQ. We correct for this by rewriting the expression for the integrand in such a way that the difference of the offending terms is multiplied by a term that becomes zero when the integration variable is zero. Using examples, we show that the new expression is stable and that we can obtain 15 SD of precision even when the OP lies on the BQ. In Section 8, we continue testing our method using the third BQ of Section 3. For all three test points we get a minimum of 14 SD. We also use integration by parts to produce a new formula that is guaranteed to be stable when the OP is on the BQ. As we point out there, all numerical experiments with the general formula yield a minimum of 14 SD; moreover, even though the OP lies on the BQ, we can move it a small distance off it without loss of precision. Thus, we may not need to use this special formula, a formula that is more computationally intensive than the general one.

In Section 9, we prove a claim we made in earlier sections and show that a certain term can be zero only if the BQ is irregular. We also give additional examples of irregular BQs and perform a sensitivity study to determine how precision is affected as we pass from a regular to an irregular BQ. As we point out there, irregular BQs should be avoided in practice.

In terms of additional investigations, we may wish to perform a more detailed validation of our formulas. We believe, however, that they will withstand any test, no matter how severe. We may also perform calculations for several OPs lying on the same BQ to determine the resulting surface and its smoothness. This is necessary for determining whether the second integration, the one with respect to the OP coordinates can be performed numerically to high precision. Alternatively, we may wish to use these points to interpolate and use the resulting expressions for an analytic integration with respect to the OP coordinates.

REFERENCES

1. J. J. H. Wang, Generalized Moment Methods in Electromagnetics. New York: Wiley – Interscience, 1991.

2. S. M. Rao, D. R. Wilton, and A. W. Glisson, “Electromagnetic Scattering by surfaces of arbitrary shape”, IEEE Trans. Antennas Propagat., Vol. AP-30, No. 3, pp. 409-418, 1982.

3. B. M. Notaroš, "Higher Order Frequency-Domain Computational Electromagnetics", invited review paper, IEEE Trans. Antennas Propagat., Vol. 56, No. 8, pp. 2251 - 2276, 2008.

4. B. M. Kolundzija and A. R. Djordjević, Electromagnetic Modeling of Composite Metallic and Dielectric Structures. Boston: Artech House, 2002. Website: http://www.wipl-d.com/

5. Y. Zhang and T. K. Sarkar, Parallel Solution of Integral Equation-Based EM Problems in the Frequency Domain. New York: Wiley – IEEE Press, 2009.

6. A. B. Manić, M. Djordjević, and B. M. Notaroš, "Duffy Method for Evaluation of Weakly Singular SIE Potential Integrals Over Curved QLs With Higher Order Basis Functions", IEEE Trans. Antennas Propagat., Vol. 62, No. 6, pp. 3338 - 3343, 2014.

7. M. G. Duffy, "Quadrature over a pyramid or cube of integrands with a singularity at a vertex", SIAM J. Numer. Anal., Vol. 19, No. 6, pp. 1260 – 1262, 1982.

8. W. Ding and G. Wang, "Treatment of singular integrals on generalized curvilinear parametric QLs in higher order method of moments", IEEE Antennas Wireless Propag. Lett., Vol. 8, pp. 1310–1313, 2009.

9. E. Jørgensen, J. L. Volakis, P. Meincke, and O. Breinbjerg, "Higher order hierarchical Legendre basis functions for electromagnetic modeling", IEEE Trans. Antennas Propag., Vol. 52, pp. 2985–2995, Nov 2004.

10. H. Yuan, N. Wang, and C. Liang, "Combining the higher order method of moments with geometric modeling by NURBS surfaces", IEEE Trans. Antennas Propag., Vol. 57, No. 11, pp. 3558–3563, Nov 2009.

11. Wolfram Research, Inc., Mathematica, Version 7.0, Champaign, IL, 2008.

12. D. J. Struik, Classical Differential Geometry. Reading, MA: Addison – Wesley, 1961.

13. I. S. Gradshteyn and I. M. Ryzhik, Table of Integrals, Series, and Products. Corrected and Enlarged Edition. New York: Academic Press, 1980.

14. P. J. Davis and P. Rabinowitz, Methods of Numerical Integration, Second ed. Orlando, FL: Academic Press, 1984.

15. H. Takahasi and M. Mori, "Double Exponential Formulas for Numerical Integration", Research Institute for Mathematical Sciences, Kyoto Univ., Vol. 9, pp. 721 – 741, 1974.

APPENDIX A: Irregular Bilinear Quadrilateral

In this appendix, we prove the oral arguments that follow (2.8). We resolve the vector $\mathbf{r}_{pq}$ with a component in the plane formed by the vectors $\mathbf{r}_p$ and $\mathbf{r}_q$ and a component perpendicular to that plane

$$\mathbf{r}_{pq} = \alpha\mathbf{r}_p + \beta\mathbf{r}_q + \gamma\left(\mathbf{r}_p \times \mathbf{r}_q\right). \tag{A.1}$$

In place of (2.8), we can then write

$$\begin{aligned}
&\frac{\partial \mathbf{r}(p,q)}{\partial p} \times \frac{\partial \mathbf{r}(p,q)}{\partial q} = \mathbf{r}_p \times \mathbf{r}_q + \left[\alpha\mathbf{r}_p + \beta\mathbf{r}_q + \gamma\left(\mathbf{r}_p \times \mathbf{r}_q\right)\right] \times \left(\mathbf{r}_q q - \mathbf{r}_p p\right) \\
&= \left(1 + \alpha q + \beta p\right)\mathbf{r}_p \times \mathbf{r}_q + \gamma\left(\mathbf{r}_p \times \mathbf{r}_q\right) \times \left(\mathbf{r}_q q - \mathbf{r}_p p\right) \\
&= \left(1 + \alpha q + \beta p\right)\left(\mathbf{r}_p \times \mathbf{r}_q\right) + \gamma\left\{\mathbf{r}_p\left[p\left(\mathbf{r}_p \cdot \mathbf{r}_q\right) - q\left|\mathbf{r}_q\right|^2\right] + \mathbf{r}_q\left[q\left(\mathbf{r}_p \cdot \mathbf{r}_q\right) - p\left|\mathbf{r}_p\right|^2\right]\right\}.
\end{aligned} \tag{A.2}$$

This is a vector for a component in the plane of the vectors $\mathbf{r}_p$ and $\mathbf{r}_q$, and one perpendicular to this plane. For this vector to be equal to zero, all three components must be zero

$$\left.\begin{aligned}
1 + \alpha q + \beta p &= 0 \\
\gamma\left[p\left(\mathbf{r}_p \cdot \mathbf{r}_q\right) - q\left|\mathbf{r}_q\right|^2\right] &= 0 \\
\gamma\left[-p\left|\mathbf{r}_p\right|^2 + q\left(\mathbf{r}_p \cdot \mathbf{r}_q\right)\right] &= 0
\end{aligned}\right\}. \tag{A.3}$$

If we assume that y is different from zero, then the last two equations yield a determinant different from zero since we have assumed that $\mathbf{r}_p$ and $\mathbf{r}_q$ are not co-linear. Thus, the system of two equations has only the trivial solution, *i.e.*, p and q are both equal to zero. For these values, however, the first equation in (A.3) is not satisfied. This leads us to the conclusion that, for the two equations to be equal to zero, y must be equal to zero. From (A.1), we conclude that, for a BQ to be irregular, the three vectors describing it must lie on the same plane. If we assume that all three are non-zero vectors, we conclude that a necessary condition for an irregular triangle is that

$$\mathbf{r}_{pq} \cdot \left(\mathbf{r}_p \times \mathbf{r}_q\right) = 0. \tag{A.4}$$

In case $\mathbf{r}_p$ and $\mathbf{r}_q$ are colinear, the first term on the right of (2.8) is zero and the second becomes zero at the origin; thus, we have an irregular BQ that lies on the plane defined by $\mathbf{r}_p$ (or $\mathbf{r}_q$) and $\mathbf{r}_{pq}$.

THIS PAGE INTENTIONALLY LEFT BLANK

APPENDIX B: Continuation of Analysis of Section 4

In Section 4, we analyzed the inner integral of the first BQ of Section 3. We found that the first integrand in (4.2) is not as smooth as stated in [4]. Here, we perform the same analysis for the remaining two BQs of Section 3.

The second BQ is shown in Figure 3.2. The position vector is given by (3.6) so that

$$\mathbf{r}^* = (3,0,0)\frac{1}{4} + (0,2,0)\frac{1}{4} + (0,0,1)\frac{1}{16} \tag{B.1}$$

and, hence,

$$\mathbf{r}(u,v) - \mathbf{r}^* = (3,0,0)u + (0,2,0)v + (0,0,1)\left[\left(u+\frac{1}{4}\right)\left(v+\frac{1}{4}\right) - \frac{1}{16}\right]. \tag{B.2}$$

The linear part of this is

$$\mathbf{r}_0(u,v) - \mathbf{r}^* = (3,0,0)u + (0,2,0)v + (0,0,1)\frac{1}{4}(u+v). \tag{B.3}$$

From the last two we get that

$$R_2(u,v) = \sqrt{(3u)^2 + (2v)^2 + \left[\left(u+\frac{1}{4}\right)\left(v+\frac{1}{4}\right) - \frac{1}{16}\right]^2} \tag{B.4}$$

and

$$R_{0,2}(u,v) = \sqrt{(3u)^2 + (2v)^2 + \left(\frac{u+v}{4}\right)^2} \tag{B.5}$$

so that

$$h_2(u,v) = \frac{\left(u+\frac{1}{4}\right)^l \left(v+\frac{1}{4}\right)^m}{\sqrt{(3u)^2 + (2v)^2 + \left[\left(u+\frac{1}{4}\right)\left(v+\frac{1}{4}\right) - \frac{1}{16}\right]^2}} - \frac{\left(\frac{1}{4}\right)^{l+m}}{\sqrt{(3u)^2 + (2v)^2 + \left(\frac{u+v}{4}\right)^2}}. \tag{B.6}$$

We have plotted this expression in Mathematica [11]. Figure B.1 shows the graph of (B.6), a graph that is anything but smooth near the origin. In Figs. B.2 and B.3, we zoom toward the origin and take cuts along both axes. We see that, on at least one side of an axis, we have a fast-changing graph that is difficult to match numerically.

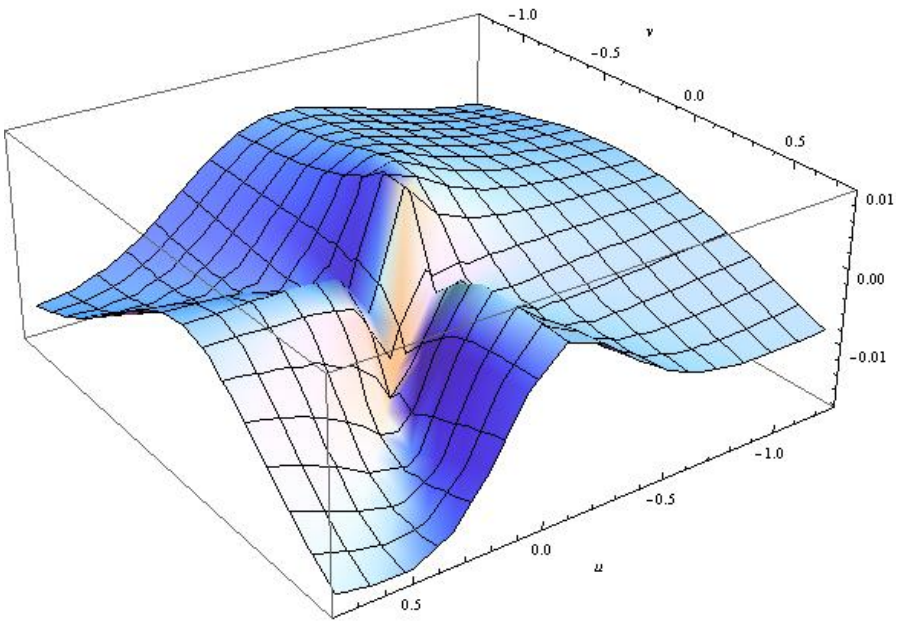

Figure B.1: Graph of the surface (B.6) for $l = 0, m = 0$; Second BQ.

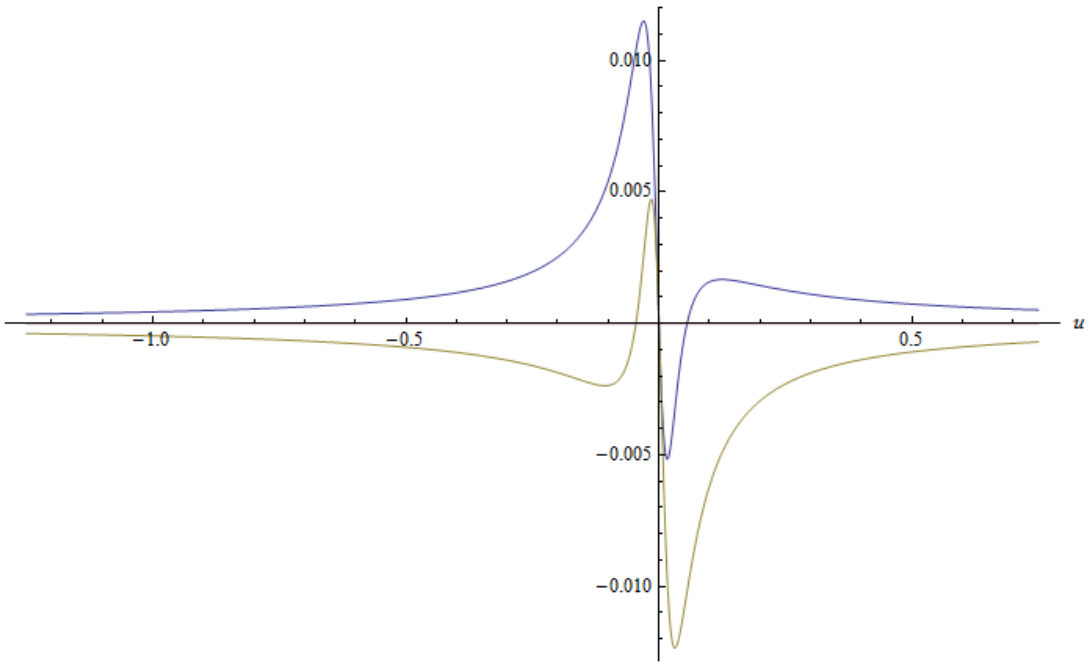

Figure B.2. Cuts of Fig. B.1 along $v = -0.05$ (blue), $v = 0$ (invisible but coinciding with the u-axis) and $v = 0.05$ (olive). Second BQ.

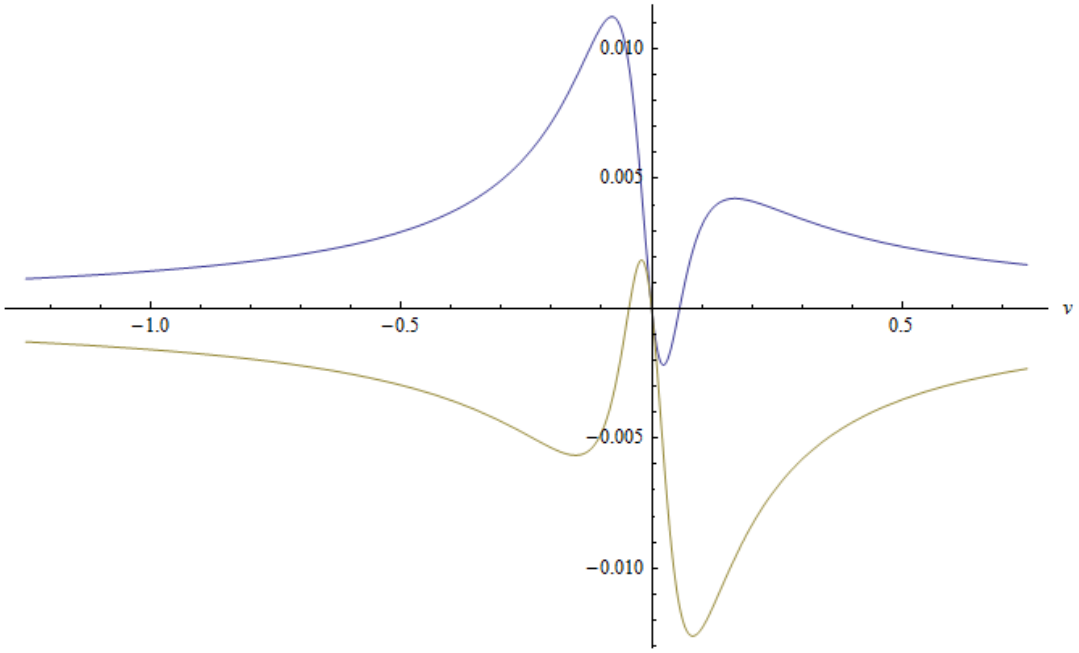

Figure B.3. Cuts of Fig. B.1 along $u = -0.05$(blue), $u = 0$ (invisible but coinciding with the *v*-axis) and $u = 0.05$ (olive). Second BQ.

In Figs. B.4 and B.5, we display the behavior of (B.6) for $l = 1, m = 0$ while, in Figs. B.6 and B.7, we display the graph of the same function for $l = 0, m = 1$. In Figs. B.8 – B.11, we display the behavior for $l = 1, m = 1$. What we observe is very similar to what we discussed in Section 4 for the first BQ of Section 3. We will not repeat those comments here.

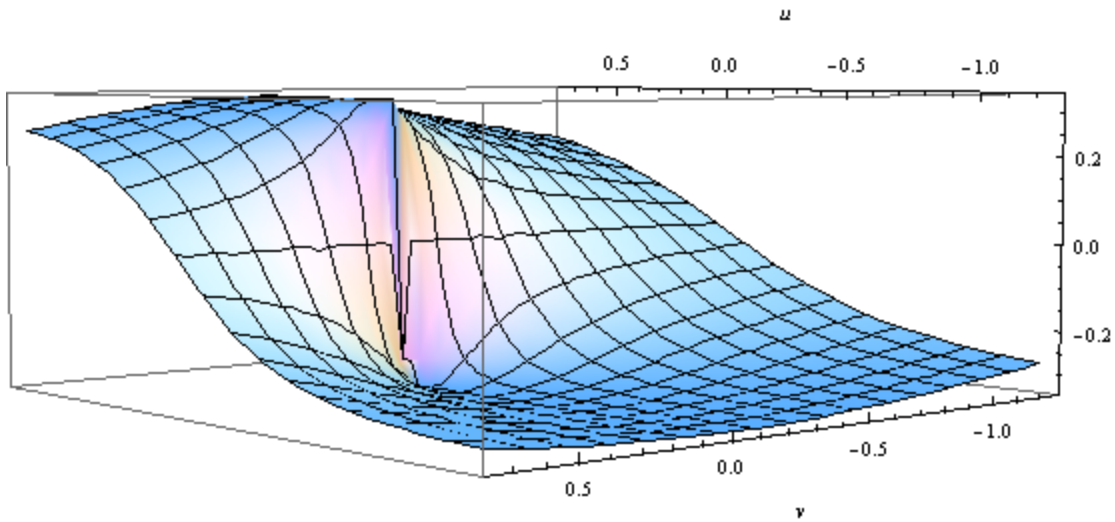

Figure B.4: Graph of (B.6) for $l = 1, m = 0$; Second BQ.

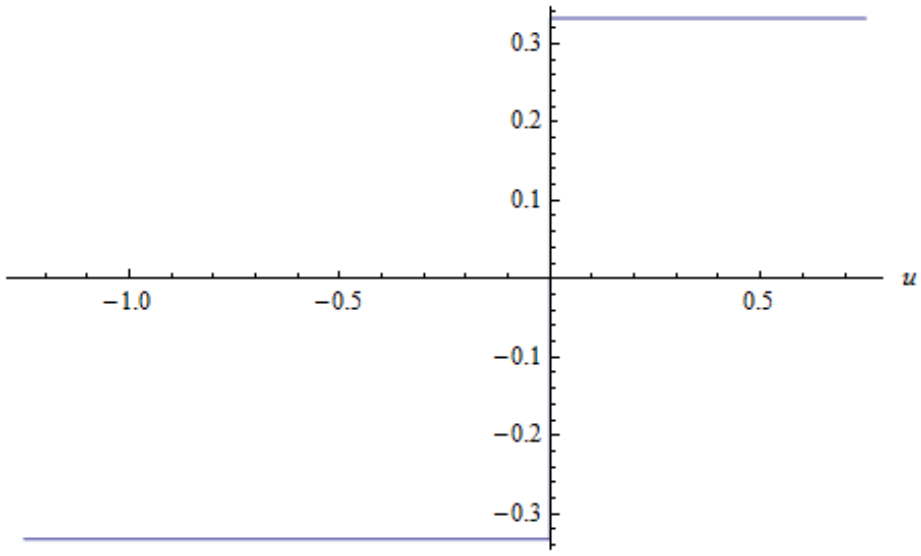

Figure B.5: Graph of the function $h_2(u,0)$, as defined in (B.6), for $l=1, m=0$; Second BQ.

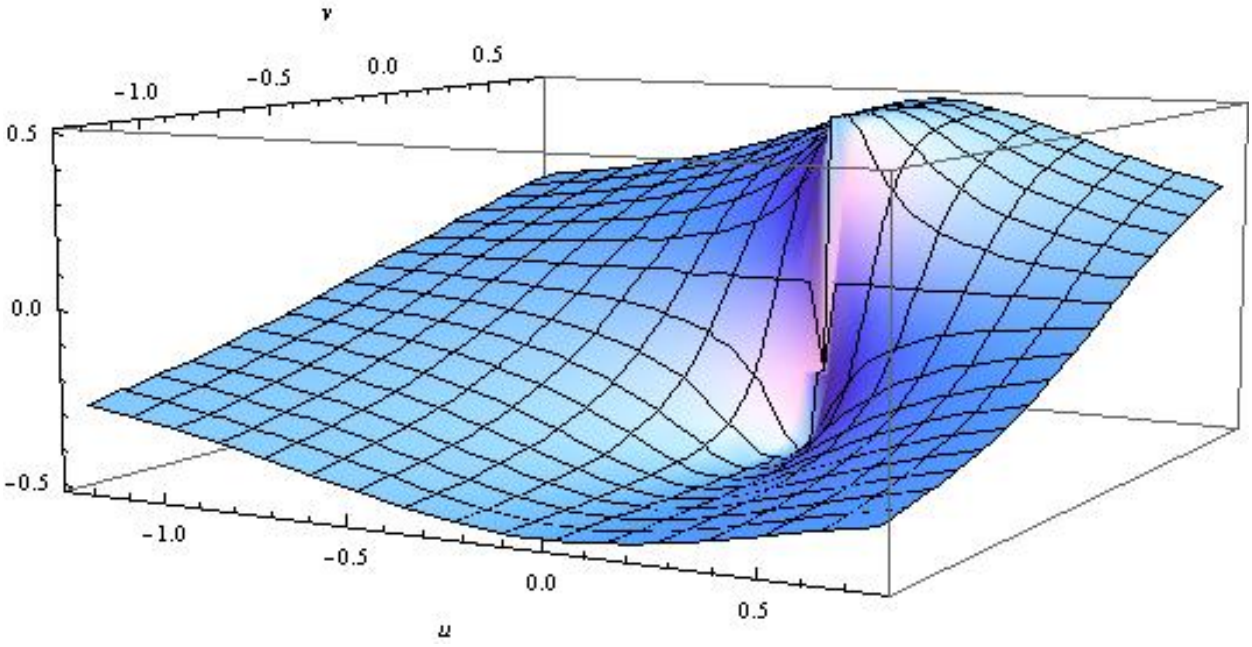

Figure B.6: Graph of (B.6) for $l=0, m=1$; Second BQ.

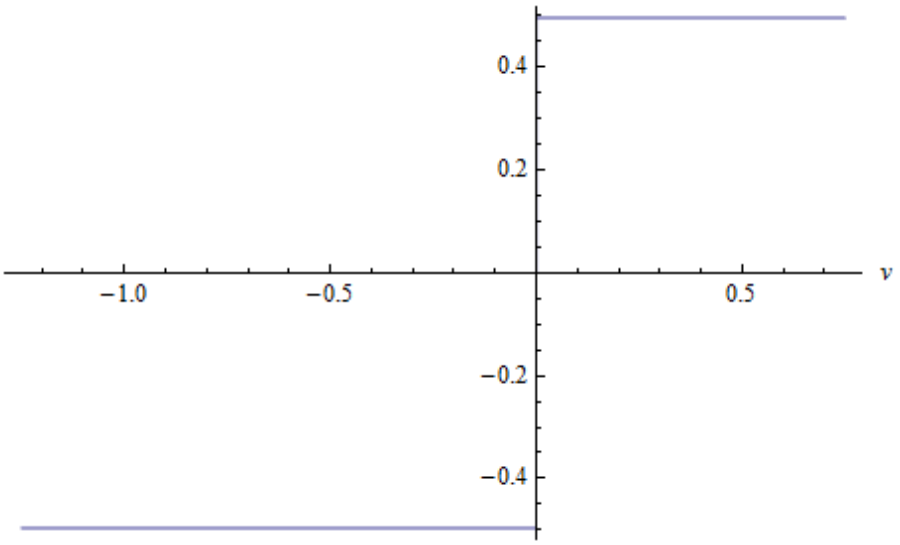

Figure B.7: Graph of the function $h_2(0,v)$, as defined in (B.6), for $l=0, m=1$; Second BQ.

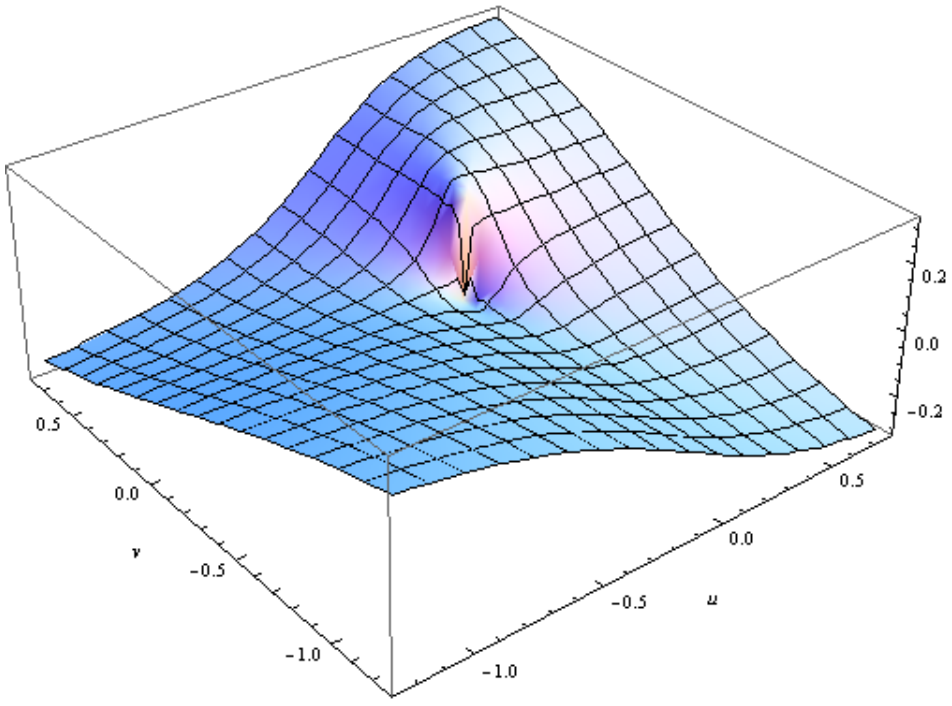

Figure B.8: Graph of (B.6) for $l=1, m=1$; Second BQ.

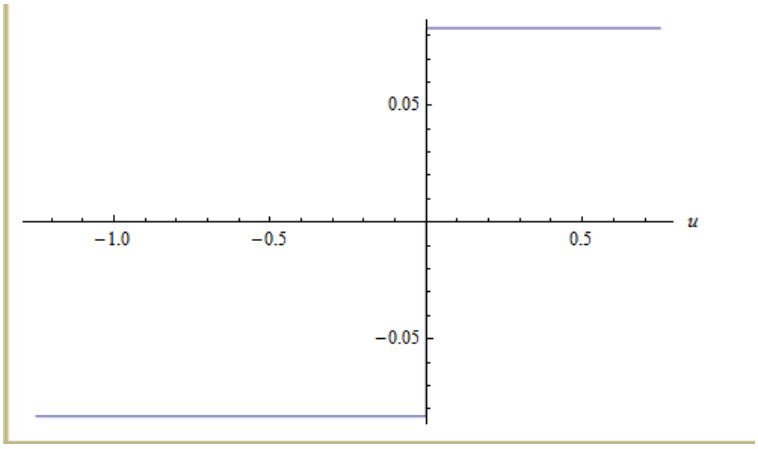

Figure B.9: Graph of the function $h_2(u,0)$, as defined in (B.6), for $l=1, m=1$; Second BQ.

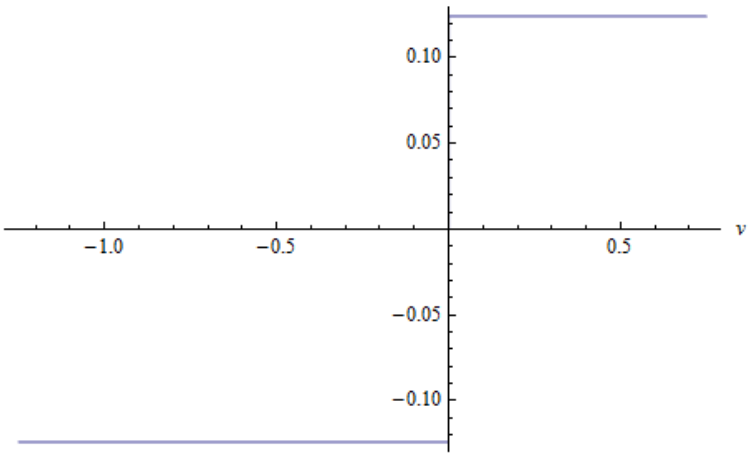

Figure B.10: Graph of the function $h_2(0,v)$, as defined in (B.6), for $l=1, m=1$; Second BQ.

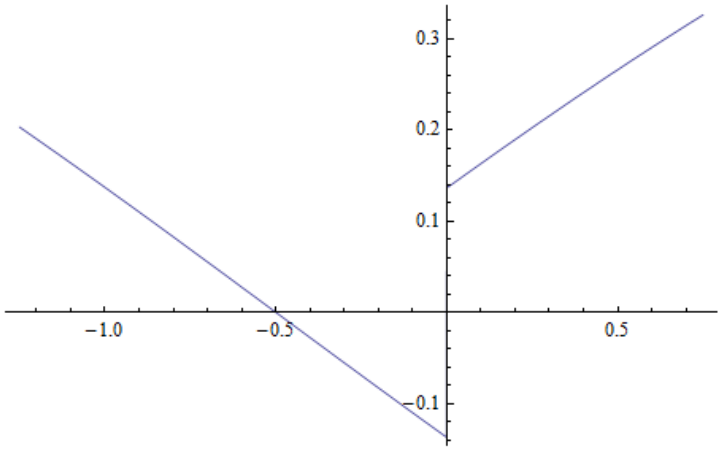

Figure B.11: Graph of the function $h_2(u,u)$, as defined in (B.6), for $l=1, m=1$; Second BQ.

We proceed next to the last BQ of Section 3. Its position vector is given by (3.9). From it

$$\mathbf{r}* = (3,0,0)\frac{1}{4} + (0,2,0)\frac{1}{4} + (0,0,10)\frac{1}{16} \tag{B.7}$$

and, hence,

$$\mathbf{r}(p,q) - \mathbf{r}* = (3,0,0)u + (0,2,0)v + (0,0,10)\left[\left(u+\frac{1}{4}\right)\left(v+\frac{1}{4}\right) - \frac{1}{16}\right]. \tag{B.8}$$

The linear part of this is

$$\mathbf{r}_0(u,v) - \mathbf{r}* = (3,0,0)u + (0,2,0)v + (0,0,10)\frac{1}{4}(u+v). \tag{B.9}$$

From the last two we get that

$$R_3(u,v) = |\mathbf{r}(p,q) - \mathbf{r}*| = \sqrt{(3u)^2 + (2v)^2 + 100\left[\left(u+\frac{1}{4}\right)\left(v+\frac{1}{4}\right) - \frac{1}{16}\right]^2} \tag{B.10}$$

and

$$R_{3,0}(u,v) = |\mathbf{r}_0(p,q) - \mathbf{r}*| = \sqrt{(3u)^2 + (2v)^2 + \left(\frac{5}{2}\right)^2 (u+v)^2} \tag{B.11}$$

so that

$$h_3(u,v) = \frac{\left(u+\frac{1}{4}\right)^l \left(v+\frac{1}{4}\right)^m}{\sqrt{(3u)^2 + (2v)^2 + 100\left[\left(u+\frac{1}{4}\right)\left(v+\frac{1}{4}\right) - \frac{1}{16}\right]^2}} - \frac{\left(\frac{1}{4}\right)^{l+m}}{\sqrt{(3u)^2 + (2v)^2 + \left[\frac{5}{2}(u+v)\right]^2}} \tag{B.12}$$

We use Mathematica [11] to produce graphs. In Figure B.12 we show the graph of (B.6), a graph that is anything but smooth near the origin. In Figs. B.13 and B.14, we zoom toward the origin and take cuts along both axes. We see that, on either side of an axis, we have a doublet-like behavior that is difficult to match numerically.

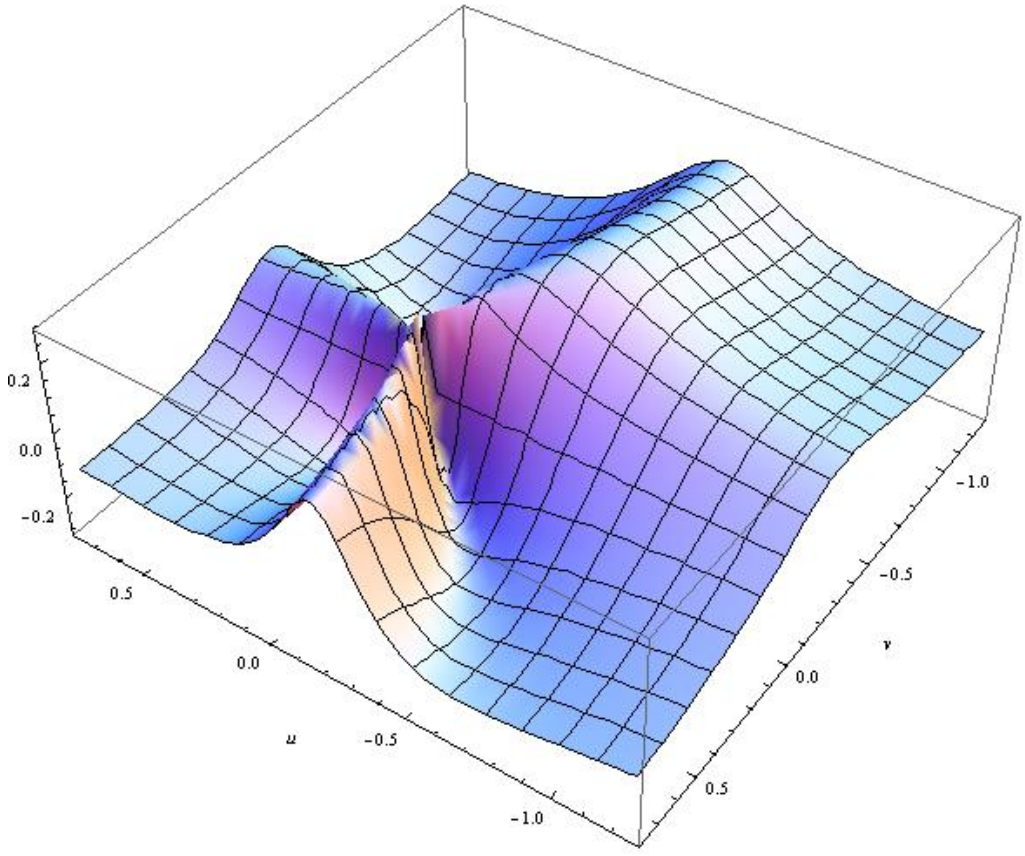

Figure B.12: Graph of the surface (B.12) for $l = 0, m = 0$; Third BQ.

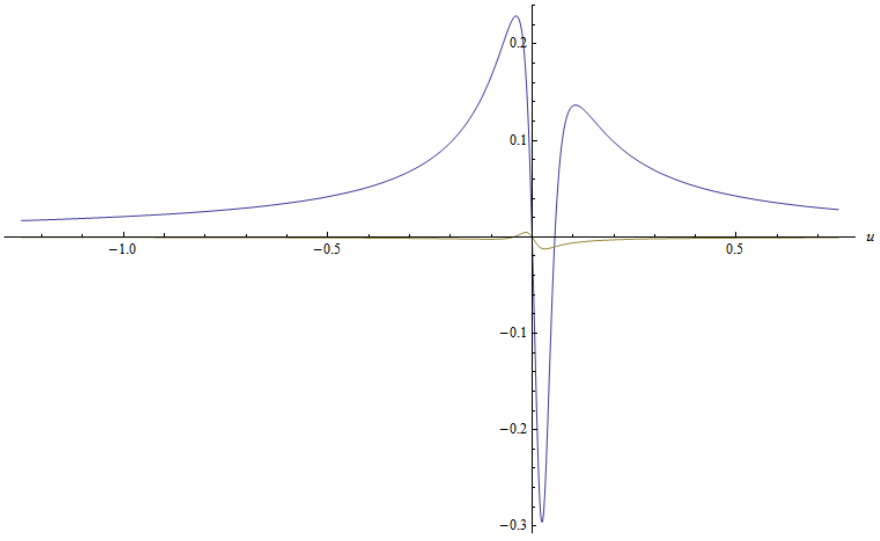

Figure B.13. Cuts of Fig. B.12 along $v = -0.05$ (blue), $v = 0$ (invisible but coinciding with the u-axis) and $v = 0.05$ (olive). Third BQ.

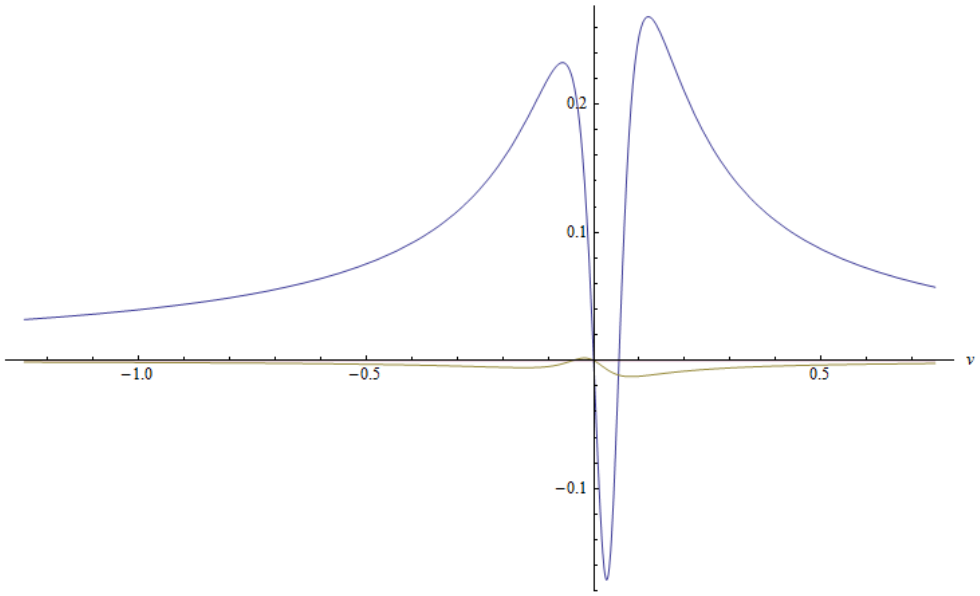

Figure B.14. Cuts of Fig. B.12 along $u = -0.05$ (blue), $u = 0$ (invisible but coinciding with the *v*-axis) and $u = 0.05$ olive. Third BQ.

In Figs. B.15 and B.16, we display the behavior of (B.12) for $l = 1, m = 0$ while, in Figs. B.17 and B.18, we display the graph of the same function for $l = 0, m = 1$. In Figs. B.19 – B.22, we display the behavior for $l = 1, m = 1$. What we observe is very similar to what we discussed in Section 4 for the first BQ of Section 3, except for the last graph, where we display the behavior along the diagonal. We verify below that the graph displays the correct behavior. From (B.12)

$$h_3(u,u) = \frac{\left(u+\frac{1}{4}\right)^2}{\sqrt{(3u)^2+(2u)^2+100\left[\left(u+\frac{1}{4}\right)^2-\frac{1}{16}\right]^2}} - \frac{\left(\frac{1}{4}\right)^2}{\sqrt{(3u)^2+(2u)^2+(5u)^2}}$$

$$= \frac{\left(u+\frac{1}{4}\right)^2}{\sqrt{(3u)^2+(2u)^2+100\left(u^2+\frac{u}{2}\right)^2}} - \frac{\left(\frac{1}{4}\right)^2}{|u|\sqrt{38}} = \frac{\left(u+\frac{1}{4}\right)^2}{|u|\sqrt{13+\left[10\left(u+\frac{1}{2}\right)\right]^2}} - \frac{\left(\frac{1}{4}\right)^2}{|u|\sqrt{38}}$$

$$= \frac{1}{|u|}\frac{\sqrt{38}\left(u+\frac{1}{4}\right)^2 - \left(\frac{1}{4}\right)^2\sqrt{13+\left[10\left(u+\frac{1}{2}\right)\right]^2}}{\sqrt{38}\sqrt{13+\left[10\left(u+\frac{1}{2}\right)\right]^2}}$$

$$= \frac{1}{|u|} \frac{38\left(u+\frac{1}{4}\right)^4 - \left(\frac{1}{4}\right)^4 \left\{13+\left[10\left(u+\frac{1}{2}\right)\right]^2\right\}}{\sqrt{38}\sqrt{13+\left[10\left(u+\frac{1}{2}\right)\right]^2}\left\{\sqrt{38}\left(u+\frac{1}{4}\right)^2+\left(\frac{1}{4}\right)^2\sqrt{13+\left[10\left(u+\frac{1}{2}\right)\right]^2}\right\}}$$

$$= \frac{1}{|u|} \frac{38\left(u^4+4\frac{u^3}{4}+6\frac{u^2}{4^2}+4\frac{u}{4^3}+\frac{1}{4^4}\right) - \left(\frac{1}{4}\right)^4 \left\{13+100\left(u^2+u+\frac{1}{4}\right)\right\}}{\sqrt{38}\sqrt{13+\left[10\left(u+\frac{1}{2}\right)\right]^2}\left\{\sqrt{38}\left(u+\frac{1}{4}\right)^2+\left(\frac{1}{4}\right)^2\sqrt{13+\left[10\left(u+\frac{1}{2}\right)\right]^2}\right\}}$$

$$= \frac{1}{|u|} \frac{38u^4+38u^3+\left(\frac{57}{4}-\frac{25}{64}\right)u^2+\left(\frac{19}{8}-\frac{25}{64}\right)u}{\sqrt{38}\sqrt{13+\left[10\left(u+\frac{1}{2}\right)\right]^2}\left\{\sqrt{38}\left(u+\frac{1}{4}\right)^2+\left(\frac{1}{4}\right)^2\sqrt{13+\left[10\left(u+\frac{1}{2}\right)\right]^2}\right\}}$$

$$= \frac{u}{|u|} \frac{38u^3+38u^3+\frac{887}{32}u+\frac{127}{64}}{\sqrt{38}\sqrt{13+\left[10\left(u+\frac{1}{2}\right)\right]^2}\left\{\sqrt{38}\left(u+\frac{1}{4}\right)^2+\left(\frac{1}{4}\right)^2\sqrt{13+\left[10\left(u+\frac{1}{2}\right)\right]^2}\right\}}, \quad u \neq 0 \qquad \text{(B.13)}$$

which explains the non-linearity of the graph in Figure B.22. Taking the limit, we have

$$\lim_{u^{\pm}\to 0} h_3(u,u) = \pm \frac{\frac{127}{64}}{\sqrt{38}\sqrt{13+\left[10\left(\frac{1}{2}\right)\right]^2}\left\{\sqrt{38}\left(\frac{1}{4}\right)^2+\left(\frac{1}{4}\right)^2\sqrt{13+\left[10\left(\frac{1}{2}\right)\right]^2}\right\}}$$

$$= \pm \frac{\frac{127}{64}}{38\left[2\sqrt{38}\left(\frac{1}{4}\right)^2\right]} = \pm \frac{127}{64}\frac{16}{2\sqrt{38}38} = \pm \frac{127}{304\sqrt{38}} = \pm 0.0678\,. \qquad \text{(B.14)}$$

This number is in agreement with the one we get from Figure B.22.

The bottom line here is that the integrand of the first integral in (4.2) is not sufficiently smooth and that a numerical evaluation of it would require very many grid points.

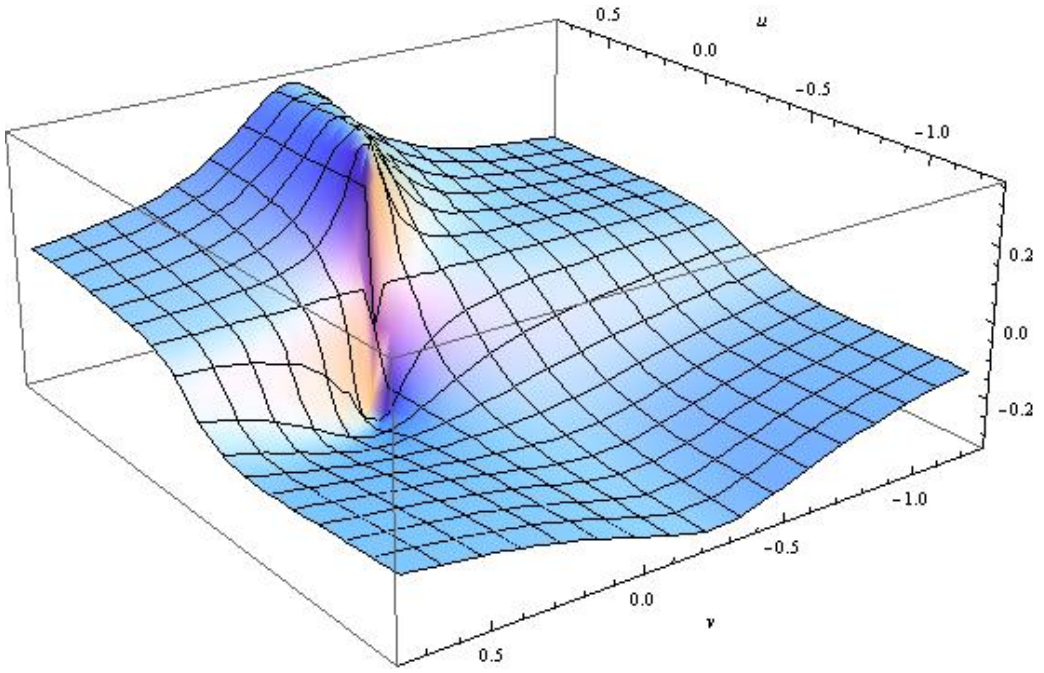

Figure B.15: Graph of (B.12) for $l=1, m=0$; Third BQ.

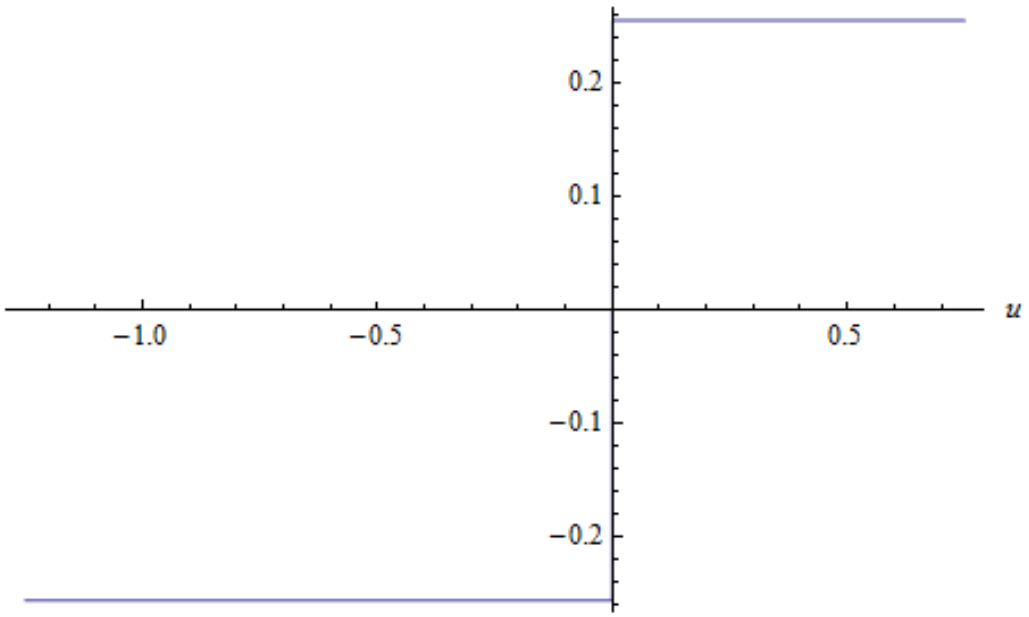

Figure B.16: Graph of the function $h_3(u,0)$, as defined in (B.12), for $l=1, m=0$; Third BQ.

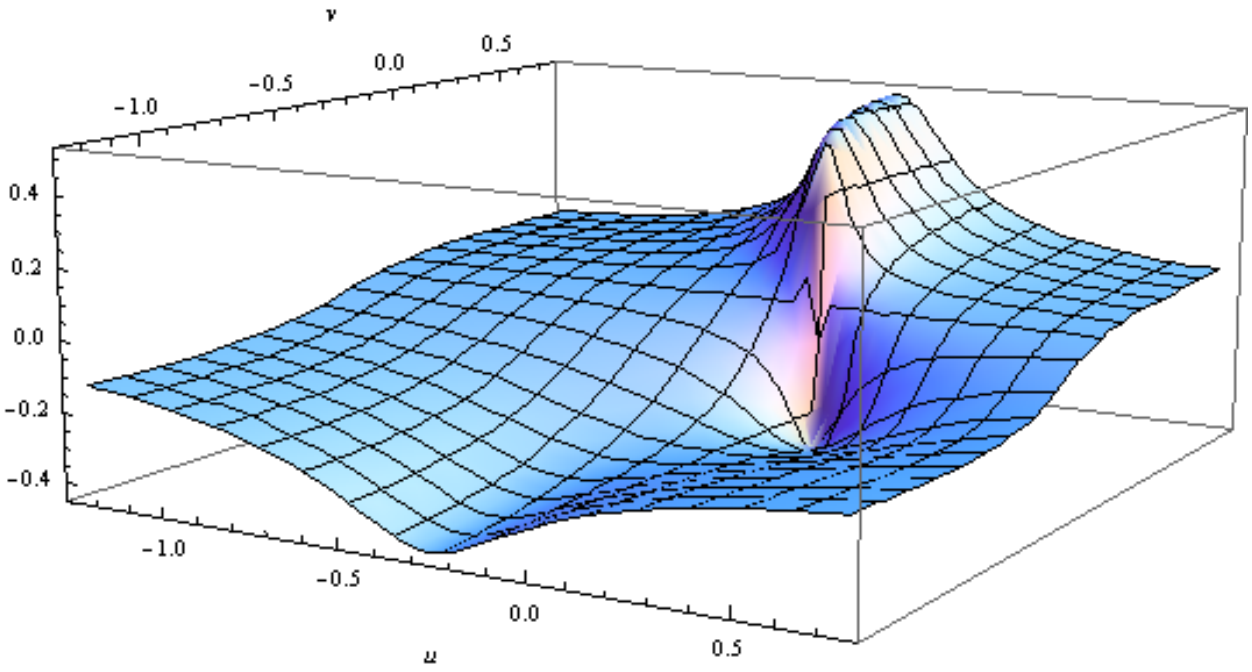

Figure B.17: Graph of (B.12) for $l=0, m=1$; Third BQ.

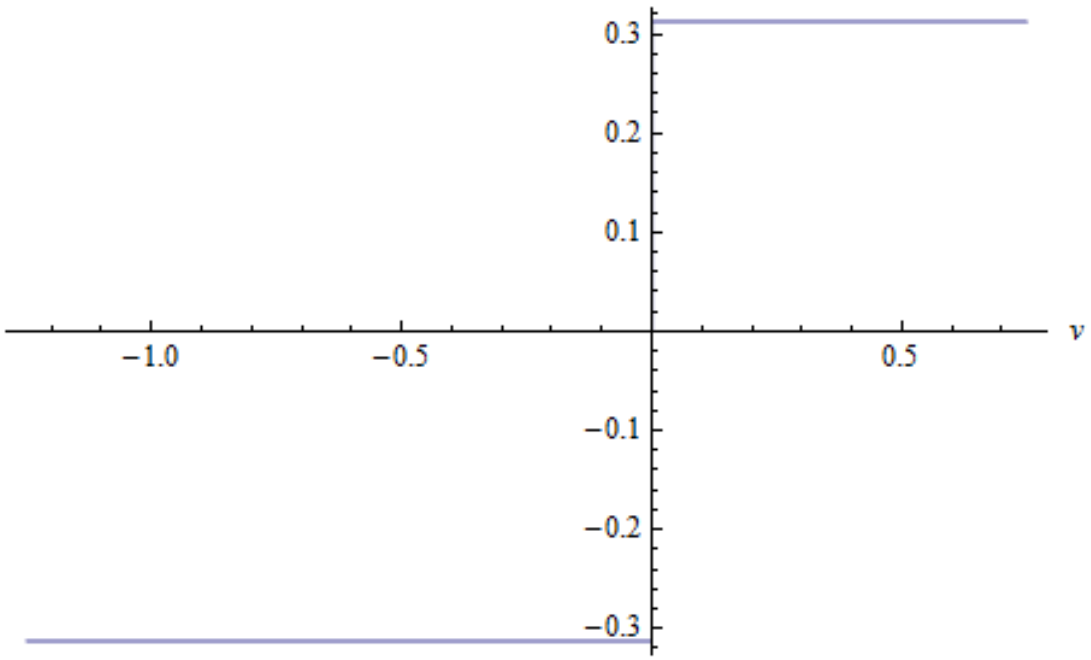

Figure B.18: Graph of the function $h_3(0,v)$, as defined in (B.12), for $l=0, m=1$; Third BQ.

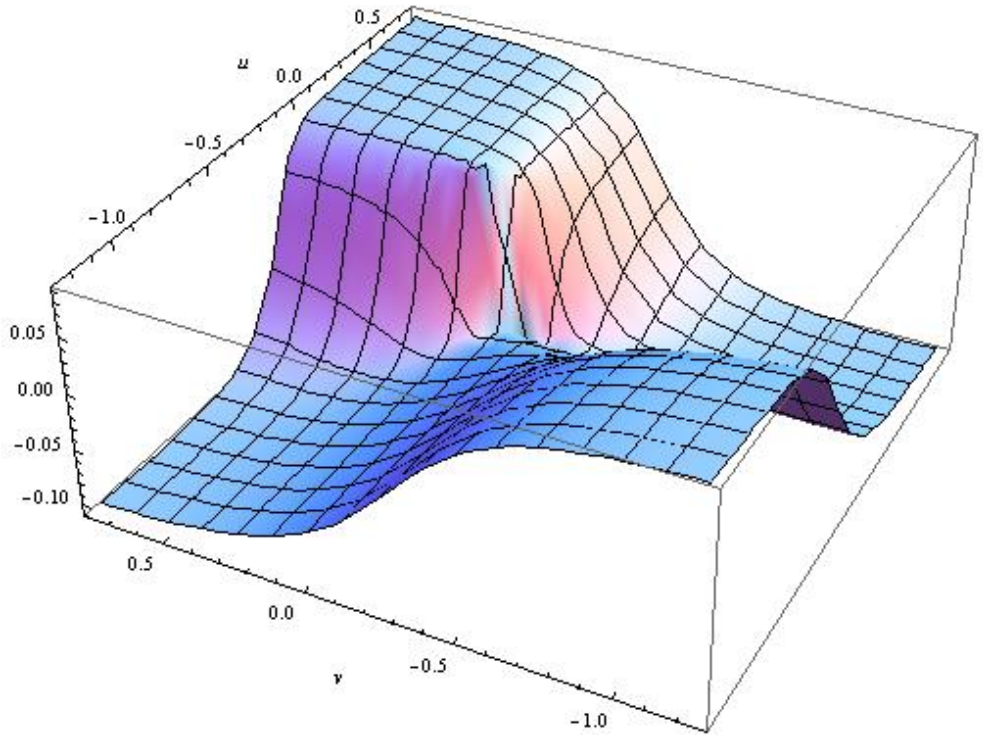

Figure B.19: Graph of (B.12) for $l=1, m=1$; Third BQ.

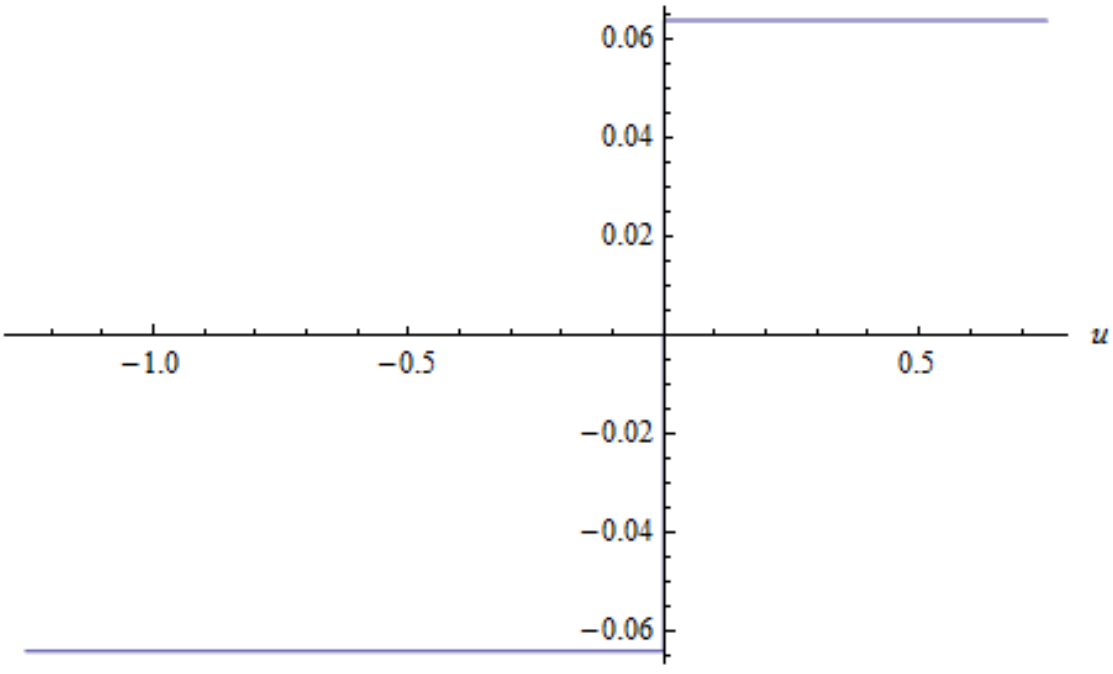

Figure B.20: Graph of the function $h_3(u,0)$, as defined in (B.12), for $l=1, m=1$; Third BQ.

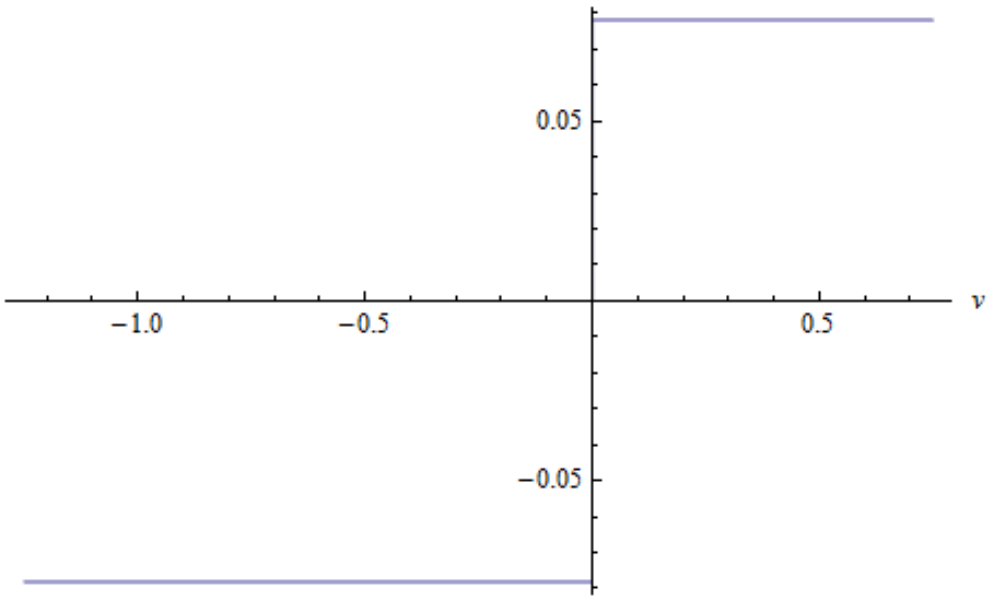

Figure B.21: Graph of the function $h_3(0,v)$, as defined in (B.12), for $l=1, m=1$; Third BQ.

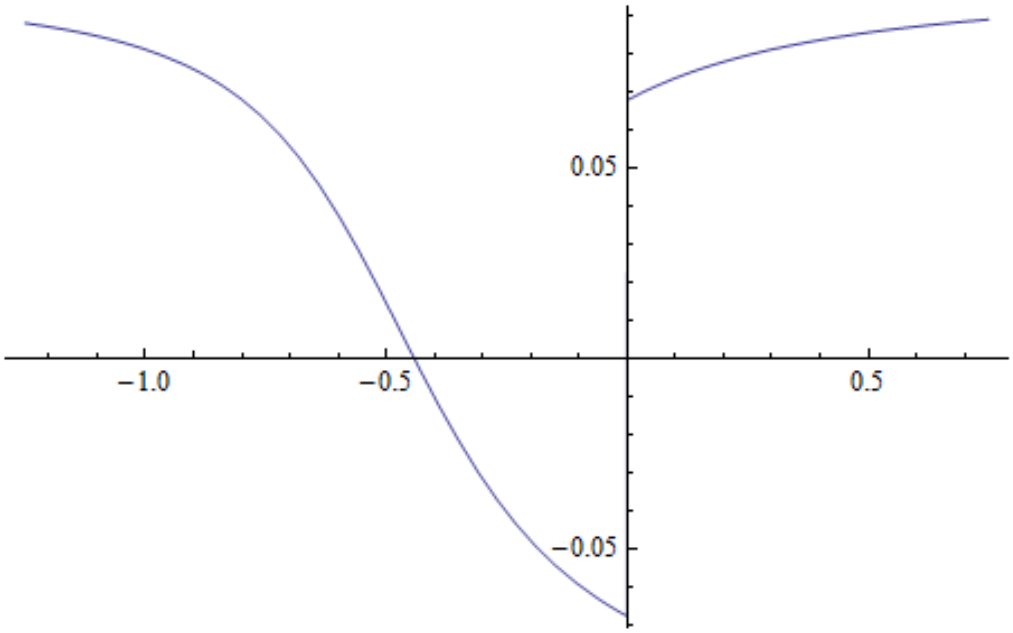

Figure B.22: Graph of the function $h_3(u,u)$, as defined in (B.12), for $l=1, m=1$; Third BQ.

DISTRIBUTION:

NAVAIRSYSCOM (AIR-4.5.5/Douglas McLaughlin), Bldg. 2187, Room 3201 (1)
48110 Shaw Road, Patuxent River, MD 20670-1906
WIPL-D d.o.o. (Prof. Branko Kolundzija), Gandijeva 7 apt. 32, (1)
11073 Belgrade, Serbia (branko.kolundzija@wipl-d.com)
University of Houston (Prof. Donald R. Wilton), E.E. Dept. (1)
N 308 Engineering Building 1, Houston, TX 77204-4005
NAVAIRSYSCOM (AIR-5.1V), Bldg. 304, Room 106A (1)
22541 Millstone Road, Patuxent River, MD 20670-1606
NAVTESTWINGLANT (55TW01A), Bldg. 304, Room 200 (1)
22541 Millstone Road, Patuxent River, MD 20670-1606
NAVAIRSYSCOM (AIR-5.1), Bldg. 304, Room 100 (1)
22541 Millstone Road, Patuxent River, MD 20670-1606
NAVAIRSYSCOM (Air-4.0T), Bldg. 407, Room 116 (1)
22269 Cedar Point Road, Patuxent River, MD 20670-1120
DTIC (1)
Suite 0944, 8725 John J. Kingman Road, Ft. Belvoir, VA 22060-6218